Real-time motion and magnetic field correction for GABA editing using EPI volumetric navigated MEGA-SPECIAL sequence: Reproducibility and Gender effects

Muhammad G. Saleh

Department of Human Biology

University of Cape Town

Thesis presented for the degree of

Doctor of Philosophy

February 2016

All praise is due to Allah, the Lord of the Worlds

Salutations and benedictions to His beloved and His beloved's immaculate family

To my beloved parents, sisters, teachers, relatives and friends

Jesus was once asked, "Who taught you ethics?" He replied, "No one. I saw the ugliness of ignorance and strayed away from it."

Introduction to Islam
Islamic Humanitarian Service

Amirul Momineen Ali ibn Abi Talib (peace be upon him) said: 'O believer, knowledge and manners are values of yourself, thus make efforts in gaining knowledge, as much as your knowledge and manners increase, your status and value would also increase, because through knowledge you would be guided to your Lord and through manners you would be able to serve the Lord in the best way and one who has good manners would become eligible for the guardianship and proximity of God. Hence, accept good advice, so that you may be saved from the punishment of God."

Introduction to Islam
Ayatollah Ibrahim Amini

ABSTRACT

γ-aminobutyric acid (GABA) is the primary inhibitory neurotransmitter and is of great interest to the magnetic resonance spectroscopy (MRS) community due to its role in several neurological diseases and disorders. Since GABA acquisition without macromolecule contamination requires long scan times and strongly depends on magnetic field (B_0) stability, it is highly susceptible to motion and B_0 inhomogeneity. In this work, a pair of three-dimensional (3D) echo planar imaging (EPI) volumetric navigators (vNav) with different echo times, were inserted in MEGA-SPECIAL to perform prospective correction for changes in the subject's head position and orientation, as well as changes in B_0. The navigators do not increase acquisition time and have negligible effect on the GABA signal. The motion estimates are obtained by registering the first of the pairs of successive vNav volume images to the first volume image. The 3D field maps are calculated through complex division of the pair of vNav contrasts and are used for estimating zero- and first-order shim changes in the volume of interest (VOI).

The efficacy of the vNav MEGA-SPECIAL sequence was demonstrated *in-vitro* and *in vivo*. Without motion and shim correction, spectral distortions and increases in spectral fitting error, linewidth and GABA concentration relative to creatine were observed in the presence of motion. The navigated sequence yielded high spectral quality despite significant subject motion.

Using the volumetric navigated MEGA-SPECIAL sequence, the reproducibility of GABA measurements over a 40 minute period was investigated in two regions, the anterior cingulate (ACC) and medial parietal (PAR) cortices, and compared for different analysis packages, namely LCModel, jMRUI and GANNET. LCModel analysis yielded the most reproducible results, followed by jMRUI and GANNET. GABA levels in ACC were unchanged over time, while GABA levels in PAR were significantly lower for the second measurement.

In ACC, GABA levels did not differ between males and females. In contrast, males had higher GABA levels in PAR. This gender difference was, however, only present in the first acquisition. Only in males did GABA levels in PAR decrease over time. These results demonstrate that gender differences are regional, and that GABA levels may fluctuate differently in different regions and sexes.

Acknowledgements

Drs. Ernesta Meintjes and A. Alhamud supervised the work. They provided the context, expert ideas, advice, support and numerous resources required for the implementation of this work. Dr. Andre J.W. van der Kouwe– from the Martinos Center for Biomedical Imaging at Massachusetts General Hospital – provided ideas, discussion and review of my work. Dr. Jamie Near provided guidance and engaged in technical discussions on different aspects of the project. Dr. Lindie du Plessis on assisting with preparation of phantom for *in vitro* scans. Dr. Frances Robertson on technical support for image segmentation. Steven Randall on assisting with recruiting healthy subjects for the project. Charles Harris constructed the moving phantom jigs. Radiographers Nailah Maroof and Alison Siljeur for assisting with data collection.

The following organizations have provided the resources used in this work: University of Cape Town and Cape Universities Brain Imaging Centre.

Funding was provided by by the NRF/DST South African Research Chairs Initiative, NIH grant R01HD071664 and the South African Medical Research Council (MRC).

Funding through the following scholarships: University of Cape Town scholarship for international students, NRF scholarships for Doctoral research, University of Cape Town international conference travel scholarship and NRF Knowledge Interchange and Collaboration scholarship.

DECLARATION

I, Muhammad Gulamabbas Saleh, hereby declare that the work on which this dissertation is based is my original work (except where acknowledgements indicate otherwise) and that neither the whole work nor any part of it has been, is being, or is to be submitted for another degree in this or any other university. I empower the university to reproduce for the purpose of research either the whole or any portion of the contents in any manner whatsoever.

Signature: …… ……

Date:…….

List of Figures

List of Tables

Table of Contents

Preface

This dissertation presents and evaluates a novel method to improve the efficacy of *in vivo* γ-aminobutyric acid (GABA) acquisition using Mescher-Garwood with spin echo full intensity acquired localisation (MEGA-SPECIAL) at 3T. There has been a long-standing interest at the University of Cape Town (UCT) to study learning deficits in children with prenatal alcohol exposure through measuring changes in GABA. The rationale for this work was to implement a technique for robust quantification of GABA in the presence of significant subject motion.

This dissertation includes three independent articles which are found in chapters three, four and five. Each chapter begins with an introduction that provides the necessary background and context to the work, documents and evaluates aspects of methodology, results and conclusion. This style permits direct access and concise evaluation of the different methodologies and follows the logical progression of the work. This format of the thesis, however, contains repetition as each core chapter is being presented as an independent article. The contribution of the co-authors to each chapter is given below:

Chapter one provides a brief background on magnetic resonance spectroscopy (MRS) followed by objectives and an outline of the dissertation.

Chapter two provides relevant background on different methods that have been used for motion and magnetic field correction in MRS, followed by a brief review of GABA studies, properties of GABA, and some background theory on J-editing and *invivo* GABA acquisition.

Chapter three is a journal article (Saleh et al., 2016) that has been peer reviewed and published in *NMR in Biomedicine* (http://www.ncbi.nlm.nih.gov/pubmed/26663075).The chapter describes the sequence and demonstrates that motion and shim correction effectively reduces subtraction artefacts resulting in well-edited GABA peaks even in the presence of subject motion. Superior spectral quality was demonstrated relative to scans with no correction. I am the primary author of this article with assistance from all co-authors. André van der Kouwe conceptualised the EPI navigator. My primary supervisor, Ernesta Meintjes, identified the problem of motion in SV GABA spectroscopy, recommended the solution and assisted with overall project supervision. My co-supervisor, A. Alhamud, provided technical assistance relevant to the project. Jamie Near first developed the MEGA-SPECIAL sequence at the University of Oxford, provided guidance on the transfer of the sequence to UCT, and engaged in technical discussions on different aspects of the sequence. It was primarily my idea to use the MEGA-SPECIAL sequence for this project. I designed the project, performed all technical work – including porting of the MEGA-SPECIAL sequence to the software

platform of the 3T Allegra MRI at UCT and inserting the volumetric navigators – collaborated with the project affiliates, planned all experiments, performed data acquisition and data analysis, drafted the journal paper and gave it to the co-authors for editorial and scientific review.

Chapters four and five are manuscripts that will be submitted for publication. These chapters investigate reproducibility of GABA measurements, tissue and gender effects to provide insight into the robustness of the technology for neuro-spectroscopy applications. In both chapters four and five, subjects' data are the same. In chapter four the data are used to determine reproducibility of MM suppressed GABA measurements obtained using three different software packages, while in chapter five the data are used to determine tissue and gender-related effects on GABA. Briefly, analyses of GABA MRS data are usually done using one of three available software packages, namely LCModel, jMRUI and GANNET. To date, the agreement on the reproducibility of macromolecule (MM) suppressed GABA has not been established between the different packages. To date, gender differences have also not been investigated using MM suppressed GABA. I am the primary author of the manuscripts with insights and assistance from all co-authors. My primary supervisor, Ernesta Meintjes, assisted with overall project supervision. My co-supervisor, A. Alhamud, provided technical assistance relevant to the project. Frances Robertson provided technical assistance on image segmentation. André van der Kouwe gave expert guidance on data capturing. Jamie Near developed the MEGA-SPECIAL sequence at University of Oxford, provided guidance on the transfer of the sequence to UCT and engaged in technical discussions on different aspects of the sequence. Jamie Near provided post-processing toolkits to develop a basis set for LCModel and *a priori* information for jMRUI. The idea of conducting said studies was primarily mine. Furthermore, I designed the project, collaborated with the project affiliates, performed all data acquisition and data analysis, drafted the journal paper and gave it to the co-authors for editorial and scientific input.

Chapter six provides a comprehensive discussion of the contribution of the present study to the GABA MRS field, and highlights limitations and possible future work.

Chapter seven presents the conclusion.

Chapter 1 Introduction

The field of spectroscopy is based on interactions between matter and electromagnetic radiation (ER). The interaction between atoms and ER is described by absorption and emission of photons, whose energy matches an energy level difference in the atom. Since the energy of a photon is directly proportional to its frequency, different forms of spectroscopy are based on the frequencies involved. One of them is nuclear magnetic resonance (NMR) spectroscopy which uses radiofrequencies (RF) in the range 10-800 MHz (De Graaf, 2008).

Magnetic resonance spectroscopy (MRS) is a non-invasive technique, based on the principles of NMR and allows direct detection of endogenous metabolites in the human body *in vivo*. Clinically, neurometabolic information provides clinicians and researchers with a powerful tool to evaluate diseases or to perform longitudinal studies of disease progression. Previously, neurometabolite measurements were generally limited to concentration levels in the blood and cerebrospinal fluid (CSF) but these are only an indirect measure of brain levels. Moreover, they cannot be attributed to a particular region of the brain to evaluate localized metabolism or regional pathology (Levy & Degnan, 2013). Neuro-MRS circumvents these challenges and allows quantitative evaluation of metabolic changes associated with disease progression, brain development, brain processes, neurological disorders and drug mediated effects (Mason et al., 2006; Sanacora et al., 2002).

The most commonly studied nuclei with MRS are hydrogen (^{1}H), carbon-13 (^{13}C), phosphorous (^{31}P) and sodium (^{23}Na), of which hydrogen, also called proton (^{1}H) MRS, is most widely used. Typical metabolites of ^{1}H MRS include N-Acetylaspartate (NAA), the choline containing compounds Glycerophosphocholine (GPC) and Phosphocholine (PCh), Phosphocreatine (PCr), creatine (Cr), Myo-Inositol (Ins) and Glutamate (Glu) (De Graaf, 2008). These metabolites can be detected robustly at 3 Tesla (T) field strengths due to the fact that they are present in detectable concentrations in the human brain and their chemical shifts are different enough that they represent distinct peaks in the ^{1}H MRS spectrum at 3T.

Recently, there has been an increasing interest in measuring γ-aminobutyric acid (GABA) levels in the brain (R. A. Edden & Barker, 2007; Near et al., 2012). GABA is the primary inhibitory neurotransmitter in the brain and accounts for almost half of the synaptic activity (Govindaraju et al., 2000). Altered concentrations of GABA have been linked to several neurological disorders such as motor disorders, mood and anxiety disorders, sleep disorders, olfactory, and gustatory disorders (Bigal et al., 2008; Hasler et al., 2007; Levy et al., 2005; Winkelman et al., 2008). At the University of Cape Town (UCT) there has been a long-standing interest in studying learning deficits in children with prenatal alcohol exposure and the ability to measure changes in GABA during

learning tasks – such as motor learning (Floyer-Lea et al., 2006) or eyeblink conditioning (Jacobson et al., 2011) – could provide new insights into the physiological basis of these learning deficits.

In vivo measurement of GABA remains challenging due to all three GABA resonances (two triplets and one quintet) overlapping with macromolecules (MM) and signals from more concentrated metabolites, namely Cr, NAA, and Glu making direct observation impossible especially at magnetic field strengths < 4T (Puts & Edden, 2012). As a result, GABA MRS requires the application of advanced spectral editing techniques, such as MEscher-GArwood (MEGA) point resolved spectroscopy (MEGA-PRESS) and MEGA spin echo full intensity acquired localisation (MEGA-SPECIAL) (Mescher et al., 1998; Near et al., 2011). These spectral editing techniques separate C4-GABA at 3 ppm from other overlapping metabolites. However, successfully suppressing MM at 3 ppm (MM7) is highly dependent upon magnetic field homogeneity, frequency selective pulse duration and editing strategy (De Graaf, 2008), as explained in the next chapter. Therefore most studies acquire GABA without MM suppression, commonly referred to as GABA+ (Mullins et al., 2012). Alternative approaches would be application of two-dimensional MRS methods or spectroscopy at higher field strengths, which is not feasible due to the unavailability of a scanner in South Africa with field strength greater than 3T (Ke et al., 2000; Puts & Edden, 2012; Tkáć & Gruetter, 2005). In this study, we employed single voxel (SV) MEGA-SPECIAL (Near et al., 2011) to acquire GABA without macromolecule (MM) contamination.

1.1 Description of the Problem

GABA acquisitions usually have long scan times (≈10-20 minutes) due to the characteristically low signal to noise ratio (SNR) of GABA, making these acquisitions highly susceptible to subject motion (Puts & Edden, 2012). Besides the long scan time, MEGA, as a difference technique, is even more motion sensitive. Subject motion can cause data to be acquired at the incorrect volume of interest (VOI) and/or induce B_0 inhomogeneity leading to line broadening, spectral distortion, and compromised spectral editing (Drost et al., 2002; Kreis, 2004), thus adversely affecting the already tiny GABA signal (Harris et al., 2013; Zhu et al., 2011). Furthermore, the MM suppression technique depends on magnetic field (B_0) stability. In the presence of B_0 instability suppression is incomplete resulting in GABA contaminated with residual MM.

1.2 Objectives of the Project

The aims of this project were:

1. to insert three dimensional (3D) echo planar imaging (EPI) volumetric navigators into the MEGA-SPECIAL sequence to perform real-time motion and shim correction and compare performance with the standard MEGA-SPECIAL sequence;
2. to apply motion and shim navigated MEGA-SPECIAL to compare reproducibility of GABA using commonly employed analysis software, namely LCModel (Provencher, 2001), jMRUI (Vanhamme et al., 1997) and GANNET (R. A. Edden et al., 2013); and
3. to apply motion and shim navigated MEGA-SPECIAL to determine tissue-specific concentrations of GABA and effects of gender on GABA concentrations.

1.3 Thesis Outline

The thesis presents a novel method to correct B_0 errors and artefacts caused by motion in single voxel spectroscopy (SVS) MEGA-SPECIAL followed by application of the technique to assess reproducibility of GABA measurements, tissue concentrations, and gender effects.

Chapter 2 presents the relevant background of the techniques that were implemented to perform motion and shim correction in MRS, followed by a literature review of GABA MRS.

Chapter 3 describes the implementation of 3D EPI volumetric navigators to perform real-time motion and shim correction for mitigating artefacts caused by motion and B_0 inhomogeneity.

Chapters 4 and 5 describe results from the application of the motion and shim navigated MEGA-SPECIAL sequence to investigate reproducibility and tissue specific concentrations of GABA, as well as gender differences in GABA levels.

Chapter 6 provides a comprehensive discussion, highlighting limitations and considerations for GABA MRS studies.

Chapter 7 presents the conclusions.

Chapter 3 has been accepted for publication in *NMR in Biomedicine*. Work from chapters 3, 4 and 5 have also been accepted for presentation at the 24th Annual Meeting of the International Society for Magnetic Resonance in Medicine (ISMRM) in May 2016. Chapters 4 and 5 have been written as manuscript and will be submitted for publication. Below are the references for the journal article and conference papers:

Saleh MG, Alhamud A, Near J, van der Kouwe AJ, Meintjes EM: **Volumetric navigated MEGA-SPECIAL for real-time motion and shim corrected GABA editing.** NMR Biomed, 29, 248-255.

Saleh MG, Alhamud A, Near J, van der Kouwe AJ, Meintjes EM: **Reproducibility of macromolecule suppressed GABA measurement using motion and shim navigated MEGA-SPECIAL with LCModel, jMRUI and GANNET.** Magnetic Resonance Materials in Physics, Biology and Medicine, *under review*.

Saleh MG, Near J, Alhamud A, du Plessis L, van der Kouwe AJW, Meintjes EM: **Volumetric Navigated MEGA-SPECIAL for real-time zero- and first-order shim and motion corrected GABA MRS.** *Proceedings of 24th Annual Meeting ISMRM: 2016; Singapore.*

Saleh MG, Alhamud A, Near J, Robertson F, van der Kouwe AJW, Meintjes EM: **Reproducibility and gender-related effects on macromolecule suppressed GABA.** *Proceedings of 24th Annual Meeting ISMRM: 2016; Singapore*.

Chapter 2 Literature review

2.1 GABA MRS Sequences

There are several sequences that could be used to acquire GABA spectra but the most common one is the MEGA-PRESS sequence (Mescher et al., 1998; Near et al., 2011; Zhu et al., 2011). In this project, we will be using MEGA-SPECIAL with MM suppression (Near et al., 2011).

2.2 Motion and Shim Correction Techniques

The MEGA-SPECIAL sequence involves four acquisitions making it more motion sensitive than the ubiquitous two-acquisition MEGA-PRESS sequence. Subject motion not only results in measurements from incorrect anatomical regions, but also in B_0 inhomogeneity, leading to signal degradation.

Currently, motion and artefact corrections in MRS data are based on i) retrospective frequency and phase corrections, and (ii) prospective motion and shim correction.

The retrospective corrections are performed using phase and frequency information from metabolites with a large signal (Waddell et al., 2007), such as NAA or Cr, or the whole spectrum (Near et al., 2015) for spectral alignment prior to averaging. This method reduces frequency and phase errors, and subtraction artefacts, however, localization errors and poor signal arising from subject motion and motion-related B_0 changes cannot be corrected retrospectively. Furthermore, this method is dependent on available SNR, which is a limiting factor for GABA editing (Near et al., 2015).

Navigator-based motion tracking methods employ properties of rigid body transformations to subsample k-space in a time efficient manner (Fu et al., 1995; van der Kouwe et al., 2006; Welch et al., 2002) to track motion throughout the scan. MRS is well suited to an imaging navigator because of its long repetition times (typically 1.5-3 s) – most of which allows for signal relaxation and as such is available for navigator acquisition. MRS also benefits greatly from such an imaging navigator due to its lack of anatomical information. One such navigator is PROspective MOtion correction (PROMO, (White et al., 2010)), which uses three orthogonal, low resolution spiral images to register head position to a reference map. Keating et al. integrated PROMO and a water-suppression cycling system into the PRESS sequence for prospective motion correction and retrospective shot to shot frequency and phase correction (Keating et al., 2010). Zaitsev et al. modified the PRESS sequence to integrate an optical tracking system and a frequency navigator for prospective motion correction and retrospective frequency correction, respectively (Zaitsev et al.,

2010). Although these techniques provide efficient motion tracking and correction, adequate MM suppression depends on B_0 stability and real-time frequency correction is needed to maintain the editing pulses symmetrically about 1.7 ppm. Keating et al. implemented a method using PROMO and navigators to correct both motion and linear shim terms in real time (Keating & Ernst, 2012). This method mitigated spectral distortions and maintained spectral quality in the presence of subject motion. To our knowledge, this technique has not been implemented in GABA editing sequences. Hess et al. implemented a pair of echo planar imaging (EPI) volumetric navigators in a single voxel PRESS sequence to correct in real-time both the volume of interest (subject motion) and zero- to first-order changes in B_0 (Hess et al., 2011). The navigator minimally affected the signals of metabolites with high concentration and maintained spectral quality when a subject moved during the scan. EPI volumetric navigators have previously been implemented in GABA+ Magnetic Resonance Spectroscopic Imaging (MRSI) using MEGA Localization by Adiabatic SElective Refocusing (MEGA-LASER) (Bogner et al., 2014). Since GABA+ acquisition does not require MM suppression, it is less sensitive to frequency drift because of the large bandwidth of the non-overlapping spectral edit-on (1.9 ppm) and edit-off (4.7 ppm) pulses. To date, real-time motion and shim correction has not been implemented in SVS J-editing MEGA-SPECIAL. The primary aim of this project was to incorporate EPI volumetric navigators into the MEGA-SPECIAL sequence to correct in real-time for both motion and B_0 inhomogeneity, for the accurate quantification of MM-suppressed GABA.

2.3 Studies on GABA

2.3.1 Reproducibility of GABA

Several studies use GABA+ (GABA+MM) as a substitute for pure MM-suppressed GABA. Previous studies have shown that GABA+ and GABA have weak to no correlation probably due to the problems related with the MM suppression technique. This also suggests that GABA+ is a weak substitute for underlying GABA (Harris et al., 2014; Mikkelsen et al., 2015; Near et al., 2011). Measuring pure GABA has become increasingly important due to its role in several neurological conditions (Bigal et al., 2008; Hasler et al., 2007; Levy et al., 2005; Winkelman et al., 2008). As explained above, measuring pure GABA is, however, challenging due to its dependence on B_0 stability.

GABA+ can be quantified using either tissue water (H_2O) or Cr as internal references (Bai et al., 2014; Bogner et al., 2010; Harris et al., 2014). To date, intra- and inter-subject variability of GABA concentrations have not been investigated using the MEGA-SPECIAL sequence. Therefore, the second aim of this project was to use the motion and shim navigated MEGA-SPECIAL sequence to

examine intra- and inter-subject variability of GABA, referenced to H_2O and Cr, using LCModel (Provencher, 2001), AMARES in jMRUI (Vanhamme et al., 1997) and GANNET (R. A. Edden et al., 2013).

2.3.2 Tissue-specific concentrations of GABA

In the healthy human brain, concentrations of GABA are highly heterogeneous (Rothman et al., 1993). The SVS sequences that are widely used to measure GABA levels typically use large VOI's due to the low SNR of GABA (Puts & Edden, 2012), inevitably including all three tissue types, namely grey matter (GM), white matter (WM) and cerebrospinal fluid (CSF). It is therefore necessary to determine the fractions of each tissue type that is present in the voxel to quantify tissue-specific brain concentrations of GABA. The ratio of GM to WM (GM/WM) concentration of GABA has been quantified across the brain previously using a two dimensional (2D) chemical shift imaging (CSI) sequence (I.-Y. Choi et al., 2006; Jensen et al., 2005). Since GABA is susceptible to B_0 changes, we employed our motion and shim corrected MEGA-SPECIAL sequence to compare here GM/WM concentrations of GABA in anterior cingulate (ACC) and medial parietal (PAR) cortices with reported values.

2.3.3 Gender-related effects on GABA

GABA-based evaluations of neurological conditions usually involve a mixed gender group of healthy controls. Gender-related differences in GABA+ have, however, been demonstrated in dorsolateral prefrontal cortex (DLPFC) and occipital cortex (OCC) (O'Gorman et al., 2011; Sanacora et al., 1999). It is possible that these differences reflect different concentrations of MM between males and females, rather than differences in pure GABA (Harris et al., 2014; Near et al., 2011). Alternatively, GABA may not be stable over time in either or both genders. Therefore, the final aim of this project was to examine gender-related differences in pure MM-suppressed GABA, referenced to H_2O and Cr, in healthy subjects in ACC and PAR.

2.4 Properties of GABA

A typical ^{1}H-MRS spectrum acquired *in vivo* at 3 T in a healthy adult is shown below Figure 2.1. The x-axis depicts the chemical shift in ppm, while the area under the curve for each peak represents the relative concentration of that metabolite.

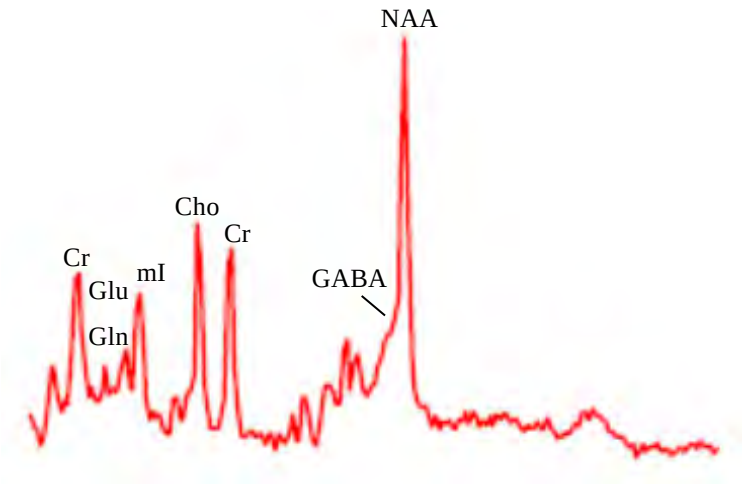

Figure 2.1: ^{1}H spectrum of the human brain acquired at 3T. Peaks correspond to N-acetyl aspartate (NAA), creatine (Cr), choline (Cho), Myo-Inositol (mI) Glutamate (Glu), Glutamine (Gln) and GABA (Hess et al., 2012).

Several brain metabolites contain ^{1}H and thus a wide range of metabolites can be detected through ^{1}H-MRS. Here we will focus only on the role of GABA, which is the main focus of this project.

GABA is an inhibitory neurotransmitter that has a brain concentration of approximately 1 mmol/L. It accounts for almost half of the synaptic activity. Altered GABA concentration are associated with the menstrual cycle (Epperson et al., 2002), alcohol and substance abuse (Behar et al., 1999), as well as numerous neurological and psychiatric disorders, such as sleep disorders, mood and anxiety disorders, motor disorders and panic disorders (Bigal et al., 2008; Goddard et al., 2001; Hasler et al., 2007; Levy et al., 2005; Winkelman et al., 2008). GABA has three methylene (CH_2) groups, giving rise to three different multiplets (Figure 2.2). The GABA-C4 and GABA-C2 triplets (each arising from two neighbouring hydrogen nuclei located on the adjacent methylene group) appear at resonances 3.01 ppm and 2.28 ppm, respectively, while the GABA-C3 quintet (arising from 4 neighbouring hydrogen nuclei on two adjacent methylene groups) appears at 1.89 ppm (Figure 2.2). These multiplets overlap with the resonances of other metabolites that are present in far higher concentrations (Figure 2.1 and Table 2.1). As a result, measurement of GABA requires the use of spectral editing techniques to observe the multiplet centred at 3.01 ppm.

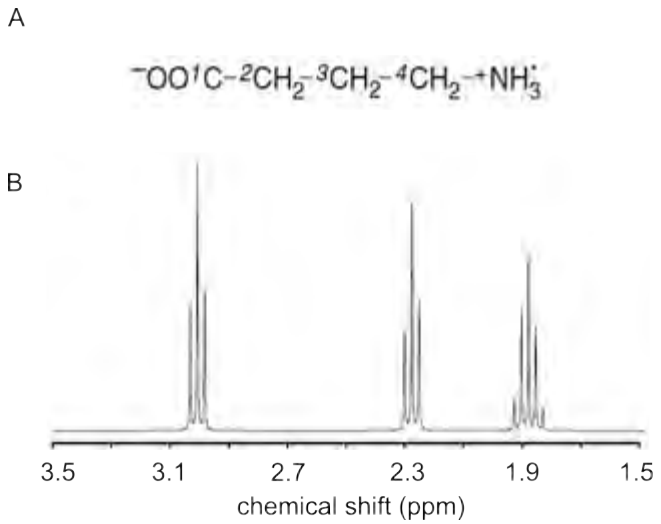

Figure 2.2: GABA A) Chemical structure and B) Simulated spectrum acquired at 300MHz with a line width of 1 Hz (De Graaf, 2008).

Table 2.1: Comparison of the characteristics of NAA and Cr compared to GABA (Levy & Degnan, 2013).

Metabolite Characteristics	Common metabolites (NAA and Cr)	Neurotransmitter (GABA)
Magnitude	Large	Small
Function	Metabolic	Physiologic
Spatial	Regional	Regional

In contrast to the neurotransmitter GABA (Table 2.1), NAA and Cr have much higher signal intensities and are easier to measure. More importantly, GABA reflects brain function, whereas NAA and Cr are more often associated with structural parameters. As such, changes in GABA levels provide useful information when evaluating different neurological disorders and the effect of therapies (Bigal et al., 2008; Levy & Degnan, 2013; Winkelman et al., 2008).

2.5 Critical Components of GABA MRS Acquisition

To achieve unambiguous detection of GABA and perform quantitative and qualitative evaluation, several challenges must be overcome.

2.5.1 Water Suppression

The most abundant compound in human tissue that dominates the MRS spectrum is water centred at 4.7 ppm. In MRS water causes baseline distortions and spurious signals due to vibrational induced signal modulation, as shown in Figure 2.3 (De Graaf, 2008). MEGA-SPECIAL uses frequency selective excitation (VAPOR) and refocusing (such as MEGA) for water suppression.

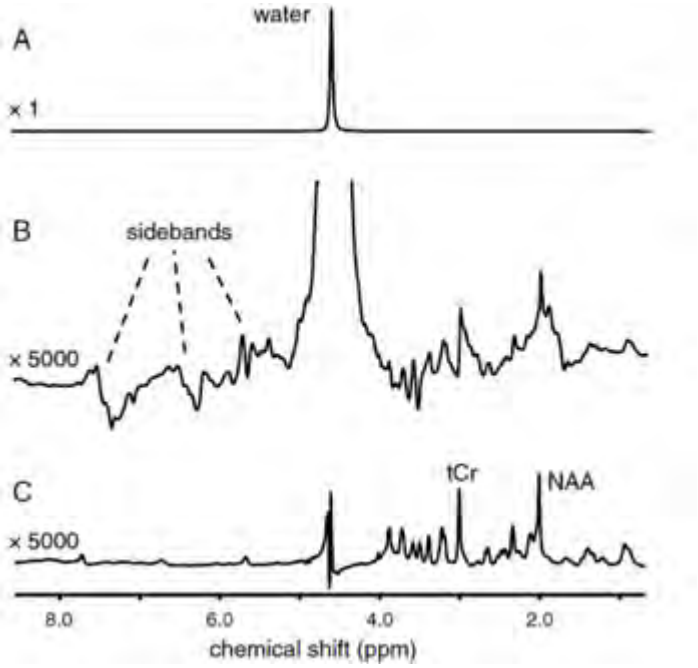

Figure 2.3: A)Water resonance dominates ^{1}H spectrum. B) Vibration induced sidebands of water obscure the metabolite resonances. C) Eradication of water resonance results in a ^{1}H MRS spectrum devoid of artefact, permitting reliable detection and quantification of metabolites (De Graaf, 2008).

2.5.2 Variable Pulse Power and Optimized Relaxation Delays (VAPOR)

Tkáć et al. developed a highly efficient water suppression method called VAPOR that utilizes seven chemical shift selective (CHESS) pulses applied at fixed time intervals followed by crusher gradients interleaved with outer volume saturation modules (Tkáć et al., 1999). The amplitudes of three of the CHESS pulses are 1.78 times greater than the other pulses (Figure 2.4) (Tkáć et al., 1999). Similar to CHESS, VAPOR is applied before localisation. The major advantage of VAPOR is that it is insensitive to variations in the T_1 of water (1 to 2 s) and can be used with a large range of flip angles (65^{o}-125^{o}, Figure 2.4). Signals outside the chemical shift region of 4.65±0.5 ppm are not affected by this scheme.

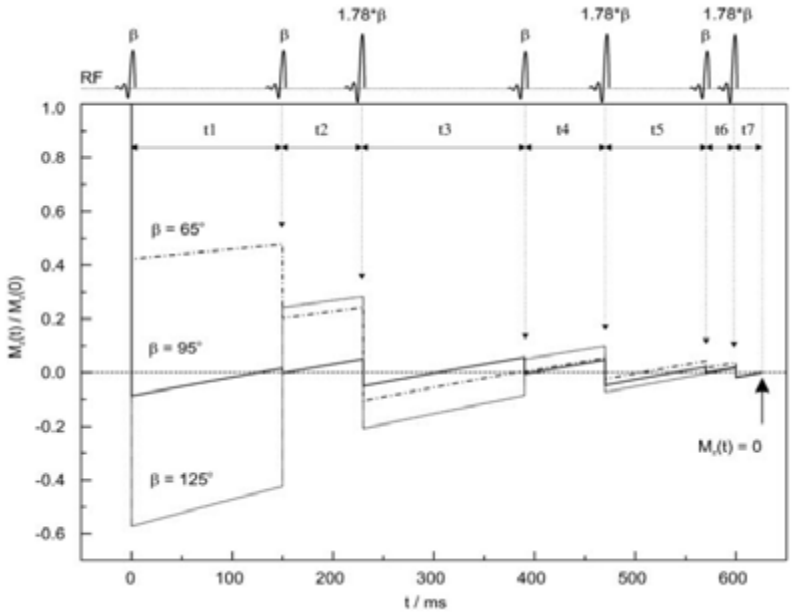

Figure 2.4: Seven CHESS elements with optimized flip angles applied at different times. Evolution of the water M_z for three different RF flip angles (β=65°, 95° and 125°). A water T_1=1.5 ms was used in the calculation (Tkáć et al., 1999).

Furthermore, VAPOR can be applied in clinical scanners without the need for careful RF power adjustment, due to lower sensitivity to applied RF power. This can considerably increase the quality and reliability of clinical MRS (Near et al., 2013; Near et al., 2011; Tkáć et al., 1999).

2.5.3 Mescher Garwood (MEGA) editing

MEGA water suppression is applied after excitation using combinations of RF pulses and magnetic field gradients. Figure 2.5 shows that two frequency selective (s) $180°_{s}$ pulses (at the water frequency) are applied before and after the broadband non-selective (ns) $180°_{ns}$ pulse, each flanked by gradients applied on two different axes (G_1 and G_2). These gradient pairs before and after the non-selective inversion pulse will refocus spins that were unaffected by the selective inversion pulses, while spins (e.g. water ^1H) inverted by the selective inversion pulses will be dephased. The third gradient (G_3) is applied along a different direction and is placed symmetrically on each side of the $180°_{ns}$ pulse which generates the primary Hahn spin echo (Mescher et al., 1996). The major advantages of this method are (1) better tolerance to flip angle errors of the frequency selective pulses relative to other suppression techniques such as WATERGATE (Figure 2.6), (2) no phase distortion of peaks outside the water resonance, (3) avoidance of inter-conversions between M_z and M_{xy}, and (4) it is easy to implement since identical $180°_{s}$ pulses are used (Mescher et al., 1998; Mescher et al., 1996). The only drawback of this technique is that the minimum TE is prolonged, though this does not hinder longer TE acquisitions, such as spectral editing techniques (e.g. TE= 68 ms for GABA). This method is most commonly used in conjunction with the PRESS sequence, known as MEGA-PRESS, for efficient suppression of water and detection of GABA (Mescher et

al., 1998; Mullins et al., 2012). Recently, this technique has been incorporated in the MEGA-SPECIAL sequence, which will be discussed later (Near et al., 2011).

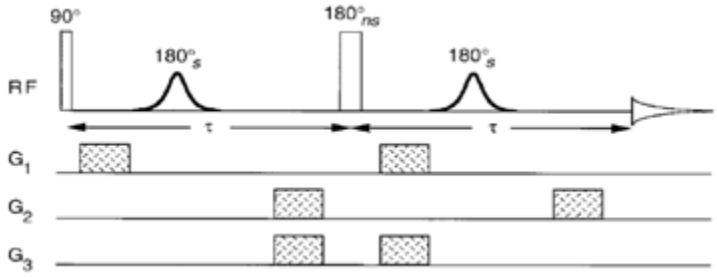

Figure 2.5: MEGA pulse sequence diagram illustrating RF pulses and gradient waveforms (Mescher et al., 1996).

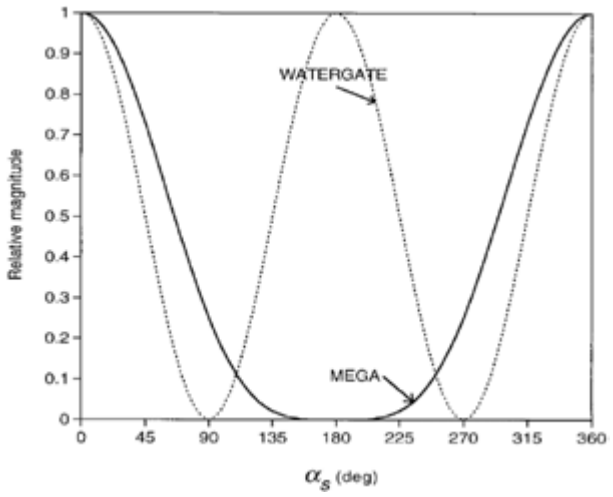

Figure 2.6: MEGA has higher tolerance to errors in the flip angles of the selective pulses (α_s) compared to the WATERGATE water suppression technique(Mescher et al., 1996).

2.6 Spatial Localisation

The two most widely used sequences for GABA MRS are MEGA-PRESS and MEGA-SPECIAL. These sequences use different methods for spatial localisation as described below.

2.6.1 Point Resolved Spectroscopy (PRESS)

The PRESS sequence (Bottomley, 1987) employs the most popular single volume localisation method in spectroscopy. Compared with the Stimulated Echo Acquisition Mode (STEAM), PRESS ensures better metabolite signal to noise ratio (SNR). The PRESS sequence is a double spin echo method, in which a 90°slice-selective pulse is combined with two slice-selective refocusing pulses (De Graaf, 2008). The slice-selective gradients are applied in three mutually orthogonal directions to achieve spatial localisation.

The slice selective 90° pulse (Figure 2.7) will excite only spins in a single slice perpendicular to the x-axis. The first slice selective 180° pulse will only invert spins in a slice perpendicular to the y-axis. As a result, only spins in a column where these two slices intersect will be refocused by this inversion pulse to produce a spin echo at time $2t_1$. Similarly, the second slice selective 180° pulse will only invert spins in a slice perpendicular to the z-axis. Only spins in a cube where all three orthogonal slices intersect will therefore be refocused to produce a spin echo at time $TE=2t_1+2t_2$. The 180^o pulses are flanked by crusher gradients, which are very important to dephase any signals arising from outside the volume of interest (VOI). The timings t_1 and t_2 vary depending on B_1 strength, gradient strength, and slew rate.

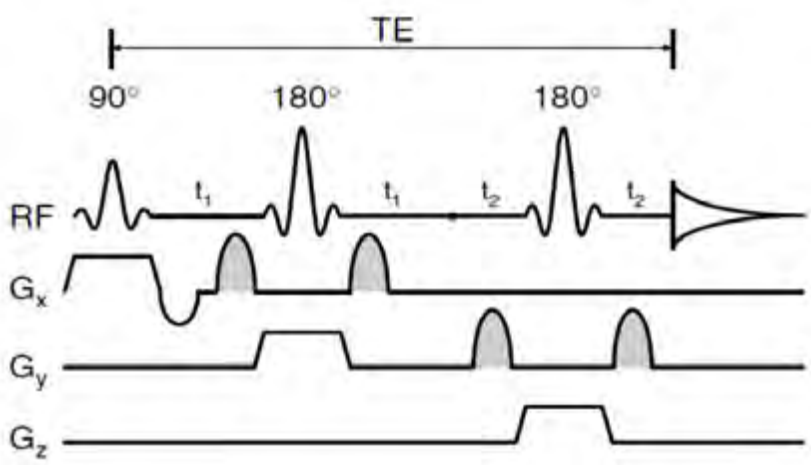

Figure 2.7: PRESS sequence for single volume localisation. G_x, G_y, G_z are gradients applied in the x, y and z directions, respectively. Trapezoidal gradients and semi-elliptical gradients (grey shade) represent slice and crusher gradients, respectively (De Graaf, 2008).

2.6.2 Spin Echo Full Intensity Acquired Localisation (SPECIAL)

The SPECIAL sequence is based on a combination of 1D image-selected *in vivo* spectroscopy (ISIS) and a slice-selective spin echo (SE) sequence (Figure 2.8A). It requires subtraction of two SE acquisitions to localise a VOI. The first SE (SE_1) is generated by a slice-selective 90° excitation pulse followed by a slice-selective 180° refocusing pulse, with the slice perpendicular to the first, which results in a spectrum arising from a column of tissue where the two slices intersect. The second SE (SE_2) acquisition is similar to the first one, but is preceded by a slice-selective 180° inversion pulse that inverts spins in a slice perpendicular to the column from which signal is being generated. The difference between these two spin echo signals will arise only from spins in a cube where the slice of the initial inversion pulse intersects the column from which the signal is being generated (Figure 2.8B) (Mlynárik et al., 2006). The major advantage of this sequence is that shorter TE's are possible (2.2-2.7 ms) because only one refocusing pulse is used (Mlynárik et al., 2006). Spectroscopy sequences with short TE minimize T_2 relaxation effects and facilitate reliable

detection and quantification of many crucial metabolites such as Glu, Gln as well as Glucose (Glc) (Michaelis et al., 1993; Tkáć et al., 1999).

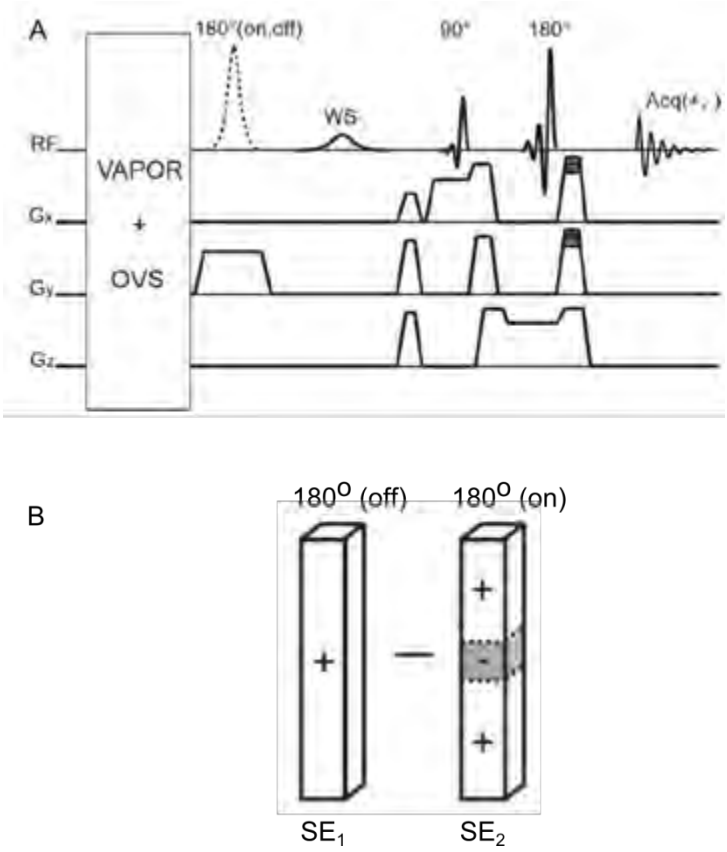

Figure 2.8: SPECIAL localization sequence. A) 180° (on, off) used for inverting spins perpendicular to the original column of tissue. It was added in even scans 180° (on) and removed in odd scans 180° (off). B) Subtraction of two SEs result in signal originating from a voxel. WS is an additional water suppression pulse (Mlynárik et al., 2006).

2.7 Spectral Editing

The ^{1}H-MRS spectrum contains several metabolites (Figure 2.1) in a small chemical shift range leading to considerable spectral overlap, impeding spectral peak assignment and quantification. The most noticeable examples are lactate and GABA. Lactate overlaps with lipids and macromolecules (R. A. Edden et al., 2006), while GABA overlaps with macromolecules, total Cr, NAA and other resonances (Henry et al., 2001). The technique implemented to separate metabolites is called spectral editing. Spectral editing utilizes scalar coupling between spins to separate scalar coupled and uncoupled spins. The information presented below is primarily from (De Graaf, 2008; Govindaraju et al., 2000).

2.7.1 Scalar Coupling Evolution

As shown previously, the splitting of resonances into multiplets can be observed at high resolution. This phenomenon is called scalar coupling or J-coupling. For a simple two-spin (I and S) system, the scalar coupling evolution (θ, Figure 2.9) is given by:

$$\theta = \pi J_{IS} \times \tau$$

where J_{IS} is the coupling constant for the two-spin spin system and τ is the time. For example, if τ=0, θ=0. If $\tau=1/(2J_{IS})$, θ=90°.

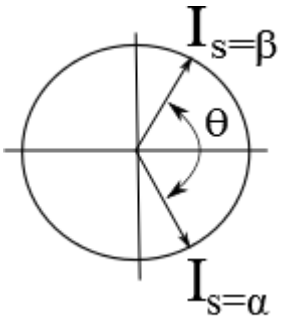

Figure 2.9: Spins undergo scalar evolution, θ, following a 90 degree pulse.

This can be illustrated using a J modulated spin echo experiment (Figure 2.10A). This spin system is characterized by a doublet with frequencies $\nu_I - J_{IS}/2$ and $\nu_I + J_{IS}/2$, resulting from the coupling of I spins with S spins in the lower energy (α) and higher energy (β) spin states, respectively.

Figure 2.10B illustrates the scalar evolution using vector diagrams. Briefly, following excitation, the I spins acquire a TE dependent phase shift θ due to scalar coupling evolution. However, dephasing resulting from magnetic field inhomogeneity and chemical shift is refocussed by the 180° pulse. The non-selective 180°pulse has two major effects on the coherences under investigation: (1) the pulse inverts the phase evolution of the I spins from $\pi(\nu_I \pm J_{IS}/2)$ to $-\pi(\nu_I \pm J_{IS}/2)$, and (2) inverts the S spin population, such that I spins attached to S spins in the α state and resonating at the lower frequency ($\nu_I - J_{IS}/2$) are attached to spins in the β state and accordingly resonate at the higher frequency ($\nu_I + J_{IS}/2$) after the 180° pulse. At TE = $1/2J_{IS}$, the transverse magnetization is in a state of complete antiphase coherence(θ=90°), while at TE = $1/J_{IS}$ it is in a state of complete in-phase coherence (θ=180°) but inverted relative to TE=0 (Figure 2.10C).

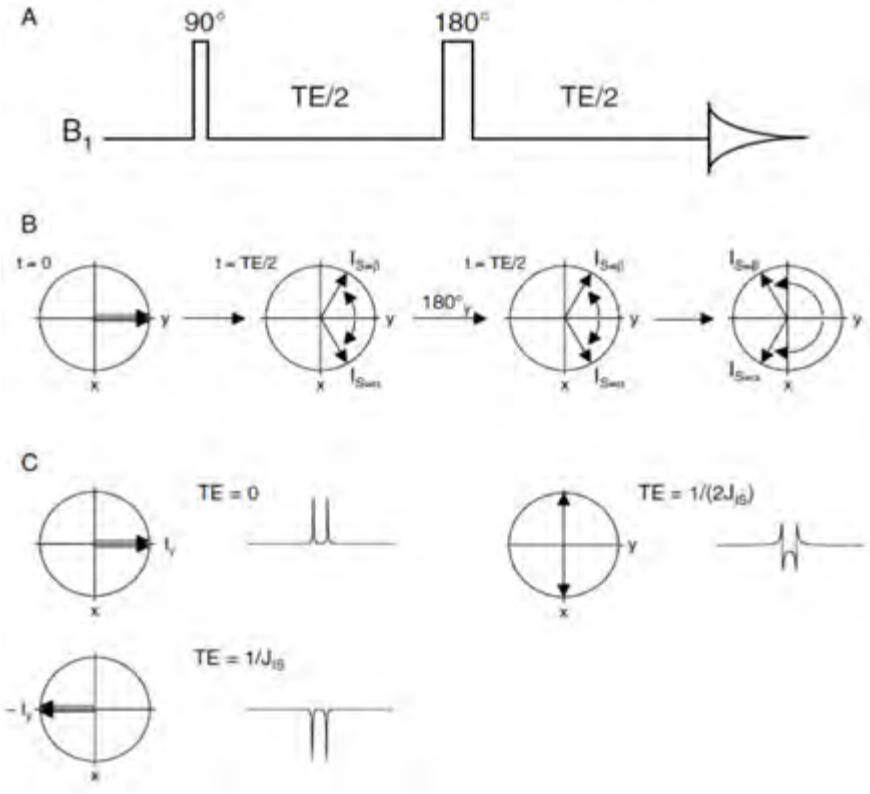

Figure 2.10: Scalar coupling evolutions of the doublet spin system during the spin echo sequence. A) Basic spin echo sequence. B) Acquired TE dependent phase shift of the I spin population. The 180° refocusing pulse inverts the acquired phase and inverts the S spin population. C) Transverse coherences and corresponding MRS spectra of I spins as a function of TE (De Graaf, 2008).

2.7.2 J-Difference Editing

The above spin echo sequence forms the basis for J-difference spectral editing. In the above example (Figure 2.10) a non-selective 180° pulse was used and resulted in a simple spin echo signal. For J-difference editing sequences both non-selective and selective 180° pulses are used (Figure 2.11A).

Following the 90° excitation pulse, I spins acquire a TE dependent phase shift θ due to scalar coupling evolution. A selective 180° ($180°_s$) pulse inverts the S spins, which reverses the direction of rotation of the scalar coupling evolution of the I spins (Figure 2.11B). This means that I spins attached to S spins in the α state and resonating at the lower frequency are attached to S spins in the β state and accordingly resonate at the higher frequency after the $180°_s$ pulse.

The non-selective pulse only refocuses phase evolution that arises from chemical shift and magnetic field inhomogeneity. During the third delay, scalar coupling evolution occurs which will be refocused by a second $180°_s$.

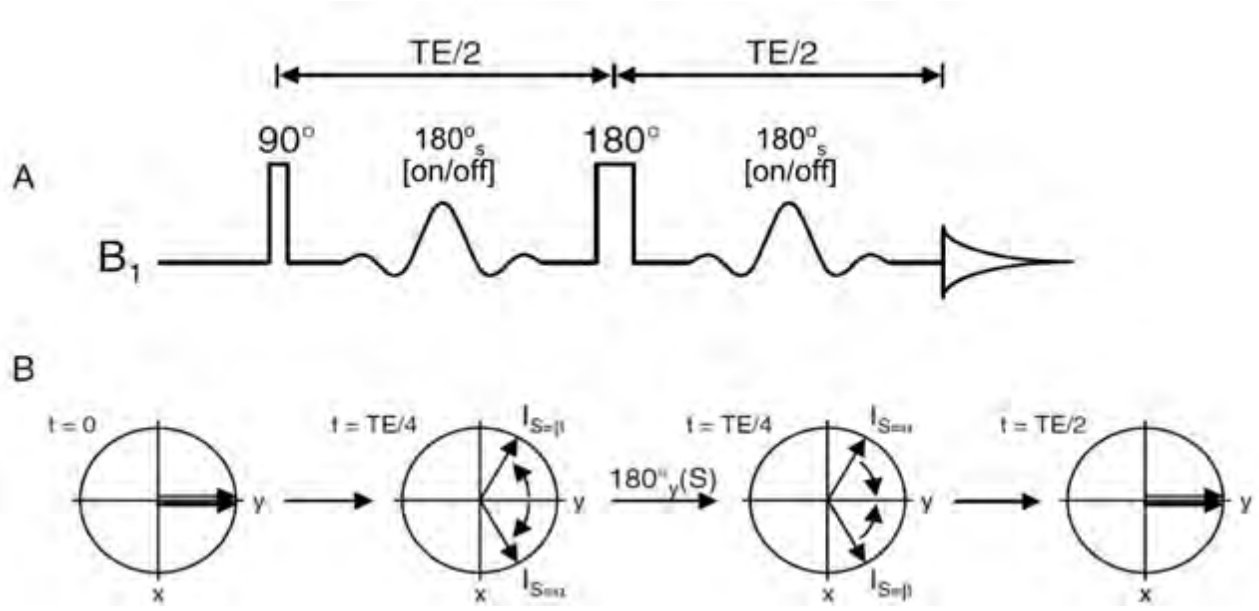

Figure 2.11: A) Basic J-difference editing sequence with both selective and non-selective180^{o} rf pulses. B) I spin population acquired TE dependent phase shift. The 180$^{o}_{s}$refocusing pulse only inverts the S spins causing the direction of rotation to be reversed(De Graaf, 2008).

Water and Cr resonances do not exhibit scalar coupling and thus acquire the same phase in the presence or absence of the 180°$_s$ pulses (Figure 2.12A). In the experiment without the slice selective inversion pulses (Figure 2.10), the phase of the doublet resonance corresponding to the I spins is inverted for TE=1/J_{IS} relative to the uncoupled spins (Figure 2.12B). In contrast, the I spin doublet will have the same phase as the uncoupled spins in the experiment with the slice selective inversion pulses (Figure 2.12C). Subtraction of the two spectra will result in cancellation of signal from the uncoupled spins and selective detection of resonances from the coupled spins (I spins) (Figure 2.12D), while addition will result in elimination of signal from I spins (Figure 2.12E).

Several sequences use the principles of J-difference editing to detect GABA in the human brain (Mescher et al., 1998; Near et al., 2011; Puts & Edden, 2012; Zhu et al., 2011), of which the two primary ones are described below.

2.7.2.1 Mescher -Garwood Point Resolved Spectroscopy (MEGA-PRESS)

The MEGA-PRESS sequence comprises PRESS localisation and MEGA elements for water suppression (Figure 2.13). It is the sequence most commonly used to measure brain concentrations of the inhibitory neurotransmitter GABA. It employs the J-difference editing technique and subtraction of two spectra. For the first (ON), selective frequency pulses are applied to GABA spins at 1.9 ppm, which also affects GABA spins at 3 ppm due to J-coupling between them. In the second non-selective dataset (OFF), non-selective refocusing pulses are applied allowing J-coupling evolution throughout the echo time. The difference between the two datasets will result in a spectrum in which GABA can be detected. Other signals close to and remote from 1.9 ppm are

affected due to the direct effect of the pulse and coupling between spins. The MEGA element requires application of selective refocusing pulses applied at the water resonance before and after the non-selective refocusing pulse. Mescher et al. developed the MEGA-PRESS sequence, which performs GABA editing and water suppression simultaneously by implementing double-banded Gaussian selective 180°$_s$ pulses (Mescher et al., 1998). One band is centred at the resonance frequency of water for water suppression, and the other at 1.9 ppm to refocus the GABA spins at 3.0 ppm as explained above. One important parameter is the TE. The value of TE is determined by the J-coupling between GABA spins at 3.00 and 1.90 ppm, which is 7.3 Hz. Therefore, the TE that would result in inversion of the doublet for the OFF acquisition equals 68 ms.

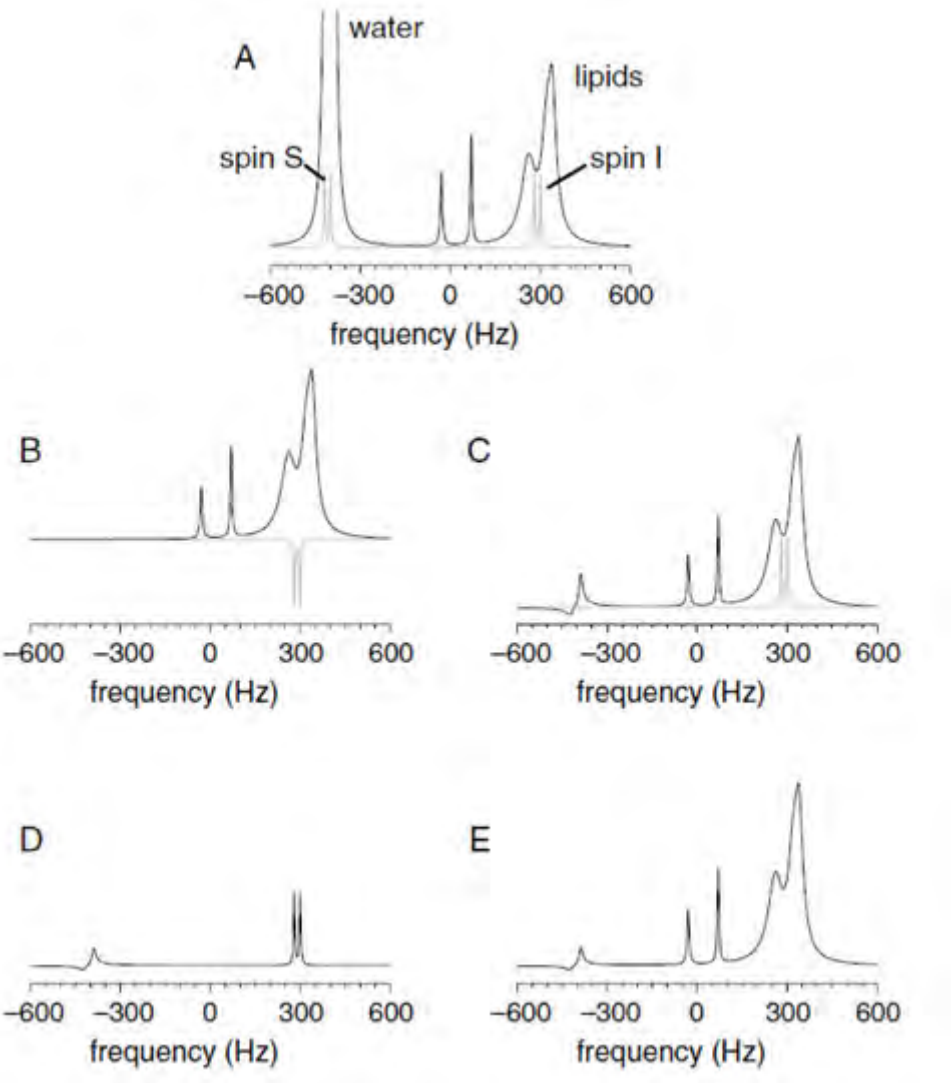

Figure 2.12: Principles of J-difference spectral editing. A) Simulated, non-edited ^{1}H MRS spectrum. Spin I overlaps with lipid resonance making it difficult to detect. B) Non-selective experiment where the phase of the doublet resonance from the I spins is inverted relative to uncoupled resonances. C) Selective experiment where I spins are in phase with uncoupled resonances. D,E) Subtraction and addition of the previous two spectra for selective detection of spin I resonance and removal of spin I, respectively(De Graaf, 2008).

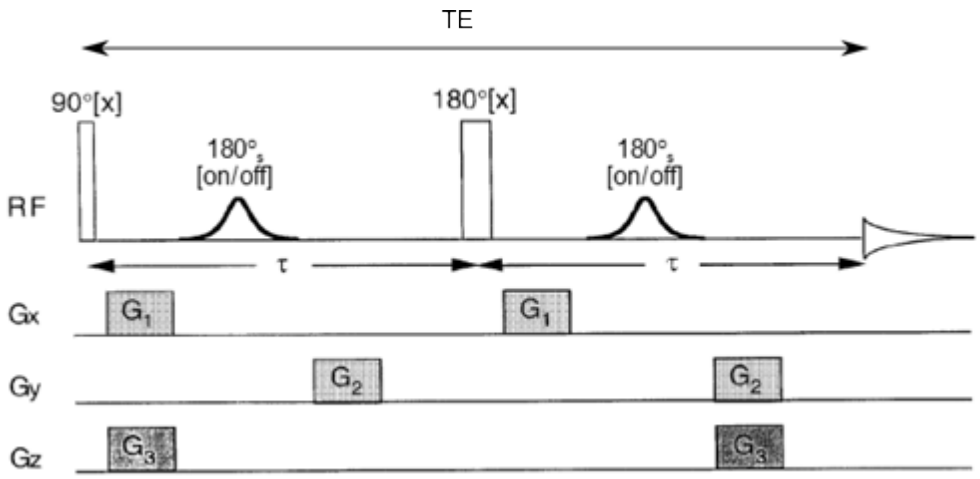

Figure 2.13: MEGA-PRESS sequence. Double banded Gaussian 180^{o}_{s}pulses are used for GABA editing and to suppress water signals. 180^{o}_{s} are flanked by gradients (G_1 and G_2) used to dephase water spins.TE =68 ms for GABA MRS(Mescher et al., 1998).

The MEGA-PRESS sequence has two major drawbacks that can hinder accurate quantitative measurements of GABA. The first drawback is the coediting of macromolecules (MM), which considerably contaminates the edited GABA signal (Rothman et al., 1993). The coedited MM signals appear at 3.0 ppm, which is coupled with the MM at 1.7 ppm, which is close to the GABA-C3 resonance at 1.9 ppm where the spectral editing pulse is applied. Several methods have been developed to avoid contamination of GABA signals. The Henry method involves using selective pulses in both the ON and OFF acquisitions (Henry et al., 2001). In the first acquisition (ON) the selective pulse is applied at the GABA resonance (1.9 ppm), while in the second (OFF) acquisition it is applied at 1.5 ppm, i.e. positioned symmetrically around the MM resonance at 1.7 ppm. The MM peak will be affected equally in both acquisitions so that the subtraction will result in a pure GABA signal devoid of MM. This method has previously successfully been applied at 7T and is highly favoured because it does not require additional scans and is not sensitive to changes in T_1 of MM or metabolites (Terpstra et al., 2002). Also, accuracy is increased by up to a factor of 2 (Henry et al., 2001). However, due to narrow spectral dispersion at 3T, the editing pulse exhibits reduced spectral selectivity, rendering it very challenging to implement the Henry method.

The second drawback is chemical shift displacement of slice-selective localisation pulses in the PRESS sequence that causes the scalar evolution of the GABA-C4 multiplet to be highly spatially dependent (Figure 2.14) (R. A. Edden & Barker, 2007). This results in substantial loss of the GABA signal (see regions II and IV in Figure 2.14C) due to reduced spectral editing efficiency and inaccurate GABA quantification.

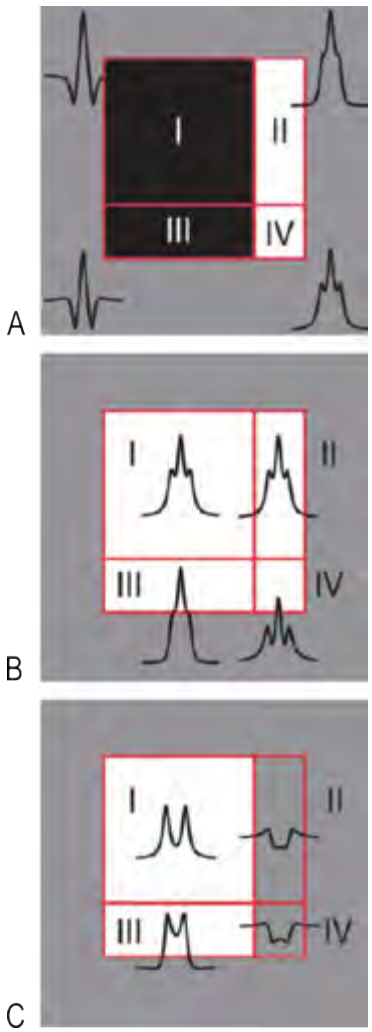

Figure 2.14: Regional modulation patterns of GABA signal in the voxel (80 x 80 mm). A) Editing pulses on. B) Editing pulses off. C) The difference between A and B. I, II, III, IV are subdivisions of the voxel illustrating variation of GABA signal due to spatial variation of scalar coupling. Subdivisions II and IV show total loss of GABA signal (R. A. Edden & Barker, 2007).

2.7.2.2 Mescher-Garwood Spin Echo Full Intensity Acquired Localized (MEGA-SPECIAL)

MEGA-SPECIAL uses SPECIAL localisation and MEGA elements for detection and measurement of GABA. Near et al. developed this sequence which comprises much longer and more frequency selective editing pulses than MEGA-PRESS, thus permitting the use of Henry's method to remove MM contamination when sufficiently narrow bandwidth editing pulses could not otherwise be achieved (Near et al., 2011).

As explained above, Henry's method requires application of editing pulses at resonances of 1.9 ppm (ON) (GABA-C3) and 1.5 ppm (OFF), respectively. The difference between the resonances is approximately 51 Hz at 3T. The OFF acquisition should not affect the GABA-C3 resonance; thus the spins at 51 Hz from the centre of the editing band should experience less than 1% inversion. Therefore, the editing pulse should have a Half Width 1% Maximum (HW1%M) of less than 51 Hz.

In MEGA-PRESS, the two slice refocusing pulses must be applied within the TE of 68 ms. Consequently, the approximate duration of each editing pulse is limited to between 14 and 20 ms (R. A. Edden & Barker, 2007; Mescher et al., 1998). Such short durations result in very broad bandwidths with HW1%M of 88 Hz and 61 Hz, respectively, assuming a time-bandwidth product of 1.128, which fails to satisfy the aforementioned HW1%M requirement for application of Henry's method (Near et al., 2011).

However, the MEGA-SPECIAL sequence has only one slice refocusing pulse within the TE of 68 ms, allowing longer editing pulses to be implemented in the sequence. The duration of the editing pulses in the sequence is about 26 ms, resulting in much narrower inversion profiles with HW1%M of 47 Hz, which fulfils the spectral selectivity requirement. Thus MEGA-SPECIAL is compatible with Henry's method.

Figure 2.15A, B and C shows the simulated spectra for two regions in a voxel for MEGA-SPECIAL and demonstrate reduced spatial variations within the VOI compared to the MEGA-PRESS sequence (Figure 2.14). Remarkably, almost perfect cancellation of the GABA-C4 signal occurs in region II as a result of temporal symmetry of the MEGA-SPECIAL sequence (Near et al., 2011). Figure 2.16 shows that MEGA-SPECIAL yields a 10% improvement in editing efficiency of GABA-C4 at 3 ppm compared to MEGA-PRESS. This is in part due to the increased amplitude of the central line of the GABA-C4 triplet.

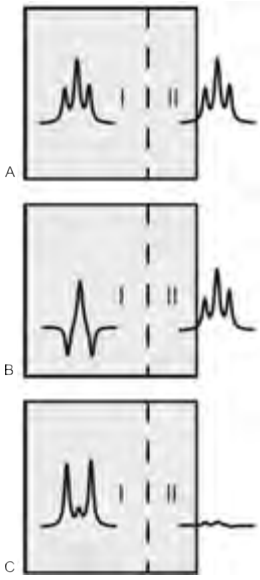

Figure 2.15: Regional modulation patterns of the GABA signal in the voxel. A) Editing pulses on. B) Editing pulses off. C) The difference between A and B. I, II are subdivisions of the voxel illustrating variation of GABA signal due to spatial variation of scalar coupling (Near et al., 2011).

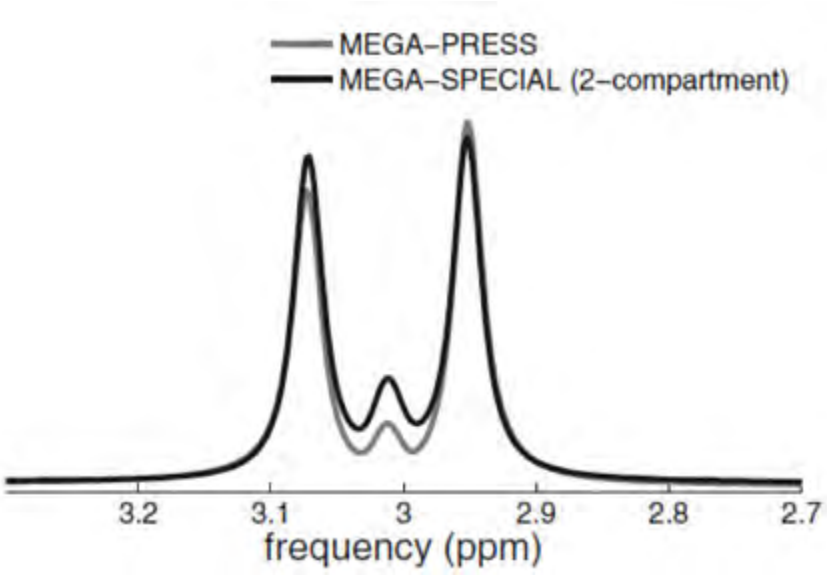

Figure 2.16: Integration of the area under the curves indicates that MEGA-SPECIAL yields 10% improvement in editing efficiency over MEGA-PRESS (Near et al., 2011).

Chapter 3 Volumetric navigated MEGA-SPECIAL for real-time motion and shim corrected GABA editing[1]

Muhammad G. Saleh[2], A. Alhamud[2], Jamie Near[3], André J.W. van der Kouwe[4], and Ernesta M. Meintjes[2]

3.1 ABSTRACT

MEGA-editing with SPECIAL localization (MSpc) is a technique to acquire γ-aminobutyric acid (GABA) without macromolecule (MM) contamination at TE of 68 ms. However, due to the requirement of multiple shot-localization, it is often susceptible to subject motion and B_0 inhomogeneity. A method is presented for real-time motion and shim correction (ShMoCo) using volumetric navigators to correct for motion and motion-related B_0 inhomogeneity during MSpc acquisition. A phantom experiment demonstrates that ShMoCo restores the GABA peak and improves spectral quality in the presence of motion, zero- and first-order shim changes. The ShMoCo scans were validated in 3 subjects who performed up-down and left-right head rotations. Qualitative assessment of these scans indicates effective reduction of subtraction artefacts and well edited GABA peaks, while quantitative analysis indicates superior fitting and spectral quality relative to scans with no correction.

3.2 INTRODUCTION

γ-aminobutyric acid (GABA) is the primary inhibitory neurotransmitter in the brain and accounts for almost half of the synaptic activity (Govindaraju et al., 2000). Altered concentrations of GABA have been linked to several neurological conditions (Levy & Degnan, 2013). *In vivo* measurements of GABA are acquired through the spectral editing methods, which enable separation of C4-GABA with overlapping resonances of creatine (Cr) and Phosphocreatine (PCr). MEGA-SPECIAL (MSpc) is a magnetic resonance spectroscopy (MRS) sequence comprising longer frequency selective editing pulses, allowing GABA acquisition without macromolecule (MM) at TE of 68 ms (Near et al., 2011). Unlike the MEGA-PRESS (Mescher et al., 1998), MEGA-LASER (Bogner et al., 2014) and MEGA-sLASER (Andreychenko et al., 2012) sequences, MSpc requires four acquisitions per

[1] Published in NMR in Biomedicine and reproduced with the permission from John Wiley & Sons Ltd
[2] University of Cape Town
[3] McGill University
[4] Massachusetts General Hospital, Harvard Medical School

localized edited spectrum, rendering it more sensitive to subject motion and magnetic field (B_0) inhomogeneity.

Subject motion can cause data to be acquired from an unintended volume of interest (VOI) and induce B_0 inhomogeneity leading to spectral distortion, thus adversely affecting the already tiny GABA signal (Harris et al., 2013; Zhu et al., 2011). Currently, motion and artefact corrections in GABA MRS data are based on retrospective corrections (Near et al., 2015; Waddell et al., 2007), and prospective corrections using water-based navigators (Bhattacharyya et al., 2007; Zhu et al., 2011). However, the prospective techniques are only able to correct for the change in B_0inhomogeneity.

Prospective correction has been implemented previously by Zaitsev et al. (Zaitsev et al., 2010) using an optical system for prospective motion correction and interleaved navigator for retrospective frequency correction. Although this technique provides efficient motion tracking and correction, the MM-suppression technique is highly dependent on B_0 field stability, necessitating real-time frequency updates to ensure frequency selective pulses are applied symmetrically about 1.7 ppm (Near et al., 2011). Keating et al. (Keating & Ernst, 2012) implemented PROMO and real-time linear shim terms correction using interleaved navigator echoes. This technique mitigated spectral distortions and maintained spectral quality in the presence of large motion. To our knowledge, this technique has not been implemented in J-editing single voxel spectroscopy (SVS) sequences.

There are several navigator-based motion tracking techniques that employ k-space properties of rigid body transformations to subsample k-space in a time efficient manner (Fu et al., 1995; van der Kouwe et al., 2006; Welch et al., 2002). GABA MRS is well suited to an imaging navigator because of its long repetition times (typically 2.5-3.5 s) (Andreychenko et al., 2012) and absence of intrinsically acquired structural images. Most of the repetition time is spent waiting for signal relaxation, and this time is available for navigator acquisitions at no cost to total acquisition time. This has been demonstrated by Hess et al. (Hess et al., 2011) who implemented volume navigators in the SVS point resolved spectroscopy (PRESS) sequence to correct in real-time for both VOI changes arising from motion and zero- to first-order B_0 inhomogeneity.

To date no real-time motion and shim correction (ShMoCo) has been incorporated into the J-editing SVS MSpc sequence for MM-suppressed GABA acquisition. Therefore, the purpose of this work was to incorporate the echo planar imaging (EPI) volume navigator into the J-editing SVS MSpc sequence to correct in real-time VOI changes, zero- and first-order B_0 inhomogeneity arising from

motion. Phantom and in vivo scans were performed to demonstrate that the vNav affects the signal minimally and maintains spectral quality in the presence of motion.

3.3 METHODS

All protocols and experiments were approved by the Human Research Ethics Committee of the Faculty of Health Sciences at the University of Cape Town and written informed consent was obtained from all subjects. All MRI/MRS experiments were performed on a Siemens Allegra 3 T scanner (Erlangen, Germany) using a single channel transmit/receive (T/R) volumetric coil.

3.3.1 MEGA-SPECIAL sequence

The MM-suppressed MSpc sequence was used for editing C4-GABA without MM contamination (Near et al., 2011). Briefly, the sequence consists of two iterations: In the first MEGA-editing iteration the editing-band is applied to the C3-GABAresonance at 1.9 ppm (edit-on), while in the second iteration the editing-band is applied at 1.5 ppm (edit-off). The water suppression band of the dual-banded editing pulses was always applied at 4.7 ppm.

One complete cycle of the MSpc sequence consists of four acquisitions: A) inversion-on, edit-on B) inversion-off, edit-on C) inversion-on, edit-off D) inversion-off, edit-off. Therefore, the final GABA spectrum is obtained by subtracting the acquisitions: GABA= A – B – (C – D). Prior to excitation, outer volume suppression (OVS) and VAPOR water suppression (Tkáć et al., 1999) pulses are applied to saturate spins outside the VOI and to improve water suppression.

3.3.2 Motion and Shim correction in the MEGA-SPECIAL sequence

To measure and correct simultaneously in real-time for head position and magnetic field inhomogeneity (shimming), two volume navigators (vNavs) with different echo times were inserted in the recovery time of each TR of the standard MSpc sequence. The vNav protocol was as follows: 3D encoded EPI, 32 x 32 x 28, flip angle 2°, TR 16 ms, TE 6.6/9 ms (ΔTE 2.4 ms for fat in-phase at 3 T). The two echoes were interleaved to minimize the effect of motion on the field map during the total navigator time of 928 ms.

Following the acquisition of the vNav, motion estimation was performed using Prospective Acquisition Correction (PACE) (Thesen et al., 2000), where magnitude images of the first navigator were used as reference for subsequent vNavs. The estimated motion parameters were applied to the MSpc to track subject motion in real time. A field map was reconstructed from the phase difference images of each pair of navigators with different TEs. The field map was masked using the navigator magnitudes images and the phase was unwrapped using PRELUDE (Jenkinson, 2003). The VOI for the MEGA-SPECIAL acquisition is smaller than the VOI for the navigator, which has to cover the

whole brain for accurate motion tracking. Multiple regression was applied to estimate shim parameters separately for the MEGA-SPECIAL VOI and the navigator VOI.

The real-time shim estimates were applied each TR starting after the first preparation scan, while the pose estimates were calculated and applied from the second TR to allow the shim to stabilize. These estimates were applied synchronously and immediately after the vNav block (but before the water suppression pulses) to all gradients and RF pulses, including the localization, MEGA-editing, OVS and VAPOR pulses.

3.3.3 *In vitro* validation

3.3.3.1 Phantom preparation

A spherical phantom with an inner cube (length 5 cm) aligned with the magnet isocentre was used to assess spectral quality in the presence of motion and shim changes. The fluid in the outer portion of the phantom (blue square, Figure 3.1) consisted of an aqueous solution of GABA, creatine (Cr), N-acetylaspartate (NAA) and Glutamate (Glu) in equal concentrations of 10 mM, and adjusted to pH 7.2. Similarly, the inner cube (red square, Figure 3.1) contained the same metabolites but without Glu.

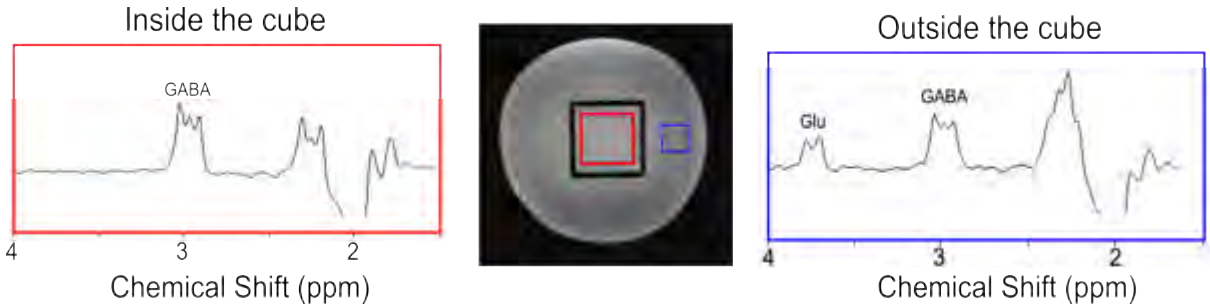

Figure 3.1: Axial image of the spherical phantom with an inner cube at the centre of the phantom used for testing performance of the vNav during motion. Red (inside the cube) and blue squares represent voxel localization and their corresponding spectra. The spectrum from the outside of the cube depicts presence of Glu at 3.75 ppm. The spectra were apodized using 5 Hz Lorentzian filter.

3.3.3.2 *In vitro* acquisition

In vitro GABA edited spectra were acquired with standard MSpc (reference) and vNavMSpc sequences from a voxel positioned in the cube. The vNavMSpc sequence included feedback from vNav for shim and motion correction (ShMoCo), and without feedback for no correction (NoCo).

Acquisitions were performed for each of the following conditions: A) static with no manual frequency or shim offsets, B) frequency (zero-order) offset by 15 Hz, C) first-order linear shim offset by 10 μT/m, D) zero- and first-order shims offset by 15 Hz and 10 μT/m, respectively, and E) a scan with intentional motion and optimal shim values.

The static scans (A) using standard MSpc and vNavMSpc with NoCo sequences were carried out thrice to quantify the mean effect of the navigator on the final edited spectra. The B, C, D and E scans were conducted to determine the efficacy of the vNav in the presence of shim instability and motion. For scans B to D, the offset values were manually added to the optimal shim values before the start of the scans to mimic typical system instabilities during a 10 minute *in vivo* MRS scan (Harris et al., 2013; Hess et al., 2011). For the motion scan (E), the phantom was placed on an MR compatible and rotatable rig to rotate the phantom from the fifth TR over multiple TRs to a total of 7^{o}.

The acquisition parameters were as follows: TR/TE 4000/68 ms, VOI 4 x 4 x 4 cm^3, bandwidth 2000 Hz, 16 averages, 2048 readout points and four dummy scans. Optimal shim values were obtained prior to the start of the initial scan using the vendor-provided shim tool; the resulting average water full width half maximum (FWHM) linewidth was 2 Hz. The number of averages for motion scan (E) was increased to 48. Finally, water unsuppressed data were acquired.

3.3.4 *In vivo* validation

3.3.4.1 Subject preparation

The *in vivo* acquisitions were performed in the medial-parietal region (Puts et al., 2013) in three volunteers. Four scans were acquired using the vNavMSpc sequence in each subject as follows: i) reference (no intentional motion) with NoCo, ii) reference (no intentional motion) with ShMoCo, iii) motion with ShMoCo, and iv) motion with NoCo. The last two acquisitions involved voluntary motion in which subjects were trained to rotate their head left-right by about 6° and up-down by about 5°. These rotations also resulted in translations of about 4 mm. Subjects performed these motions upon receiving audio cues. After every data acquisition involving motion, subjects were instructed to return to their original positions. All subjects were trained and instructed on how to move before the experiments.

3.3.4.2 *In vivo* acquisition

Prior to the 4 vNavMSpc scans, three-dimensional (3D) T1-weighted sagittal images of the subjects' brains were acquired using MEMPRAGE (van der Kouwe et al., 2008) and were re-sliced for accurate voxel placement. Parameters for vNavMSpc were similar to *in vitro* acquisition, except for VOI 3 x 3 x 3 cm^3 and 148 averages. The long TR was necessary to reduce the specific absorption rate effects due to strong outer volume suppression (OVS) pulses. Previous *in vivo* study has demonstrated that increasing TR up to 4 s leads to increase in GABA signal by 20 to 30 % (Puts et al., 2013). Moreover, effective acquisition of GABA has been established at TR of 4s (Andreychenko et al., 2012). Finally, water unsuppressed data with eight averages were acquired.

3.3.5 Post-processing and analysis

Data were analysed using the Gannet 2.0 toolkit, a tool for analysing only MEGA-PRESS data (R. A. Edden et al., 2013). Therefore, the following steps were implemented for post-processing MSpc data for non-linear fitting through the GannetFit module of Gannet.

3.3.5.1 Post-processing

The motion corrupted edit-on/off spectra were removed by first calculating the 'unlikeness metrics' for each individual scan through subtracting the scan from the mean of all scans to obtain a difference spectrum, followed by the computation of the root-mean square of all the spectral points in this spectrum. Scans with unlikeness metric of 2.5 standard deviations (SD) above the average were considered to have been corrupted and were removed. The value was derived from the reference scans with no voluntary motion and we found that the SD value of 2.5 was fairly effective at removing outlier averages without removing uncorrupted averages and did not result in substantial loss of SNR. A similar value (SD =2.6) has been reported in a previous study (Near et al., 2013). On average 8 edit on/off spectra were removed from NoCo and ShMoCo scans. This was followed by frequency and phase correction (Klose, 1990; Near et al., 2015), apodization using a 5-Hz Lorentzian filter and zero padding by a factor of 16. Finally, the fully processed edit-on/off scans were subtracted to generate GABA-edited spectra.

3.3.5.2 Analysis

The GannetFit module uses a single Gaussian model with a linear baseline to fit the edited GABA signal between 2.8-3.5 ppm and Cr signal from the edit-off scan from 2.72-3.12 ppm. From the fit, GABA FWHM (expressed as ppm), fitting error (FitErr), SNR and GABA/Cr ratio were estimated, as described previously (R. A. Edden et al., 2013) i.e. GABA/Cr ratio was estimated as the ratio of the signal integrals of GABA and Cr. Due to variations of peak amplitude in the presence of motion, GABA FitErr was defined as the SD of the fitting residual normalised to the average amplitude of GABA in the NoCo reference scan. SNR was computed in the frequency domain as the GABA amplitude divided by the SD of the fitting residual.

The static *in vitro* edited spectra acquired by standard MSpc and vNavMSpc with NoCo sequences were quantified to determine the effect of the navigator on the final edited GABA peaks. For this, an additional 5-Hz line broadening was applied to the *in vitro* data to be consistent with the *in vivo* data (Puts et al., 2013), followed by the estimation of GABA/Cr ratio and FWHM using GannetFit module.

Visual assessment of the spectra was the index for qualitative analysis to identify subtraction artefacts, line-broadening and baseline distortions. The parameters FWHM, FitErr, SNR and

GABA/Cr were indices for quantitative analysis. These indices are frequently applied to gauge spectral quality (Bhattacharyya et al., 2007; Keating & Ernst, 2012), and for our study, to determine the efficacy of volume navigators to recover spectra in the presence of motion. All spectra are compared to reference scans and all values are expressed as mean ± standard error of mean (SEM).

3.4 RESULTS

3.4.1 *In vitro* validation

The static scans acquired using the standard MSpc (reference) and vNavMSpc sequences produced similarly excellent quality and fully resolved edited spectra (Figure 3.2A). The parameters derived from standard MSpc (GABA/Cr: 0.125 ± 0.002, FWHM: 0.147 ± 0.001) and vNavMspc with NoCo (GABA/Cr: 0.128 ± 0.002; FWHM: 0.147 ± 0.001 ppm) sequences were similar.

For the vNavMSpc with NoCo acquisitions, the manually applied zero-order shim offset led to a distorted and inverted C4-GABA peak and slightly noisy baseline (Figure 3.2B), while manually applied first-order shim offset caused substantial GABA peak degradation and NAA line broadening (Figure 3.2C: arrows 1 and 2). The combination of zero- and first-order shim offsets affected the NoCo scan in a similar manner to the first-order shim offset, resulting in a loss of the pseudo-doublet pattern (Near et al., 2012) of the GABA peak (Figure 3.2D: arrow 3). The corresponding ShMoCo scans adjusted the shim offsets, improved the quality of the spectra and compare favourably with the reference scan. The 7^{o} rotation caused distortion of the GABA peak (Figure 3.2E: arrow 4), so that the multiplet could not be resolved. The ShMoCo scan improved spectral quality, but the pseudo-doublet pattern of GABA was less prominent relative to the static scans.

3.4.2 *In vivo* validation

Although subjects were fairly successful in remaining still throughout the reference scans with average translations of -0.04 ± 0.01 mm and rotations of -0.08 ± 0.06 degrees, these minor changes led to uncorrected shim changes in the NoCo scans. For the scans involving intentional motion, subjects moved as instructed according to a pre-defined schedule.

Figure 3.3 shows edited spectra from NoCo and ShMoCo scans, acquired with and without intentional motion, and GABA fitting overlaid over the reference scans to demonstrate the fitting quality. The edited spectra from the NoCo and ShMoCo reference scans have comparable and excellent spectral quality. The motion scans with NoCo demonstrate different effects of motion on the edited spectra. Subject 1 shows a distorted and broadened GABA peak and slanted baseline between about 2.2 and 3 ppm. Subject 2 exhibits subtraction artefact and elevated GABA

amplitude, which is also evident in subject 3. In subject 3, motion was not large enough to substantially degrade edit-off spectral quality, but the NoCo edit-on spectrum of the third subject shows insufficient suppression of the NAA peak. The ShMoCo scans reduced the artefacts substantially and compare favourably with reference scans.

The artefacts in subject 1's edited spectrum are substantial relative to the other two subjects' edited spectra, originating from baseline distortions and line-broadening in edit-on/off scans (Figure 3.3: Artefact A) due to larger head motions (up-down 4.0° versus 3.1° ± 0.0°, left-right: 4.5° versus 3.0° ± 0.0°) relative to the other two subjects. The resulting absolute first order-shim changes ($\sqrt{(\Delta Gx)^2 + (\Delta Gy)^2 + (\Delta Gz)^2}$), derived from maximum shim changes in G_x, G_y, and G_z, from subject 1 were larger relative to the other two subjects during up-down (5.8 versus 3.6 ± 0.7 μT/m) and left-right (3.6 versus 2.9 ± 0.0 μT/m) rotations. These distortions are attributable primarily to distortions along the Y-axis (perpendicular to coronal plane (G_y): up-down: 5.2 versus 3.3 ± 0.8 μT/m; left-right: 2.4 versus 1.4 ± 0.0).

The quantitative parameters for the three subjects are presented in Figure 3.4. Although the NoCo and ShMoCo reference scans without intentional motion show similar results, NoCo scans have slightly larger standard errors in FitErr (±0.81 versus ±0.31) and SNR (±3.2 versus ±1.68) than ShMoCo scans. NoCo motion scans show increases in all parameters (FWHM: 0.25 ± 0.12 ppm; FitErr: 15.22 ± 2.43; SNR: 15.31 ± 5.53; GABA/Cr: 0.22 ± 0.17), while ShMoCo recovers the data yielding values similar to the reference values (FWHM: 0.13 ± 0.01 ppm; FitErr: 9.98 ± 1.92; SNR: 10.42 ± 2.01; GABA/Cr: 0.037 ± 0.01).

3.5 DISCUSSION

In this work, we implemented a pair of 3D EPI vNav in the J-editing SVS MSpc sequence to correct in real-time changes in VOI localisation due to motion and zero- to first-order shim terms. Firstly, we investigated in a phantom whether (i) the presence of vNav in the sequence affect the GABA signal. Secondly, the accuracy of the vNav in measuring and correcting changes in position and B_0.

The static scans acquired using the standard MSpc and vNavMSpc sequences show excellent agreement and well-resolved GABA peaks. The vNavMSpc with NoCo scan revealed that the inclusion of the navigator had minimal effect on the edited spectrum. Applying zero- and first-order shim offsets led to distortion, line-broadening and depreciated peaks in the NoCo scans (arrows 1-4; Figure 3.2B, C and D), while ShMoCo scans compare favourably with the reference scans. Our data suggest that broadening of peaks and loss of the GABA multiplet structure arise largely due to changes in the first-order shim terms, while frequency drift appears to cause subtraction artefacts.

Keating et al. and Zhu et al. demonstrated that suboptimal shim terms led to broadened metabolite peaks (Keating & Ernst, 2012) and unresolved GABA peaks at the peripheral voxels (Zhu et al., 2011). Harris et al., demonstrated altered GABA peaks in the presence of frequency drifts (Harris et al., 2013). Future research to assess the effect of individual shim terms on the GABA spectrum will be valuable.

The 7^{o} rotation was chosen to mimic *in vivo* motion without introducing Glu signal from outside the inner cube. This level of motion was enough to cause substantial shim changes as demonstrated by the poor spectral quality in the NoCo scan, which were largely recovered by the ShMoCo scan (Figure 3.2E). Small differences relative to static scans remain, similar to those reported previously in GABA spectra acquired using real-time motion and shim corrected adiabatic spiral MRSI (Bogner et al., 2014). In our study this may be due to fluid flow induced by the displacement of the phantom.

In our study, we acquired C4-GABA without MM – a loss of about 50% of the total GABA+ (GABA+MM) signal (Near et al., 2011) – with VOI dimensions and scan duration of 27 ml and 10 minutes, respectively. This resulted in sufficient SNR for detection and quantification of the metabolite (Figure 3.3 and Figure 3.4). The fitting quality (FitErr) of the reference scans in our study are relatively larger than reported values (approximately 5.6 %) from similar location and dimensions of VOI (Bai et al., 2014). This is due to reduction in peak amplitude in the absence of MM while the fitting residuals remain the same (Harris et al., 2014). The FWHM of the reference scans are similar indicating comparable spectral quality.

The edited spectra were sensitive to motion and were adversely affected during the NoCo scans. Subject 1's larger head motion resulted in significant distortions in the edit-on/off scans, which were translated to the edited spectrum (Figure 3.3). Similar effects of large motion have been demonstrated in previous studies (Hess et al., 2011; Keating & Ernst, 2012), including baseline distortions and line-broadening in the final spectra largely attributable to shim changes along Y-axis. The remaining subjects revealed subtraction artefacts and increases in peak amplitude (Figure 3.3). These errors also led to lower fitting quality, line broadening and overestimation of the GABA/Cr ratio (Figure 3.4A, C and D). The SNR from the NoCo scan (with motion) is higher relative to reference scans and should be interpreted with caution (Figure 3.4B) as this could be due to incomplete MM suppression. Moreover, the large variation in the SNR reflects instabilities in the signal amplitudes and lack of consistency. The ShMoCo scans reduced the subtraction artefacts and compared favourably with the reference scans (Figure 3.3 and Figure 3.4).

The MM-suppression technique used in our sequence can be susceptible to subtraction errors due to frequency drifts because (i) the MEGA-editing pulses implemented are frequency selective and (ii) the inversion-pulse profiles for edit-on and edit-off experiments overlap (Harris et al., 2014). Briefly, in the presence of frequency drift, the editing pulses are applied off-resonance, thus reducing the efficiency of inversion. In the case of GABA editing, the C3-GABA resonance experiences only partial inversion leading to a C4-GABA peak with errors. Although post-acquisition frequency correction (Near et al., 2015) reduces the subtraction errors, the GABA concentration is still overestimated (Terpstra et al., 2002). This phenomenon was observed in our study, where frequency changes of up to 14 Hz led to overestimation of GABA/Cr (Figure 3.4D) and almost no suppression of NAA (Figure 3.3: arrow E) in the edit-on spectrum of subject 3. Additional effects of motion were corrected by our real-time motion and shim correction technique. GABA is often reported relative to the Cr or NAA concentrations of the edit-off spectrum (Bai et al., 2014; Donahue et al., 2010). In view of the distortions mentioned above that may arise due to motion or B_0 inhomogeneity, referencing relative to metabolites of the edited spectrum should be performed with extreme caution (Durst et al., 2015).

The ubiquitous technique for motion correction is retrospective frequency and phase correction (Near et al., 2015). Although this method reduces subtraction artefacts, localization errors remain uncorrected and corrupted signal arising from poor shimming cannot be corrected retrospectively. Furthermore, this method is dependent on the available SNR, which is a limiting factor for GABA editing (Bhattacharyya et al., 2007; Near et al., 2015).

Some studies have implemented navigators alongside MEGA-editing sequences. Bhattacharyya et al. (Bhattacharyya et al., 2007) utilized a water-based navigator to discard data from the point where motion is first detected. Although this method may reduce misinterpretation of data, it may suffer from substantial SNR loss and does not guarantee localization accuracy. Zhu et al. (Zhu et al., 2011) implemented navigators to compensate only for field drift and Zaitsev et al. (Zaitsev et al., 2010) implemented optical tracking for motion correction, both of which are insufficient for MM-suppressed GABA acquisition during motion. Keating et al. (Keating & Ernst, 2012) implemented PROMO and a navigator as an efficient alternative method to simultaneously correct in real-time for subject motion and B_0 inhomogeneity. To our knowledge, this technique has not been implemented in J-editing single voxel spectroscopy (SVS) sequences.

Real-time motion and shim correction have been applied in MRSI MEGA-LASER sequence for GABA+ acquisition using volumetric navigators (Bogner et al., 2014). Our implementation involves MM-suppression technique, demanding stronger B_0 stability, which can be impaired by the presence of motion especially when using motion sensitive MSpc sequence.

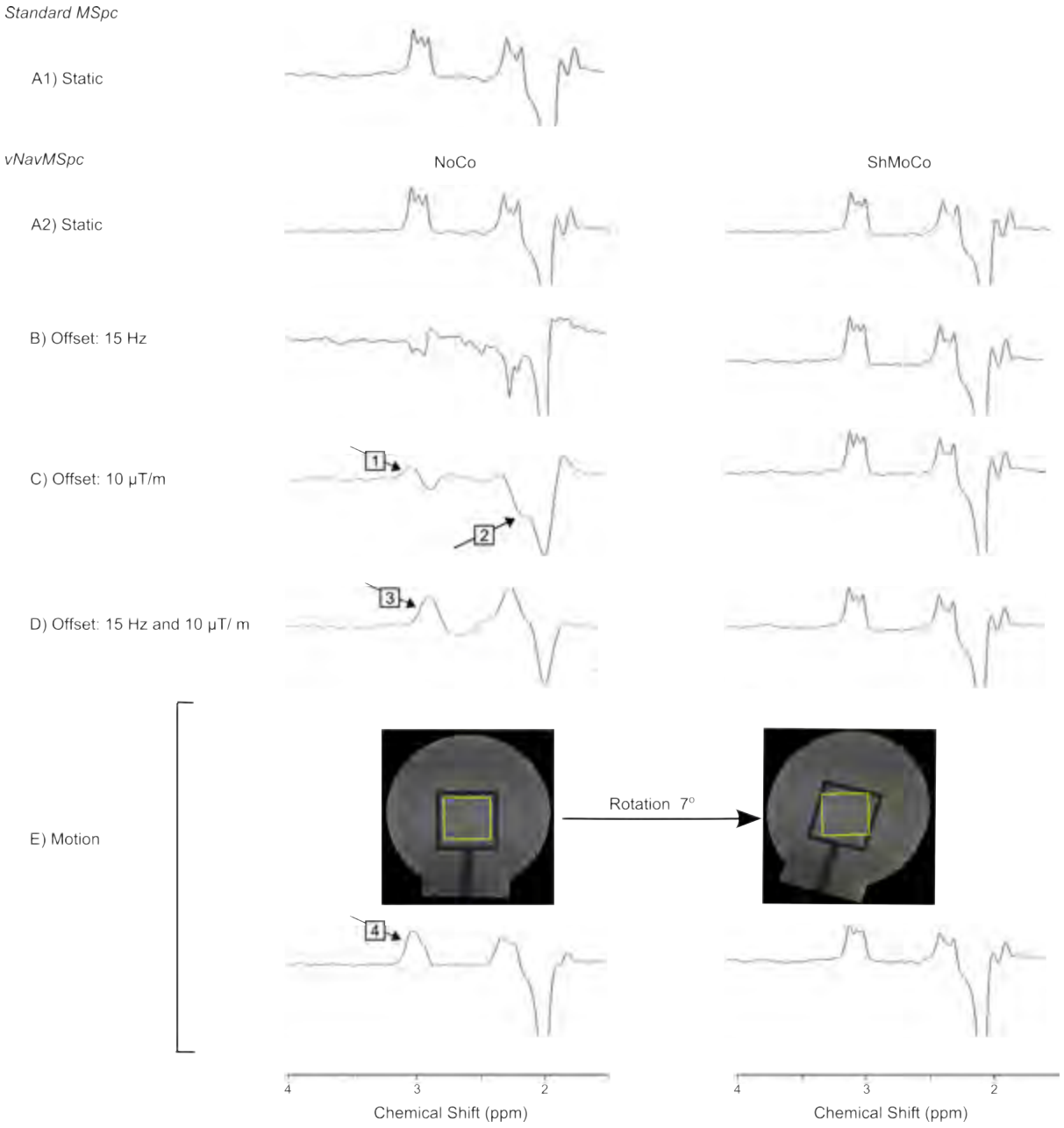

Figure 3.2: Scans of the spherical phantom acquired using the standard MEGA-SPECIAL (MSpc; A1) and volume navigated MSpc (vNavMSpc) sequences for different scenarios: (A) at rest; (B) with a frequency offset; (C) with a first-order shim offset; (D) with a frequency and first-order shim offset; and (E) a scan during which the inner cube was rotated through 7 degrees during the scan. vNavMSpc scans were acquired without (NoCo) and with (ShMoCo) shim and motion correction applied. In B, C, and D frequency and first-order shim offsets led to poor quality spectra from NoCo scans while ShMoCo scans recovered the spectra. The first-order shim offset caused loss of the pseudo-doublet pattern of the GABA peak 4(indicated by 1 and 3) and NAA line broadening (2). Similarly, motion in the NoCo scan also caused loss of the GABA multiplet (indicated by 4).

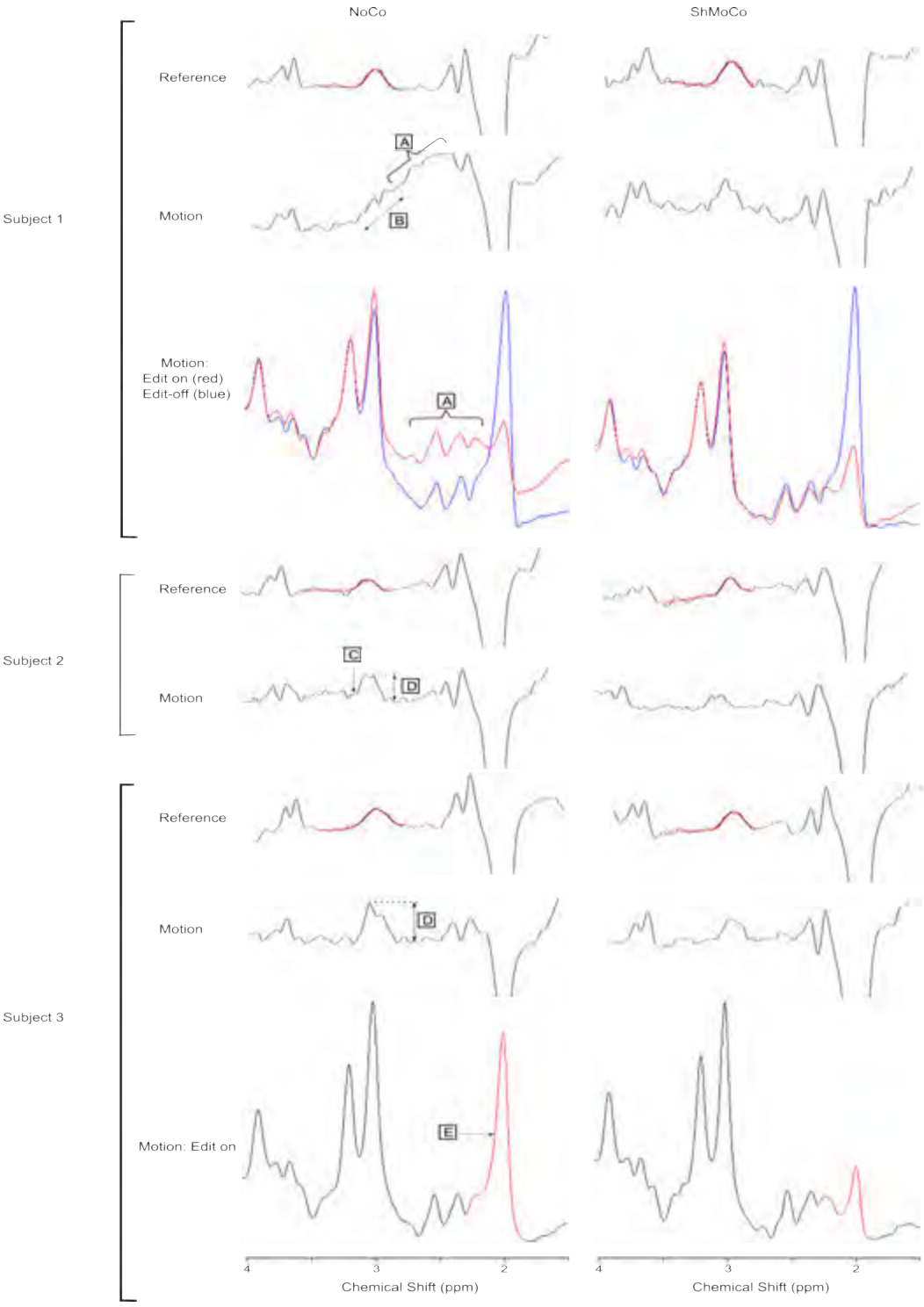

Figure 3.3: Scans in three volunteers without (reference scans) and with intentional motion, respectively, acquired using the volume navigated MEGA-SPECIAL (vNavMSpc) sequence with either no correction (NoCo) or both shim and motion correction (ShMoCo) applied prospectively during the scan. The GABA fitting is shown on the reference scans. Effects of motion on the NoCo acquisitions are indicated with arrows and include a slanted baseline (A) and distorted and broadened (B) GABA peak in subject 1, subtraction artefact (C) in subject 2, increased GABA amplitude (D) in subjects 2 and 3, and insufficient NAA suppression (E) in the edit-on spectrum in subject 3.

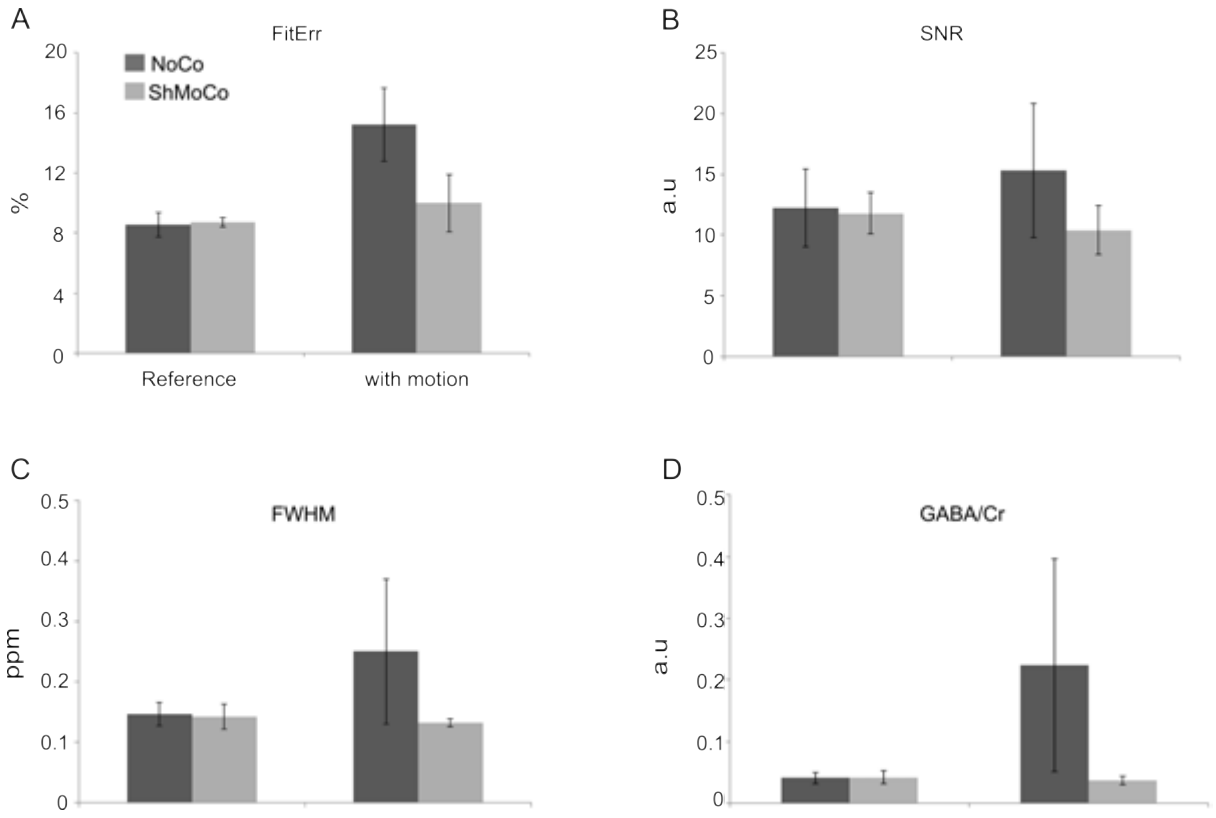

Figure 3.4: Means of the fitting parameters A) FitErr, B) SNR, C) FWHM and D) GABA/Cr ratio for the edited spectra without (NoCo) and with shim and motion correction (ShMoCo), both in the absence (reference) and presence (motion) of intentional motion. (a.u: arbitrary units; ppm: parts per million; % percentage).

There are no direct comparisons between MEGA-LASER or MEGA-sLASER and MSpc sequences, but when referenced to MEGA-PRESS, MEGA-LASER and MEGA-sLASER demonstrate lower spatial variations, are less sensitive to motion and yield more GABA signal than MSpc (Andreychenko et al., 2012; Bogner et al., 2014; Near et al., 2011). This suggests that the real-time motion and shim correction is a necessity for MSpc sequence to ensure proper C4-GABA acquisition. Further studies involving comparison between different real-time motion and shim corrected J-editing sequences will be valuable.

Finally, this work has not addressed reacquisition (Zaitsev et al., 2010) to further improve spectral quality. To avoid prolonging scan time, we decided instead to remove corrupted data during post-processing, as previously done (Near et al., 2013). Higher order shims can also be calculated from the field maps but the current Siemens hardware does not permit real-time control of the higher order shims. While the linear gradients are eddy current compensated, the higher order shims are not, and switching these shims in real time would result in eddy currents that would compromise image and spectral quality.

3.6 CONCLUSION

Subject motion causes detrimental effects on the GABA edited spectra. We have demonstrated that the addition of volume navigators to the MEGA-SPECIAL sequence mitigates spectral distortions due to motion and B_0 inhomogeneity without increasing scan time or compromising SNR.

3.7 ACKNOWLEDGEMENTS

Support was provided by the NRF/DST South African Research Chairs Initiative, NIH grant R01HD071664 and the South African Medical Research Council (MRC).

Chapter 4 Reproducibility of macromolecule suppressed GABA measurement using motion and shim navigated MEGA-SPECIAL with LCModel, jMRUI and GANNET[1]

Muhammad G. Saleh[2], Jamie Near[3], A. Alhamud[2], Frances Robertson[2], André J.W. van der Kouwe[4], Ernesta M. Meintjes[2]

4.1 ABSTRACT

Measuring the pure form of GABA has become increasingly important due to its link with pathology and behaviour. The aim of this study is to assess reproducibility of GABA using a shim and motion navigated MEGA-SPECIAL sequence with LCModel, jMRUI and GANNET software. 20 healthy subjects were scanned. For every subject, four motion and shim navigated MEGA-SPECIAL scans were acquired in a single session. Two acquisitions were performed for each of two regions, the anterior cingulate (ACC) and medial-parietal cortices (PAR). Absolute GABA concentrations ($GABA_{H2O}$) and GABA/Cr were quantified using the three different software packages. The GABA concentrations from the two acquisitions in the PAR were statistically different ($p < 0.05$) from each other. The reproducibility measured as coefficient of variation within-subjects (CV_{ws}) was ≈13-22% in both the ACC and PAR determined using all three software packages. Based on CV_{ws}, GABA concentrations are reproducible in both the ACC and PAR using a shim and motion corrected MEGA-SPECIAL sequence with three different software packages. This study shows the potential to quantify the pure form of GABA using any of the three software packages in studies relating GABA to pathology and healthy behaviour.

4.2 INTRODUCTION

γ-aminobutyric acid (GABA) is a primary inhibitory neurotransmitter and accounts for almost half of synaptic activity (Levy & Degnan, 2013). GABA quantification remains challenging due to overlapping resonances arising from macromolecules (MM) and metabolites such as creatine (Mullins et al., 2012). Currently one preferred method for measuring C4-GABA is through spectral

[1] Chapter written as an article intended for review and publication
[2] University of Cape Town
[3] McGill University
[4] Massachusetts General Hospital, Harvard Medical School

editing methods, such as MEGA-PRESS and MEGA-SPECIAL. Most studies acquire C4-GABA with macromolecule (MM) contamination, commonly referred to as GABA+ (Mullins et al., 2012).

Several studies have established test-retest reproducibility of GABA+ within- and between-subjects using LCModel, jMRUI and GANNET (Bogner et al., 2010; Evans et al., 2010; Mikkelsen et al., 2015; Near et al., 2014; O'Gorman et al., 2011). These studies employed coefficient of variation (CV) as an index to determine reproducibility of GABA+, which was referenced to either tissue water ($GABA_{H2O}$) or creatine (GABA/Cr). Bogner et al., performed a reproducibility study in the occipital cortex (OCC) and found average within-subjects CV (CV_{ws}) ranging between 10 to 12% and between-subjects CV (CV_{bs}) ≈13% using AMARES package in jMRUI (Bogner et al., 2010). Evans et al., measured CV_{ws} and CV_{bs} in the OCC (CV_{ws} ≈7% and CV_{bs} ≈9%) and sensorimotor cortex (SMC: CV_{ws} of ≈9% and CV_{bs} ≈12%) using MATLAB (The Mathworks, Natick, MA), which was similar to GANNET software (Evans et al., 2010). O'Gorman et al., measured GABA+ in the dorsolateral prefrontal cortex (DLPFC) and demonstrated CV_{ws} of 7%, 9% and 12% using, respectively, LCModel, AMARES in jMRUI and MATLAB, which was similar to GANNET software (O'Gorman et al., 2011). Near et al., found CV_{ws} in the OCC of about 4% using AMARES in jMRUI (Near et al., 2014). Mikkelsen et al., found CV_{ws} of about 15% and 4% in the anterior cingulate cortex (ACC) and OCC using GANNET (Mikkelsen et al., 2015).

Previous studies (Harris et al., 2014; Near et al., 2011) have shown that the MM contribution varies between subjects, resulting in a very weak correlation between GABA+ and GABA (MM-suppressed). Another reason for weak correlation could be due to the problems related with the MM suppression technique. Measuring the pure form of GABA is becoming increasingly important due to its relationship with several neurologic conditions including Alzheimer's disease (Bai et al., 2014), epilepsy (Yamamoto et al., 1985), alcohol and drug abuse (Ticku, 1990), insomnia (Winkelman et al., 2008) and depression (Block et al., 2009; Sanacora et al., 2002). GABA levels are also correlated with hemodynamic contrasts measured through blood-oxygen level dependent (BOLD) functional magnetic resonance imaging (fMRI) and cerebral blood flow (CBF)-weighted arterial spin labelling (ASL) (Donahue et al., 2010; Muthukumaraswamy et al., 2009). Furthermore, variations in GABA levels are observed with motor learning (Floyer-Lea et al., 2006) and working memory (Michels et al., 2012) tasks.

GABA acquisition is challenging due to the requirement of high magnetic field (B_0) stability for adequate MM-suppression, which can be hampered by several factors, including incidental motion. Furthermore, a previous pilot study suggested that removal of MM from GABA+ reduces the reliability of GABA measurements (determined by Cramer Rao Lower Bound increasing from 20% to 40%) (O'Gorman et al., 2007). Therefore, it is important to establish reproducibility of GABA

prior to GABA-based evaluation of aforementioned studies, including pathology and healthy behaviour.

GABA measurements are performed using a range of software, however most commonly employed (Bogner et al., 2010; Mikkelsen et al., 2015; Mullins et al., 2012; Near et al., 2014) are LCModel (Provencher, 2001), the AMARES (Vanhamme et al., 1997) package in jMRUI (Naressi et al., 2001) and GANNET (R. A. Edden et al., 2013). The commercial LCModel software utilises prior knowledge of the individual metabolite basis spectra (a basis set) to fit GABA in the frequency domain. The jMRUI software is freely available to non-profit organizations, and through the AMARES package, performs time-domain fitting by utilizing user-defined a priori information. The MATLAB-based software, GANNET, is open-source and specifically developed for quantitative analysis of GABA through nonlinear least-squares Gaussian fitting in the frequency domain. Several studies implement different software which – given the different techniques implemented in performing GABA measurements – will introduce bias and variance in GABA measurements (Levy & Degnan, 2013; Mullins et al., 2012; Puts & Edden, 2012).

To our knowledge, two studies using MEGA-PRESS with the MM suppression technique have investigated reproducibility of GABA, of which one study quantified GABA at 7 T through manual integration of the area under the C4-GABA peak and found CV_{ws} ≈14% and ≈13% in the ACC and DLPFC, respectively (Wijtenburg et al., 2013). The second study employed GANNET software to quantify GABA in the ACC and OCC (Mikkelsen et al., 2015). The study found CV_{ws} ≈13% and CV_{bs} ≈14% in the ACC and CV_{ws} ≈5-9% and CV_{bs} ≈15% (Mikkelsen et al., 2015).

A motion and shim navigated MEGA-SPECIAL sequence has recently been demonstrated that acquires the J-edited spectrum with superior spectral quality, permitting more accurate quantification of GABA (Saleh et al., 2016). To date, the extent of intra- and inter-subject variability of GABA acquired by motion and shim navigated MEGA-SPECIAL has not been investigated and compared between commonly employed spectral fitting methods (R. A. Edden et al., 2013; Provencher, 2001; Vanhamme et al., 1997). GABA+ concentration has been quantified using internal references, such as water (H_2O) and creatine (Cr) (Bai et al., 2014; Bogner et al., 2010; Harris et al., 2014). Cr is widely used as a reference for GABA+ (Bogner et al., 2010; Near et al., 2014). Therefore, the aim of this study was to use motion and shim navigated MEGA-SPECIAL (Saleh et al., 2016) to assess intra- and inter-subject variability in GABA concentration in two brain regions, referenced to H_2O and Cr, as determined with LCModel (Provencher, 2001), AMARES (Vanhamme et al., 1997) in jMRUI (Naressi et al., 2001) and GANNET (R. A. Edden et al., 2013).

4.3 METHODS

All protocols and experiments were approved by the Human Research Ethics Committee of the Faculty of Health Sciences at the University of Cape Town and written informed consent was obtained from all subjects. All MRI/MRS experiments were performed on a Siemens Allegra 3 T scanner (Erlangen, Germany) using a single channel transmit/receive (T/R) head coil.

4.3.1 Subjects

20 healthy subjects (10 female; age: 23 ± 2 (mean ± standard deviation (SD))) were recruited for the study. Two J-edited spectra were acquired from each of two regions (Figure 4.1), the anterior cingulate cortex (ACC) and medial-parietal cortex (PAR), with the order interleaved.

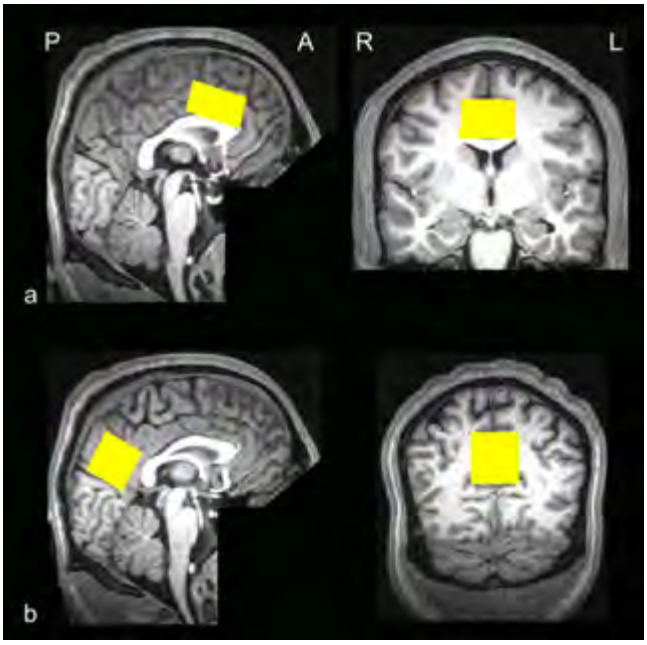

Figure 4.1: Voxel positioning in the (a) ACC and (b) PAR. A: Anterior. P: Posterior. R: Right. L: Left.

4.3.2 MR imaging and MR spectroscopy acquisition

Prior to voxel placement, three-dimensional (3D) T1-weighted sagittal scans of the subjects' brains were acquired using MEMPRAGE (van der Kouwe et al., 2008) with 1.3 × 1.0 × 1.0 mm^3 resolution for accurate voxel placements.

The motion and shim navigated MEGA-SPECIAL sequence (Saleh et al., 2016) was used for acquiring C4-GABA without MM contamination, as explained previously (Near et al., 2011). MEGA-SPECIAL comprises two iterations of SPECIAL localization and MEGA-editing pulses for GABA editing and water suppression. All editing pulses are dual-banded, Gaussian shaped and have a duration of 27 ms with a half width at 1% maximum (HW1%M) of less than 48 Hz. In the

first MEGA-editing iteration the editing-band is applied to the C3-GABA resonance at 1.9 ppm (edit-on), while in the second iteration the editing-band is applied at 1.5 ppm (edit-off). The water suppression band of the dual-band editing pulses was always applied at 4.7 ppm. Prior to all acquisitions, outer volume suppression (OVS) pulses were applied to saturate spins outside the VOI (Near et al., 2011).

The MEGA-SPECIAL parameters were as follows: TR/TE 4000/68 ms, bandwidth 2 kHz, 160 averages, 2048 readout samples; scan duration 11 min. The voxel sizes of every region were: ACC: 20 × 30 ×40 mm^3, PAR: 30 × 30 ×30 mm^3. Shimming was performed using vendor-specific shim tool prior to the start of every acquisition. The resulting average water full width at half maximum (FWHM, mean ± standard error of mean) was 15 ± 0.3 Hz and 14 ± 0.2 Hz for ACC and PAR, respectively. Finally, water unsuppressed data with four averages were acquired from every region.

4.3.3 Post-processing and analysis

The T1 images of every subject were segmented using SPM12 (http://www.fil.ion.ucl.ac.uk/spm). Subsequently, the segmented images were multiplied by a mask representing the voxel to determine grey matter (f_{GM}), white matter (f_{WM}) and cerebrospinal fluid (CSF, f_{CSF}) composition of the voxel.

4.3.3.1 Frequency and Phase correction

The post-processing procedure was semi-automated using MATLAB processing routines. Briefly, subspectra from interleaved SPECIAL inversion on/off acquisitions were subtracted, resulting in edit-on/off scans. The motion corrupted edit-on/off scans were removed as described previously (Saleh et al., 2016). Subsequently, eddy current correction (Klose, 1990) was applied, followed by frequency correction using the Cr peak position so that line broadening due to minor frequency drifts could be reduced (Fuchs et al., 2013). The averaged edit-on and edit-off spectra were manually frequency aligned and phase adjusted to minimize the choline difference signal (Near et al., 2014). This was followed by removal of residual water (A. Hess et al., 2014) and DC offset (Stagg et al., 2009; Zhu et al., 2011). Finally, fully processed edit-on/off scans were subtracted to generate GABA-edited spectra. ACC spectra of two males and two females, as well as PAR spectra of a different two males and two females, were rejected due to a large residual choline artefact.

4.3.3.2 Analysis

Figure 4.2 shows spectral fitting of a subject's GABA-edited spectra from the ACC and PAR using LCModel (Provencher, 2001), AMARES in jMRUI (Vanhamme et al., 1997) and the GannetFit module within GANNET (R. A. Edden et al., 2013). For LCModel (version: 6.3-1E), measurements were obtained using a simulated basis set that was generated using FID-A toolbox (O'Gorman et al., 2007). For LCModel, GABA/Cr was defined as the ratio of GABA from the edited spectrum to

total Cr (creatine + phosphocreatine) from the edit-off spectrum. For jMRUI (version 5.2), GABA and Cr were modelled as double and single Lorentzian peaks, respectively. The frequency, phases and linewidths of the peaks were all constrained relative to either the residual NAA peak for GABA or the NAA peak of the edit-off spectrum for Cr at 3 ppm. For GANNET (version 2.0), a Gaussian doublet with linear baseline was used to fit the GABA signal between 2.8 and 3.4 ppm, while a Gaussian singlet was used to fit Cr between 2.72 and 3.12 ppm. For jMRUI and GANNET analyses, apodization using a 5 Hz Lorentzian filter and zero padding to a factor of 16 were applied prior to fitting.

Tissue H_2O and Cr were used as internal references. The water concentration along with partial volume correction were estimated as shown in equation 1 and used in all three spectral fitting toolkits (Provencher, 2001). The absolute concentration of GABA ($GABA_{H2O}$) and the ratio of GABA to Cr (GABA/Cr) from jMRUI and GANNET were estimated as shown in equations 2 and 3, respectively.

$$WCONC = \frac{43300 f_{GM} + 35880 f_{WM} + 55556 f_{CSF}}{1 - f_{CSF}} \quad \textbf{[1]}$$

$$[GABA_{H2O}]_{corr} = \frac{S_{GABA}}{S_{H2O}} \times WCONC \times \frac{1 - e^{-TR/T1_{H2O}}}{1 - e^{-TR/T1_{GABA}}} \times \frac{e^{-TE/T2_{H2O}}}{e^{-TE/T2_{GABA}}} \times \frac{1}{eff_{GABA}} \quad \textbf{[2]}$$

$$[GABA/Cr]_{corr} = \frac{S_{GABA}}{S_{Cr}} \times \frac{H_{Cr}}{H_{GABA}} \times \frac{1 - e^{-TR/T1_{Cr}}}{1 - e^{-TR/T1_{GABA}}} \times \frac{e^{-TE/T2_{Cr}}}{e^{-TE/T2_{GABA}}} \times \frac{1}{eff_{GABA}} \quad \textbf{[3]}$$

where WCONC: concentration of water in institutional units (i.u), f_{GM}: fraction of grey matter, f_{WM}: fraction of white matter, f_{CSF}: fraction of CSF, S_{GABA}: integral of the modelled GABA signal, S_{H2O}: integral of the modelled water signal, S_{Cr}: integral of the modelled Cr signal, H_{Cr}/ H_{GABA}: ratio of ^1H in Cr to GABA, eff_{GABA}: editing efficiency of GABA, T1 and T2: relaxation times of metabolites and water. The editing efficiency (eff) of GABA is 0.45 (Near et al., 2011). The H_{Cr}/H_{GABA} ^1H ratio is 3/2.

All concentrations and ratios were corrected for T1 and T2 relaxation effects using published values (R. Edden, Intrapiromkul, et al., 2012; Mlynárik et al., 2001; Puts et al., 2013). All $GABA_{H2O}$ are reported in institutional units (i.u). Estimates of GABA fit error were used to evaluate spectral quality. In LCModel Cramer-Rao Lower Bounds (CRLB) were used, and fitting error (FitErr) for jMRUI and GANNET. AMARES within jMRUI provides the Cramer-Rao standard deviation (CRSD) and amplitude of every Lorentzian peak. We computed the ratio of the CRSD to the amplitude for every Lorentzian peak and defined the FitErr for jMRUI ($FitErr_{jMRUI}$) as the average of these ratios. The FitErr from GANNET ($FitErr_{GANNET}$) was defined as the SD of the fitting residuals normalized to the Gaussian amplitude of the GABA peak.

4.3.4 Statistical analysis

Statistical analyses were performed in SPSS 22. All data were tested for normality using the Shapiro-Wilk test.

4.3.4.1 Test-retest Reproducibility

The repeated measures were compared using paired t-tests; non-normally distributed data were log transformed. The extent of intra- and inter-subject variability of GABA measurements from the three different software packages was compared in each region using coefficients of variation within subjects (CV_{ws}) and between subjects (CV_{bs}) as described by the previous studies (Mikkelsen et al., 2015; Near et al., 2014). Firstly, the CV of each subject (CV_s) was estimated as follows:

$$CV_s = \frac{\sigma_s}{\mu_s} 100$$

where μ_s and σ_s are the mean and SD, respectively, of GABA concentrations measured for each subject. Then the CV_{ws} was measured as the average of CV_s:

$$CV_{ws} = \overline{CV_s}$$

The 95% confidence interval (CI) of CV_{ws} was estimated using a bootstrapping technique to resample with replacement 10,000 times, as described previously (Mikkelsen et al., 2015; Near et al., 2014). Finally, the CV_{bs} was estimated as the ratio of the SD of subject means (σ) to the mean of the subject means (μ):

$$CV_{bs} = \frac{\sigma}{\mu} 100$$

The relationship between pairs of GABA measurements acquired for each subject in each region were examined for each of the software packages using either Pearson (r) or Spearman (ρ) correlation for normally and non-normally distributed data, respectively.

A two-factor analysis of variance (ANOVA) was used to compute the proportional contribution of variance between the subjects (between-subjects variability excluding individual differences, σ^2_p) and variance due to error (error, σ^2_e) to the total variance in the dataset, as described previously (Mikkelsen et al., 2015). As a measure of intra-software reliability, intraclass correlation (ICC) between repeated measures was computed for each software package in each brain region using a two-way mixed effects model with measures of consistency (Weir, 2005).

4.3.4.2 Comparison between software packages

Intra-subject variability (CV_s) was compared in each region for the different software packages using either ANOVA with repeated measures or the Friedman test for normally and non-normally distributed data, respectively. Prior to ANOVA, equality of variances was tested using Mauchly's test. When the assumption of sphericity (equality of variance) was violated, Greenhouse-Geisser correction was employed. In addition, inter-software reliability of $GABA_{H2O}$ and GABA/Cr measurements from every acquisition was computed using ICC to determine agreement between different software packages (Weir, 2005). Unless stated, all values are henceforth presented as mean or mean ± standard error of mean (SEM).

4.4 RESULTS

A total of 64 spectra (16 subjects × 2 scans per region × 2 regions) were analysed using all three software packages. The average CRLB from LCModel fitting in ACC and PAR were 10.2 ± 0.3 % and 9.0 ± 0.2 %, respectively. JMRUI yielded average fitting errors in ACC and PAR of 5.5 ± 0.3 % and 4.7 ± 0.3 %, respectively, while fitting errors in ACC and PAR for GANNET were 10.6 ± 0.6 % and 6.4 ± 0.4 %, respectively. Table 4.1, Table 4.2 and Table 4.3 summarise measures of reproducibility in each region from LCModel, AMARES in jMRUI, and GANNET, respectively. Table 4.4 summarises measures of inter-software reliability of both $GABA_{H2O}$ and GABA/Cr measurements. GABA measurements in each region were normally distributed (Shapiro-Wilk test, $p > 0.05$), except for GABA concentrations in the ACC estimated by GANNET. For each of the software packages, the CV_s data in ACC were normally distributed (Shapiro-Wilk test, $p > 0.05$), while the CV_s data in PAR were not.

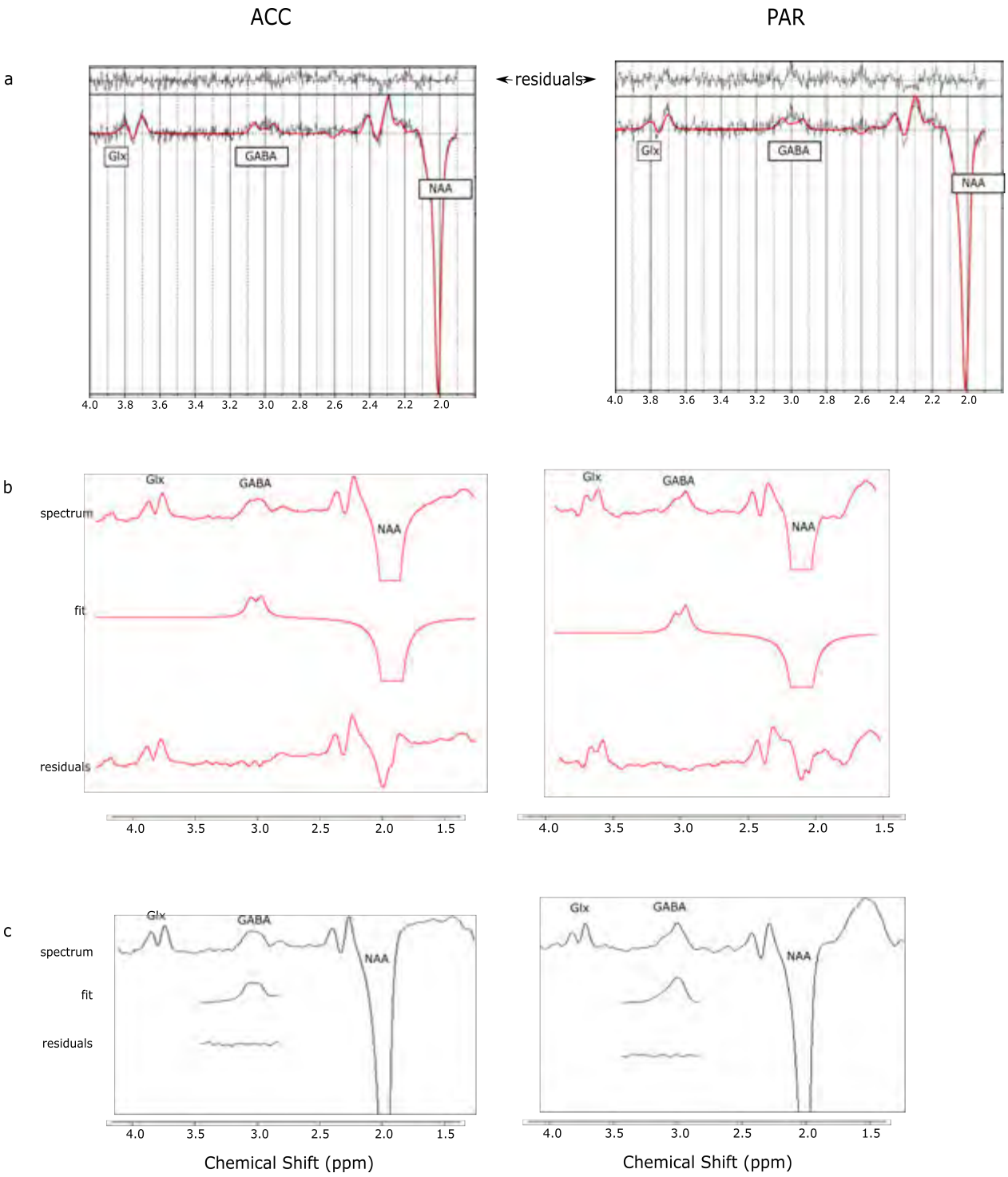

Figure 4.2: Spectral fitting of a subject's GABA-edited spectra from the ACC (left) and PAR (right) using A) LCModel, B) AMARES in jMRUI and C) GANNET. The Glx (Glutamate + Glutamine) peak at 3.75 ppm and inverted NAA peak at 2 ppm are co-edited with GABA. Apodization using a 5 Hz Lorentzian filter and zero filling to a factor of 16 were applied prior to jMRUI and GANNET fitting. The spectral fitting plots generated by the different software packages are not on the same scale.

ACC

In ACC, $GABA_{H2O}$ and GABA/Cr did not differ significantly between the two acquisitions for any of the three software packages. Although the mean CV_{ws} was lower for LCModel and jMRUI than GANNET, these differences were not significant ($GABA_{H2O}$: F = 2.422, p = 0.128 and GABA/Cr: F = 2.787, p = 0.103, repeated measures ANOVA with Greenhouse-Geisser correction). The CV_{bs} from GANNET for both $GABA_{H2O}$ and GABA/Cr was also higher than for LCModel and jMRUI.

The correlation between the pair of acquisitions was stronger for GANNET. The component of variance associated with differences between participants (σ^2_p) was lower for LCModel and jMRUI compared to GANNET. This resulted in comparatively lower ICC using these two packages.

PAR

In PAR, repeated measures for $GABA_{H2O}$ and GABA/Cr differed significantly (all p's < 0.05) irrespective of which software package was used. CV_{ws} and CV_{bs} for all software were similar for both $GABA_{H2O}$ and GABA/Cr. The Friedman test confirmed that variability between repeated measures (CV_{ws}) did not differ significantly between software packages ($GABA_{H2O}$: $\chi^2(2) = 0.50$, p = 0.78; GABA/Cr: $\chi^2(2) = 3.13$, p = 0.21). Repeated measures were significantly correlated *only* for $GABA_{H2O}$ from GANNET. ICC was highest for GANNET and lowest for jMRUI.

With respect to inter-software reliability, from Table 4.4, the σ^2_p were higher than σ^2_e and similar across the two acquisitions for both $GABA_{H2O}$ and GABA/Cr resulting in consistent and comparatively high ICCs.

4.5 DISCUSSION

Although several studies have reported reproducibility of GABA+ in the ACC and OCC (Bogner et al., 2010; Evans et al., 2010; Near et al., 2014; O'Gorman et al., 2011), this study is the first, through motion and shim navigated MEGA-SPECIAL, to compare intra- and inter-subject variability of GABA measurements in the ACC and PAR regions using three widely employed analysis tools: LCModel, jMRUI and GANNET.

Table 4.1: Measures of reproducibility for GABA measurements using LCModel

		ACC		PAR	
		$GABA_{H2O}$	**GABA/Cr**	**$GABA_{H2O}$**	**GABA/Cr**
Concentration (i.u) [a]	**Acquisition 1**	1.08 ± 0.06	0.097 ± 0.005	1.24 ± 0.11	0.105 ± 0.004
	Acquisition 2	1.08 ± 0.04 *p*=0.92	0.097 ± 0.004 *p*=0.95	1.03 ± 0.04 *p*<0.01	0.090 ± 0.003 *p*=0.01
Mean CV_{ws}(%)		13.3	12.9	14.2	13.3
95% CI (%)		10.0–16.7	9.6–16.2	8.7–20.2	8.2–19.0
CV_{bs} (%)		13.8	14.6	14.0	12.6
Pearson (r)		0.21 (*p*=0.44)	0.29 (*p*=0.28)	0.34 (*p*=0.20)	0.28 (*p*=0.30)
σ^2_p (%)		60	64	66	63
σ^2_e (%)		40	36	34	37
ICC		0.33	0.44	0.50	0.42

[a]Concentrations are expressed as mean ± standard error of mean (SEM), *p*-values are from paired t-test between acquisitions; 95% CI: 95% confidence interval generated by bootstrapping the CV_s; σ^2_p: between-subjects component of variance; σ^2_e: variance due to error; ICC: Intraclass correlation coefficient.

Table 4.2: Measures of reproducibility for GABA measurements using AMARES in jMRUI

		ACC		PAR	
		$GABA_{H2O}$	**GABA/Cr**	**$GABA_{H2O}$**	**GABA/Cr**
Concentration (i.u) [a]	**Acquisition 1**	2.81 ± 0.15	0.170 ± 0.009	3.79 ± 0.16	0.220 ± 0.009
	Acquisition 2	2.90 ± 0.10 *p*=0.62	0.180 ± 0.007 *p*=0.50	3.30 ± 0.15 *p*=0.02	0.190 ± 0.008 *p*=0.04
Mean CV_{ws}(%)		15.2	14.2	14.5	14.9
95% CI (%)		10.4–20.2	9.1–19.3	9.1–20.8	9.3–21.1
CV_{bs} (%)		12.9	15.0	13.4	12.5
Pearson (r)		0.03 (*p*=0.91)	0.22 (*p*=0.42)	0.17 (*p*=0.52)	0.05 (*p*=0.86)
σ^2_p (%)		51	61	59	52
σ^2_e (%)		49	39	41	48
ICC		0.06	0.35	0.30	0.09

[a]Concentrations are expressed as mean ± standard error of mean (SEM), *p*-values are from paired t-test between acquisitions; 95% CI: 95% confidence interval generated by bootstrapping the CV_s; σ^2_p: between-subjects component of variance; σ^2_e: variance due to error; ICC: Intraclass correlation coefficient.

Table 4.3: Measures of reproducibility for GABA measurements using GANNET

		ACC		PAR	
		$GABA_{H2O}$	GABA/Cr	$GABA_{H2O}$	GABA/Cr
Concentration (i.u) [a]	**Acquisition 1**	1.72 ± 0.18	0.130 ± 0.014	2.55 ± 0.10	0.18 ± 0.008
	Acquisition 2	1.58 ± 0.14	0.120 ± 0.012	2.07 ± 0.13	0.15 ± 0.009
		p=0.56	*p*=0.65	*p*<0.01	*p*<0.01
Mean CV_{ws}(%)		22.1	22.2	17.6	17.6
95% CI (%)		15.1–29.7	15.0–30.0	11.5–24.1	11.7–23.9
CV_{bs} (%)		32.7	35.5	17.0	16.6
Pearson (r)/Spearman (ρ)		ρ=0.37 (*p*=0.17)	ρ=0.43 (*p*=0.09)	r=0.57 (*p*=0.02)	r=0.38 (*p*=0.15)
σ^2_p (%)		72	75	73	69
σ^2_e (%)		28	25	27	31
ICC		0.60	0.66	0.62	0.56

[a]Concentrations are expressed as mean ± standard error of mean (SEM), *p*-values are from paired t-test between acquisitions; 95% CI: 95% confidence interval generated by bootstrapping the CV_s; σ^2_p: between-subjects component of variance; σ^2_e: variance due to error; ICC: Intraclass correlation coefficient.

Table 4.4: Inter-software reliability of $GABA_{H2O}$ and GABA/Cr measurements

	$GABA_{H2O}$		GABA/Cr	
	Acquisition 1	**Acquisition 2**	**Acquisition 1**	**Acquisition 2**
σ^2_p (%)	76	78	77	77
σ^2_e (%)	24	22	23	23
ICC	0.69	0.72	0.70	0.70

σ^2_p: between-subjects component of variance; σ^2_e: variance due to error;ICC: Intraclass correlation coefficient.

Suppressing MM is beneficial for GABA-based evaluation of neurologic conditions (Levy & Degnan, 2013), especially those involving correlational designs. For instance, Aufhaus et al., demonstrated age-related increase in GABA+, but when MM is suppressed, the relationship between GABA and age no longer exists (Aufhaus et al., 2013). However, the MM-suppressed GABA acquisition is challenging due to its strong dependence on B_0 stability, which can be exacerbated in the presence of motion. Furthermore, a previous pilot study demonstrated that removal of MM by subtracting MM – acquired from metabolite nulled scan – from GABA+ reduces reliability (based on CRLB) of GABA measurements from 20% to 40% (O'Gorman et al., 2007). The technique of removal of MM in (O'Gorman et al., 2007) increases the level of noise in the final edited GABA spectrum, thus reducing reliability of GABA measurements (Mullins et al., 2012). It also prolongs scan duration and involves subtraction of non-interleaved acquisitions, thus increasing sensitivity to subject motion (Mullins et al., 2012).

In this study, we implemented 3D EPI volumetric navigators along with MEGA-SPECIAL to prospectively correct for motion and B_0 drift (Saleh et al., 2016) throughout the acquisition. Pairwise motion and shim updates, i.e. once for every pair of edit-on/off measurements, have been shown previously to reduce subtraction artifacts (e.g. choline artefatcs) in MEGA-PRESS and MEGA-LASER (Bogner et al., 2014; Evans et al., 2013). Since the MEGA-SPECIAL sequence requires four acquisitions (4 ×TR = 16 s for this study) to acquire a single GABA edited spectrum, it is more sensitive to motion than MEGA-PRESS and MEGA-LASER that each require two TRs per edited spectrum. In view of this, the motion and shim estimates were updated every TR, rather than once for every set of measurements, to reduce the impact of motion and B_0 drift on the final GABA spectrum (Saleh et al., 2016). Nevertheless, comparison between the individual and pairwise updates of motion and shim terms during MEGA-SPECIAL acquisition would be favourable.

This strategy resulted in spectra with high quality as evidenced by the low values of the CRLB (ACC: ≈10%, PAR: ≈9%) from LCModel, and low fitting errors for jMRUI and GANNET. Differences in GABA fit errors between the two regions reflect differences in signal to noise ratio (SNR). The SNR was calculated in GANNET as the ratio of the amplitude of the fitted Gaussian to the SD of the noise between 0.2 and 0.5 ppm. The average SNR from ACC (6 ± 0.9) was lower than the SNR from PAR (11 ± 0.6). A previous study demonstrated higher SNR in posterior regions of the brain such as OCC, compared to mid-brain regions, such as SMC (Evans et al., 2010). This may be due to RF magnetic field (B_1) inhomogeneity. Another contributor to the higher SNR in PAR was that the VOI for PAR was larger (27 cm^3) relative to the VOI for ACC (24 cm^3). The intrinsic concentration of GABA in PAR could also be higher than that in ACC, thus influencing the SNR.

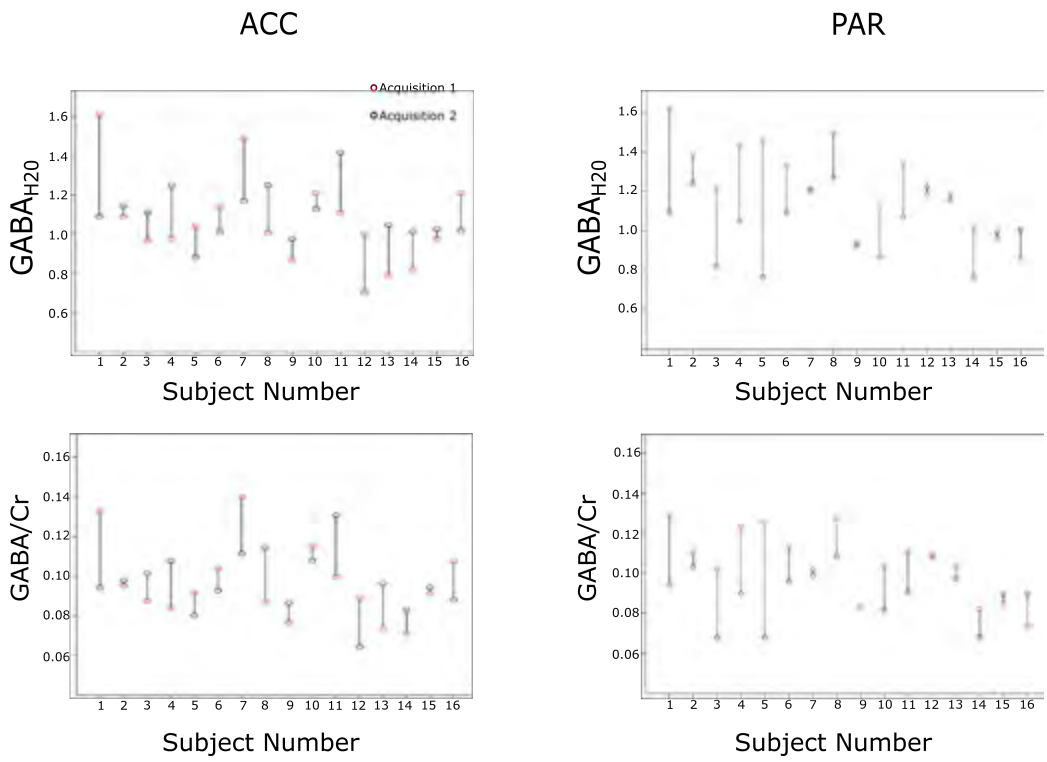

Figure 4.3: LCModel measurements of $GABA_{H2O}$ and GABA/Cr from the ACC (left) and PAR (right) regions. The red circle (O) represents data from acquisition 1 and the black circle (O) from acquisition 2.

In this study we assessed reproducibility between repeated measures using a paired t-test, ICC, and Pearson (or Spearman) correlation. Figure 4.3 shows GABA levels computed using LCModel for each subject in each of the two regions for the pairs of acquisitions. We used the paired t-test to detect systematic differences between repeated measures. In ACC there were no statistically significant differences between repeated measures for GABA levels computed using any of the software tools (all *p*'s > 0.50). Despite the absence of differences, ICC's were low (< 0.5) except for measurements obtained using GANNET. In contrast, the second measurements in the pair of repeats yielded lower GABA levels in PAR for all three software packages. Similar to results in ACC, ICC's and correlations were, however, again low and not significant, except for data obtained using GANNET.

In ACC, CV_{ws} ranged from 13% for LCModel (Figure 4.3) to 22% for GANNET. In PAR, CV_{ws} ranged from 13% for LCModel (Figure 4.3) to 18% for GANNET. These results are similar to those of a previous GABA+ reproducibility study performed in the dorsolateral prefrontal cortex (DLPFC) (O'Gorman et al., 2011) where the lowest CV_{ws} were obtained using LCModel followed by jMRUI and MATLAB-based fitting, the latter being similar to GANNET (Mullins et al., 2012).

Differences between CV_{ws} for different software packages were not significant in either region. Unlike LCModel and jMRUI, GANNET estimated higher CV_{ws} in the ACC than PAR. This is

consistent with a previous study that has demonstrated higher CV_{ws} from GANNET in the ACC than OCC (Mikkelsen et al., 2015). This is probably due to higher SNR from the OCC and PAR relative to ACC. However, the regional difference in SNR did not modulate the CV_{ws} from LCModel and jMRUI, suggesting that CV_{ws} from GANNET is dependent on SNR.

Similarly, the CV_{bs} values from GANNET were higher in the ACC and could have been influenced by larger between-subject variability in tissue fractions in the ACC than PAR. However, regional differences in between-subject variability in tissue fractions did not affect CV_{bs} from LCModel and jMRUI, suggesting that CV_{bs} values from GANNET, similar to the corresponding CV_{ws} values, are SNR dependent. Future research comparing SNR and both CV_{ws} and CV_{bs} from GANNET in different regions of the brain would be informative.

For both regions, between-subject variability appears to be higher when using GANNET as evidenced by higher CV_{bs} and σ^2_p relative to values obtained using the other two software packages. This high variance improved the ICC values for GANNET. Near et al. (Near et al., 2014) previously reported an ICC value greater than 0.50 using jMRUI, while Harada et al. (Harada et al., 2011) reported ICC values greater than 0.7 using LCModel. Mikkelsen et al., reported ICC values greater than 0.40 using GANNET (Mikkelsen et al., 2015). Our study yielded similar ICC values for GANNET, while LCModel and jMRUI ICC values were lower. This is probably due to the fact that the two previous studies using jMRUI and LCModel measured GABA+ (Harada et al., 2011; Near et al., 2014).

The inter-software ICC values (Table 4) are above 0.60 across the acquisitions for both $GABA_{H2O}$ and GABA/Cr. Since ICC values ranging from 0.60 to 0.74 are considered good (Buckens et al., 2013; Hodkinson et al., 2013; Near et al., 2014), these values suggest good agreement between the three software packages. However, the large differences in $GABA_{H20}$ and GABA/Cr levels found in this study when using the three different software packages, indicate that direct comparison between studies implementing different analysis software should be performed with great caution.

Although Cr is widely used as a referencing method (Bai et al., 2014; Bogner et al., 2010; Near et al., 2014), some studies have shown that it might not be a stable choice for comparisons in some neurological disorders (Deicken et al., 2001; Gruber et al., 2003). In view of the inter-software agreement, measurements of $GABA_{H2O}$ could be used to detect changes between healthy and unhealthy subjects.

To the author's knowledge, only two studies using MEGA-PRESS (with MM-suppression) have investigated reproducibility of GABA. One study by Wijtenburg et al. scanned 4 subjects at 7T in the ACC and dorsolateral prefrontal cortex (DLPFC) using a 32 channel coil, 27 ml isotropic voxel,

160 averages and 8 min scan duration (Wijtenburg et al., 2013). This study found CV_{ws} of 14% and 13% in the ACC and DLPFC, respectively, for GABA relative to H_2O using manual integration. In a second study, Mikkelsen et al. acquired GABA at 3T in two groups of participants, each comprising 15 participants. In the first group, GABA-edited spectra were acquired from the ACC and OCC with the following parameters: 8 channel coil, 24 ml (ACC) and 27 ml (OCC) voxels, 332 averages and ≈10 min scan duration. In the second group of participants, GABA-edited spectra were acquired only from the OCC with the same acquisition parameters, except that the number of averages was increased to 512 (Mikkelsen et al., 2015). The study found CV_{ws} ≈13% in the ACC. In the OCC, the first group revealed CV_{ws} ≈9%, while the second group with the higher number of averages (higher SNR) revealed CV_{ws} ≈5%, suggesting that increased SNR leads to better CV_{ws} when using GANNET (Mikkelsen et al., 2015).

In the present study, the CV_{ws} for $GABA_{H2O}$ and GABA/Cr in ACC were not statistically different between software packages. The CV_{ws} from LCModel and jMRUI (CV_{ws} ≈13-15%) are in agreement with values reported previously in the ACC (Mikkelsen et al., 2015; Wijtenburg et al., 2013). The CV_{ws} from GANNET (CV_{ws} ≈22%) is, however, higher than the previously reported values (Mikkelsen et al., 2015; Wijtenburg et al., 2013) probably due to lower SNR in our study, since CV_{ws} from GANNET – as suggested above – is SNR dependent. In the previous studies (Mikkelsen et al., 2015; Wijtenburg et al., 2013) the use of a multi-channel coil, larger voxel size, greater B_0 strength and higher number of averages would all contribute to higher SNR.

The scanning protocol for almost all subjects was such that GABA measurements in PAR were performed ≈15 minutes apart. Subjects were requested not to move during the scanning session as this could cause data to be acquired from an incorrect region. It is, however, feasible that subject motion may have occurred between the two acquisitions due to the length of the protocol, resulting in variations in GABA levels. The significant variation in GABA concentration from PAR could be due to differences in GABA concentration from neighbouring regions. Another possible reason could be the involvement of GABA in regulating circadian rhythm (Liu & Reppert, 2000) due to cyclical expression of clock genes in the PAR (Masubuchi et al., 2000). Future research to assess diurnal stability of GABA levels in the PAR will be valuable.

The long scan time (about an hour) may have rendered it difficult for subjects to remain motionless. The risk of inter-scan motion was minimized by placing close fitting pillows or soft pads around the subjects' heads and a marker in front of their eyes to aid them in maintaining their position. The long scan duration was largely due to the long TR (4s) that was required to reduce specific absorption rate (SAR) due to the strong OVS pulses. Long TRs ranging between 4 s and 5 s have

been implemented successfully in previous studies and have been shown to result in improved SNR (Puts et al., 2013; Saleh et al., 2016).

4.6 CONCLUSION

GABA concentrations are reproducible (CV_{ws}: ≈13-22%) using a shim and motion corrected MEGA-SPECIAL sequence with three different software packages in both the ACC and PAR, using either absolute concentrations or ratios relative to Cr. GABA levels were, however, significantly lower for the second measurements in PAR. This study shows the potential of quantifying pure GABA using any of the three available software packages to determine its relationship with pathology and healthy behaviour.

4.7 ACKNOWLEDGEMENTS

Support was provided by the NRF/DST South African Research Chairs Initiative, NIH grant R01HD071664 and the South African Medical Research Council (MRC).

Chapter 5 Effects of Tissue and Gender on Macromolecule suppressed GABA acquired by Motion and Shim navigated MEGA-SPECIAL[1]

Muhammad G. Saleh[2], Jamie Near[3], A. Alhamud[2], André J.W. van der Kouwe[4], Ernesta M. Meintjes[2]

5.1 ABSTRACT

The aims of this study are to implement a motion and shim navigated MEGA-SPECIAL sequence to determine the ratio of grey to white matter (GM/WM) concentration of GABA and compare with literature values, and to investigate gender-related differences in GABA in healthy subjects. 20 healthy subjects were scanned. For every subject, two acquisitions were performed for each of two regions, the anterior cingulate cortex (ACC) and medial-parietal cortex (PAR), with the order interleaved. Absolute GABA ($GABA_{H2O}$) and GABA/Cr concentrations were measured using LCModel. LCModel fitting revealed an overall average Cramer-Rao Lower Bound ≈10%. The GM/WM concentrations of $GABA_{H2O}$ and GABA/Cr were 3 and 1.5, respectively, in agreement with literature. The ACC revealed no gender-related differences in GABA. The PAR revealed time-related changes in concentrations of GABA in male participants and thus gender-related differences. The higher GM/WM concentrations of GABA found in this study and literature might be reflective of heterogeneous distribution of GABA around the brain. The gender- and time-related differences in the PAR emphasize that gender- and time-matching are critical for GABA scans.

5.2 INTRODUCTION

γ-aminobutyric acid (GABA) is the primary inhibitory neurotransmitter accounting for almost half of synaptic activity. Measuring GABA is becoming increasingly important due to its relationship with several neurological conditions, including epilepsy (Yamamoto et al., 1985), motor disorders (Jacobson et al., 2011), alcohol and drug abuse (Ticku, 1990) and diseases (Bai et al., 2014; Wong et al., 2003). GABA concentrations are also correlated with changes in blood-oxygen level dependent (BOLD) functional magnetic resonance imaging (fMRI) and cerebral blood flow (CBF)-weighted arterial spin labelling (ASL) (Donahue et al., 2010; A. D. Harris et al., 2015;

[1] Chapter written as an article intended for review and publication
[2] University of Cape Town
[3] McGill University
[4] Massachusetts General Hospital, Harvard Medical School

Muthukumaraswamy et al., 2009). Temporal changes in GABA are observed in motor learning (Floyer-Lea et al., 2006) and working memory (Michels et al., 2012) tasks.

In vivo measurements of GABA are challenging; firstly, GABA concentrations are an order of magnitude lower than that of other metabolites like NAA (1mM vs 10mM), resulting in difficult and ambiguous detection. Secondly, the GABA resonances overlap with other peaks, such as creatine (Cr), rendering direct observation impossible. Therefore, GABA acquisitions are performed using single voxel (SV) spectral editing techniques, such as MEGA-SPECIAL (Near et al., 2011), which separate C4-GABA at 3 ppm from Cr. Several studies acquire C4-GABA without macromolecule (MM) suppression, commonly referred to as GABA+, and relate levels to neurological diseases and disorders (Bai et al., 2014; Levy & Degnan, 2013; Long et al., 2013; Wong et al., 2003; Yamamoto et al., 1985). Recent studies that demonstrated very low to no correlation between GABA and GABA+ raise concerns that differences between healthy and diseased subjects could be driven by differences in MM levels (Harris et al., 2014). Acquiring MM-suppressed GABA is, however, challenging because of its strong dependence on magnetic field homogeneity (B_0), which can be hampered by subject motion and B_0inhomogeneity. A motion and shim navigated MEGA-SPECIAL sequence has recently been demonstrated that acquires a J-edited spectrum with superior spectral and fitting quality, permitting accurate quantification of MM-suppressed GABA (Saleh et al., 2016).

In the healthy human brain, the concentration of GABA is highly heterogeneous (Rothman et al., 1993). Due to the low signal to noise ratio (SNR) of the GABA peak in the spectrum from the single voxel (SV) J-editing sequences that are commonly employed (Puts & Edden, 2012), large voxels that include different tissue types are typically required. To determine tissue-specific GABA concentrations, the fractions of grey matter (GM), white matter (WM) and cerebrospinal fluid (CSF) in the voxel need to be quantified. The ratio of GABA concentrations in GM to WM (GM/WM) has previously been quantified across the brain using 2D chemical shift imaging (CSI) (I.-Y. Choi et al., 2006; Jensen et al., 2005). In this study we compare GM/WM ratios of GABA concentration in anterior cingulate and medial parietal cortices obtained using a SV J-editing sequence with reported values.

Further, studies investigating the effect of neurological conditions on GABA+ concentrations usually involve a cohort of mixed-gender healthy controls and potential gender-related differences are typically not considered. Gender-related differences in GABA+ have been demonstrated in healthy participants. For example, O'Gorman et al. and Sanacora et al. respectively showed that GABA+ levels differ in males and females in dorsolateral prefrontal cortex (DLPFC) and occipital cortex (OCC) (O'Gorman et al., 2011; Sanacora et al., 1999). In contrast, Gao et al. (Gao et al.,

2013) found no gender differences in GABA+ in anterior cingulate and medial parietal regions. These differences may be due to regional variations in GABA+. The fact that the relative contribution of MM to the total GABA+ signal varies from 40% to 60% in individuals (Harris et al., 2014; Near et al., 2011), and may differ in different regions, may further impact the results (O'Gorman et al., 2011; Sanacora et al., 1999). To date, only one study has investigated gender-related differences in MM-suppressed GABA and only in one region (Aufhaus et al., 2013). The absence of gender differences in GABA in the anterior cingulate cortex found in that study (Aufhaus et al., 2013) needs to be validated and it is required to establish whether this result persists over different brain regions.

The aims of this study were therefore to use a motion and shim navigated MEGA-SPECIAL sequence (i) to determine in anterior cingulate and medial parietal regions the relative concentration of GABA in GM compared to WM (for both water and Cr internal references), and (ii) to investigate gender differences in GABA levels in healthy subjects in both these regions.

5.3 METHODS

All protocols and experiments were approved by the Human Research Ethics Committee of the Faculty of Health Sciences at the University of Cape Town and written informed consent was obtained from all subjects. All MRI/MRS experiments were performed on a Siemens Allegra 3 T scanner (Erlangen, Germany) using a single channel transmit/receive (T/R) volumetric coil.

5.3.1 Subjects

20 healthy subjects (10 female; age: 23 ± 2 years (mean ± SD)) were recruited for the study, with no history of neurological or psychiatric disorders. Two J-edited spectra were acquired from each of two regions(Figure 5.1), the anterior cingulate cortex (ACC) and medial-parietal cortex (PAR), with the order interleaved.

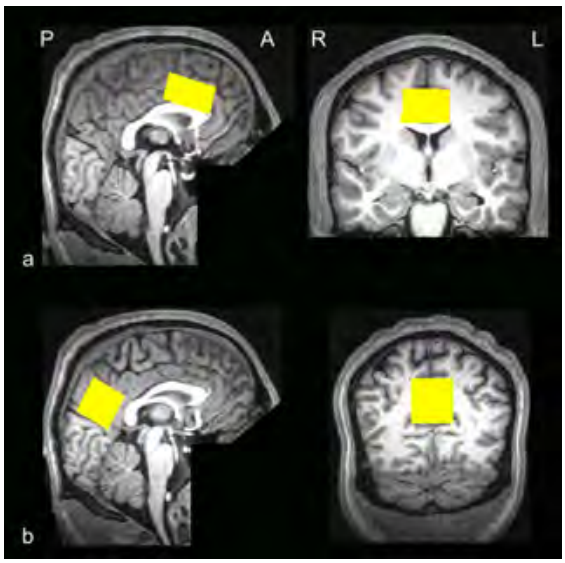

Figure 5.1: Voxel localization on T1 structural image for (a) anterior cingulate cortex (ACC) and (b) medial parietal cortex (PAR). The acquisitions were performed in an interleaved manner. A: Anterior. P: Posterior. R: Right. L: Left.

5.3.2 MR imaging and MR spectroscopy acquisition

Prior to voxel placement, three-dimensional (3D) T1-weighted sagittal scans of the subjects' brains were acquired using MEMPRAGE (van der Kouwe et al., 2008) with 1.3 × 1.0 × 1.0 mm^3 resolution for accurate voxel placement.

The C4-GABA edited spectra were derived from the motion and shim navigated MEGA-SPECIAL sequence without MM contamination, as explained previously (Saleh et al., 2016). Briefly, there are two iterations of MEGA-editing. In the first iteration, the editing-band is applied to the C3-GABA resonance at 1.9 ppm (edit-on), while in the second iteration the editing-band is applied at 1.5 ppm (edit-off). The water suppression band of the dual-banded editing pulses was always applied at 4.7 ppm.

The MEGA-SPECIAL parameters were as follows: TR/TE 4000/68 ms, bandwidth 2 kHz, 160 averages, 2048 readout samples and four dummy scans; scan duration 11 min. The voxel sizes were: ACC: 20 × 30 × 40 mm^3 and PAR: 30 × 30 × 30 mm^3, respectively. Prior to all acquisitions, outer volume suppression (OVS) pulses were applied to saturate spins outside the VOI (Near et al., 2011). Finally, water unsuppressed data with four averages were acquired from every region.

5.3.3 Post-processing

The T1 images of every subject were segmented using SPM12's New Segment (Ashburner & Friston, 2005). Subsequently, the segmented images were multiplied by a mask representing the

voxel to determine fractions of GM (f_{GM}), WM (f_{WM}), and CSF (f_{CSF}) in the voxel and to compute GM ratio (GM_{ratio}), defined as the fraction of brain tissue that is GM ($GM_{ratio}=f_{GM}/(f_{GM}+f_{WM})$).

5.3.3.1 Frequency and Phase correction

The subspectra from interleaved SPECIAL inversion-on/off acquisitions were subtracted resulting in edit-on/off spectra. The motion corrupted edit-on/off spectra were removed as described previously (Saleh et al., 2016). Subsequently, eddy current correction (Klose, 1990) was applied, followed by frequency correction using the position of the Cr peak to reduce line broadening arising from minor frequency drifts, as described previously (Fuchs et al., 2013). The averaged edit-on and edit-off spectra were manually frequency aligned and phase adjusted to minimize the choline difference signal (Near et al., 2014). This was followed by removal of residual water (A. Hess et al., 2014) and DC offset (Stagg et al., 2009; Zhu et al., 2011). Two ACC and two PAR spectra were rejected from both males and females due to a large residual choline artefact. Finally, fully processed edit-on/off spectra were subtracted to generate GABA-edited spectra (Figure 5.2).

5.3.3.2 Spectral Analysis

The GABA-edited spectra were analysed using LCModel version 6.3-1E (Provencher, 2001) using a simulated basis set (Figure 5.3) that was generated by FID-A toolbox (O'Gorman et al., 2007). Tissue water (H_2O) and total creatine (Cr: creatine + phosphocreatine) were used as internal concentration references. Water concentration (*WCONC*) along with partial volume correction (Provencher, 2005) was estimated using

$$WCONC = \frac{43300 f_{GM} + 35880 f_{WM} + 55556 f_{CSF}}{1 - f_{CSF}}$$

where f_{GM} is the fraction of grey matter, f_{WM} is the fraction of white matter, and f_{CSF} is the fraction of CSF. Absolute concentrations of GABA ($GABA_{H2O}$) and total creatine (Cr_{H2O}) were determined. Absolute concentrations are reported in institutional units (i.u). GABA/Cr is defined here as the ratio of the absolute concentration of GABA ($GABA_{H2O}$) from the edited spectrum to the absolute concentration of creatine (Cr_{H2O}) from the edit-off spectrum. All concentrations and ratios were corrected for T1 and T2 relaxation effects using published values (R. Edden, Intrapiromkul, et al., 2012; Mlynárik et al., 2001; Puts et al., 2013). Cramer-Rao Lower Bounds (CRLB) from LCModel were used as a measure of spectral quality and GABA fit error.

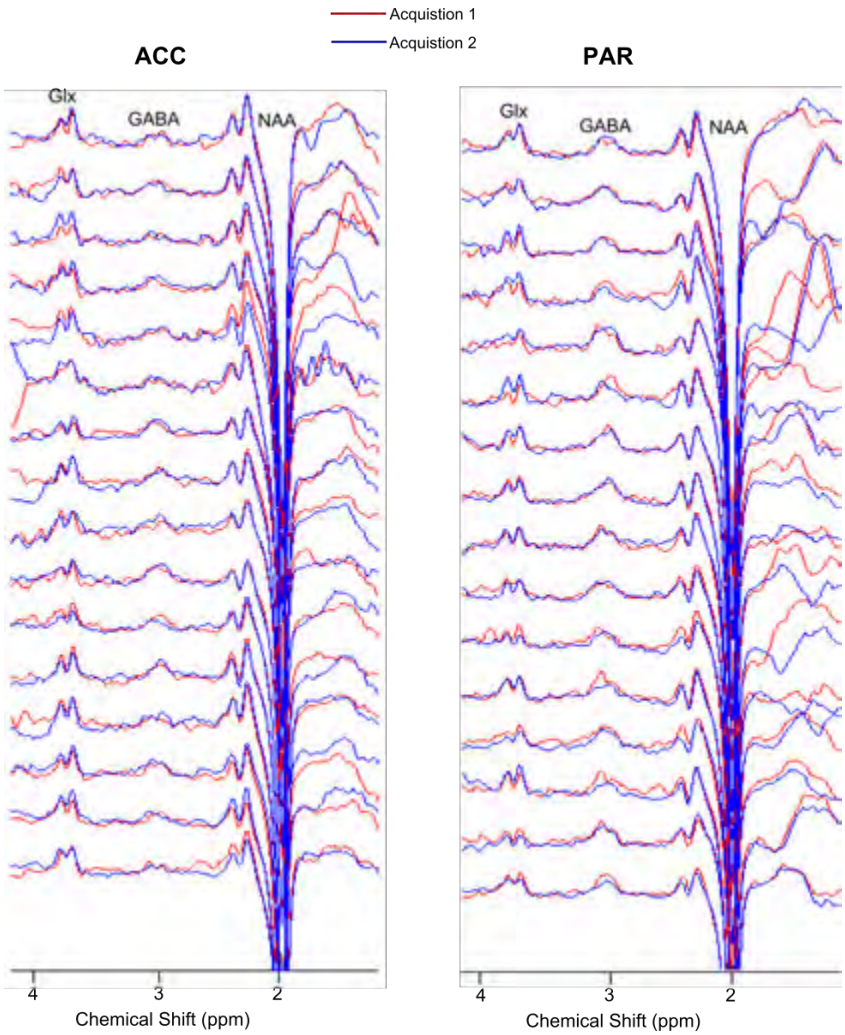

Figure 5.2: GABA-edited spectra from ACC (left) and PAR (right). GABA is clearly observed at 3 ppm. Other visible metabolites include Glx (Glutamate+Glutamine) at 3.75 ppm and inverted NAA at 2 ppm. Apodization using a 5 Hz Lorentzian filter was applied to the spectra.

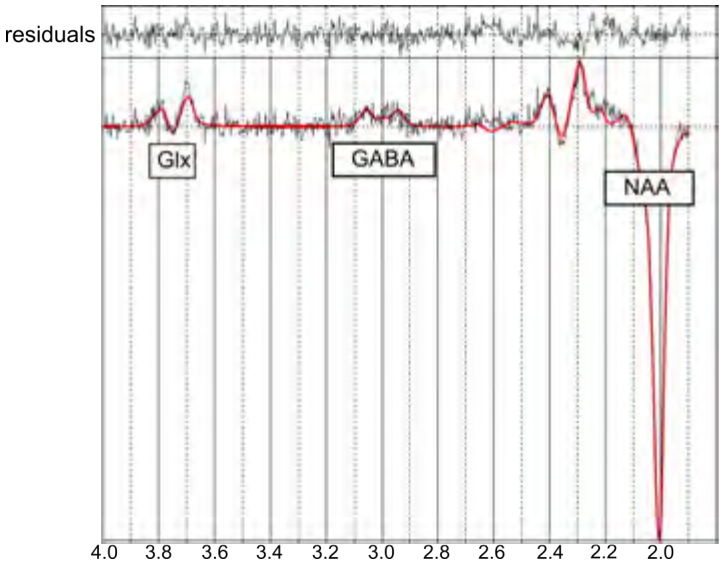

Figure 5.3: LCmodel fit of GABA at 3 ppm, Glx (Glutamate + Glutamine) at 3.75 ppm and NAA at 2 ppm.

5.3.4 Statistical analysis

All measures were normally distributed (Shapiro-Wilk test), except for $GABA_{H2O}$ and GABA/Cr in the ACC. Non-normally distributed data were inverted ($1/GABA_{H2O}$ and 1/(GABA/Cr)) following the procedure described in (Pallant, 2001).

5.3.4.1 GABA levels for pure GM and WM

f_{GM}, f_{WM}, f_{CSF} and GM_{ratio} were averaged in each region, as well as for males and females separately in each region. Gender-related differences were examined in each brain region using unpaired t-tests with unequal variance assumed.

Pearson correlation was used to examine associations between levels of $GABA_{H2O}$ or GABA/Cr and GM_{ratio}. Data from all acquisitions for all participants and in both regions were used for this analysis. Linear regression analysis was performed to determine GM and WM concentrations of $GABA_{H2O}$ and GABA/Cr, as shown in previous works (C. Choi et al., 2007; I.-Y. Choi et al., 2006; Jensen et al., 2005). The levels of $GABA_{H2O}$ and GABA/Cr in pure GM and WM were estimated by plotting $GABA_{H2O}$ and GABA/Cr against GM_{ratio} and fitting a linear least squares line. The pure GM and WM concentrations of $GABA_{H2O}$ and GABA/Cr were then estimated by extrapolating the regression line to GM_{ratio} equal to 1 and 0, respectively.

5.3.4.2 Effects of Gender and Time on GABA levels

Gender-related differences in $GABA_{H2O}$ and GABA/Cr were examined using two-way analysis of variance (ANOVA) for repeated measures (SPSS 22 software package), with time as the repeated measure. Post hoc tests with Bonferroni correction were performed to compare effects of time and gender on $GABA_{H2O}$ and GABA/Cr.

Unless stated otherwise, all values are henceforth reported as mean ± standard error of mean (SEM) and the error bars represent ± SEM.

5.4 RESULTS

A total of 64 spectra were analysed, 32 from male and 32 from female participants, of which half were in the ACC and half in the PAR. Figure 5.2 shows the J-edited spectra from the two acquisitions performed in each participant for ACC and PAR. Figure 5.3 shows a typical LCModel fit of the J-edited spectrum. Low residuals indicate a good fit. Moreover, average CRLB from male and female participants were not significantly different for both ACC (male: 9.8 ± 0.3% and female: 10.6 ± 0.6%, $p = 0.28$) and PAR (male: 8.6 ± 0.3% and female: 9.3 ± 0.3%, $p = 0.19$).

Table 5.1: Comparison of tissue fractions (Mean ± SEM) in males and females in ACC and PAR

		Male	Female	Allsusbjects
ACC	f_{GM}	0.59 ± 0.02*	0.54 ± 0.01	0.57 ± 0.01
	f_{WM}	0.36 ± 0.01*	0.42 ± 0.01	0.39 ± 0.01
	f_{CSF}	0.06 ± 0.01*	0.03 ± 0.01	0.05 ± 0.00
	GM_{ratio}	0.62 ± 0.01*	0.56 ± 0.01	0.59 ± 0.01
PAR	f_{GM}	0.64 ± 0.01*	0.60 ± 0.01	0.62 ± 0.01
	f_{WM}	0.30 ± 0.01*	0.34 ± 0.01	0.32 ± 0.01
	f_{CSF}	0.06 ± 0.01	0.05 ± 0.00	0.06 ± 0.00
	GM_{ratio}	0.68 ± 0.01*	0.64 ± 0.01	0.66 ± 0.01

*Denotes significant (p<0.05) differences between males and females.

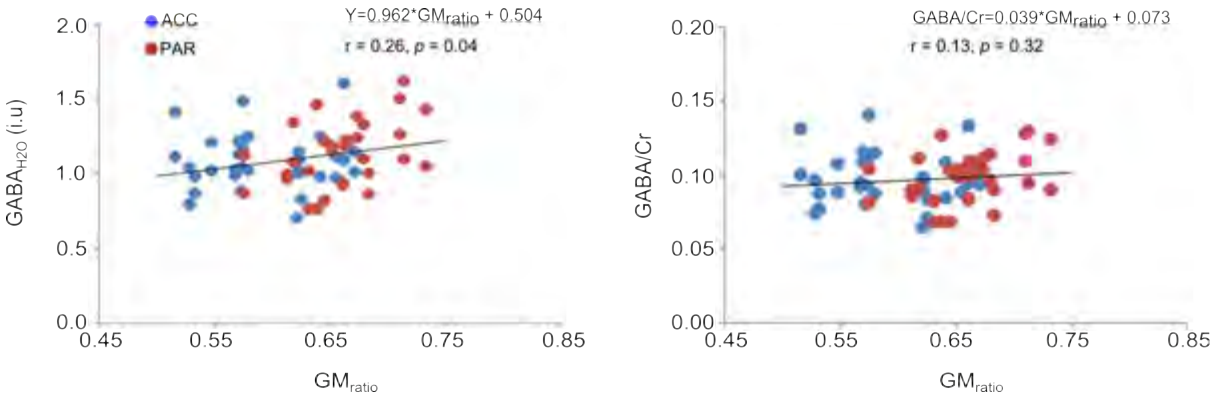

Figure 5.4: Linear regression analysis to determine, by extrapolation, $GABA_{H2O}$ (left) and GABA/Cr (right) in pure GM (GM_{ratio}=1) and WM (GM_{ratio}=0). i.u: institutional units. GM_{ratio}: grey matter ratio. *r*: Pearson's correlation coefficient.

GABA levels for pure GM and WM

Table 5.1 shows the mean tissue fractions for the voxels in ACC and PAR. In both regions, male participants had significantly higher f_{GM} and GM_{ratio} than female participants. The fraction of CSF was higher in males only in the ACC voxel.

Associations of $GABA_{H2O}$ and GABA/Cr with GM_{ratio} are shown in Figure 5.4. In this analysis data from ACC and PAR were combined and no gender differences were assumed. Increasing GM_{ratio} was associated with higher $GABA_{H2O}$ (r=0.26, p = 0.04). From the plot of $GABA_{H2O}$ vs GM_{ratio}, $GABA_{H2O}$ of pure GM (GM_{ratio}=1) was found to be 1.47 ± 0.17 i.u, while $GABA_{H2O}$ of pure WM

(GM_{ratio}= 0) was 0.50 ± 0.28 i.u. Similarly, GABA/Cr of pure GM was found to be 0.112 ± 0.015, while GABA/Cr of pure WM was 0.073 ± 0.024. These results yield GM to WM ratios (GM/WM) for $GABA_{H2O}$ and GABA/Cr of 2.94 and 1.53, respectively.

Effects of Gender and Time on GABA levels

In the ACC, there were no statistically significant differences in $GABA_{H2O}$ (male: 1.14 ± 0.07 i.u vs female:1.02 ± 0.06 i.u, F(1,14) = 3.38, p= 0.09) or GABA/Cr (male: 0.101 ± 0.006 vs female: 0.092 ± 0.006, F(1,14) = 2.31, p= 0.15) between male and female participants. In contrast, in PAR both $GABA_{H2O}$ (male: 1.23 ± 0.08 i.u vs female: 1.04 ± 0.06 i.u, F(1,14) = 8.99, p = 0.01) and GABA/Cr (male: 0.104 ± 0.007 vs female: 0.091 ± 0.005, F(1,14) = 5.58, p = 0.03) were significantly higher in males compared to females.

The effect of time (Acquisition 1 (Acq 1) vs Acquisition 2 (Acq 2)) on $GABA_{H2O}$ and GABA/Cr was examined in both regions. In the ACC, there was no effect of time for $GABA_{H2O}$ (F(1,14) = 0.01, p = 0.93) or GABA/Cr (F(1,14) = 0.05, p = 0.83), while in PAR there was a significant effect of time for both $GABA_{H2O}$ (F(1,14) = 17.84, p< 0.01) and GABA/Cr (F(1,14) = 15.40, p< 0.01).

Figure 5.5a shows estimated marginal means of $GABA_{H2O}$ and GABA/Cr in PAR for each acquisition, revealing significantly larger gender-related differences in both $GABA_{H2O}$ (male: 1.39 ± 0.05 vs female: 1.08 ± 0.06, p < 0.01) and GABA/Cr (male: 0.12 ± 0.01 vs female: 0.09 ± 0.01, p < 0.01) for the first acquisition compared to the second acquisition. Figure 5.5b shows for males and females separately how $GABA_{H2O}$ and GABA/Cr levels differ between the first and second acquisitions in PAR. Post hoc tests using Bonferroni correction revealed that $GABA_{H2O}$ (Acq 1: 1.39 ± 0.05 vs Acq 2: 1.07 ± 0.06, *p(Bonf)*< 0.01) and GABA/Cr (Acq 1: 0.117 ± 0.005 vs Acq 2: 0.094 ± 0.005, *p(Bonf)*< 0.01) differ significantly between acquisitions in the male participants *only*.

5.5 DISCUSSION

Several studies have acquired GABA from different brain regions using 2D J-resolved chemical shift imaging (CSI), multiple quantum filtering (MQF) CSI and single voxel (SV) J-editing techniques (Bhattacharyya et al., 2011; I.-Y. Choi et al., 2006; Jensen et al., 2005). The J-editing SV sequences (SVS) are widely implemented due to conceptual simplicity and ease of implementation (Puts & Edden, 2012). However, acquiring GABA without MM is challenging as it requires editing pulses to be consistently applied symmetrically about 1.7 ppm to adequately suppress MM, which can be hampered by subject motion and B_0 inhomogeneity. The other possible means of removing MM is by subtracting MM – attained by a separate metabolite nulled scan using

an inversion pulse prior to MEGA-PRESS – from the GABA spectrum, as demonstrated by Terpstra et al. (Terpstra et al., 2002). This technique, however, is more sensitive to motion because of the long scan time and subtraction of non-interleaved acquisitions (Mullins et al., 2012).

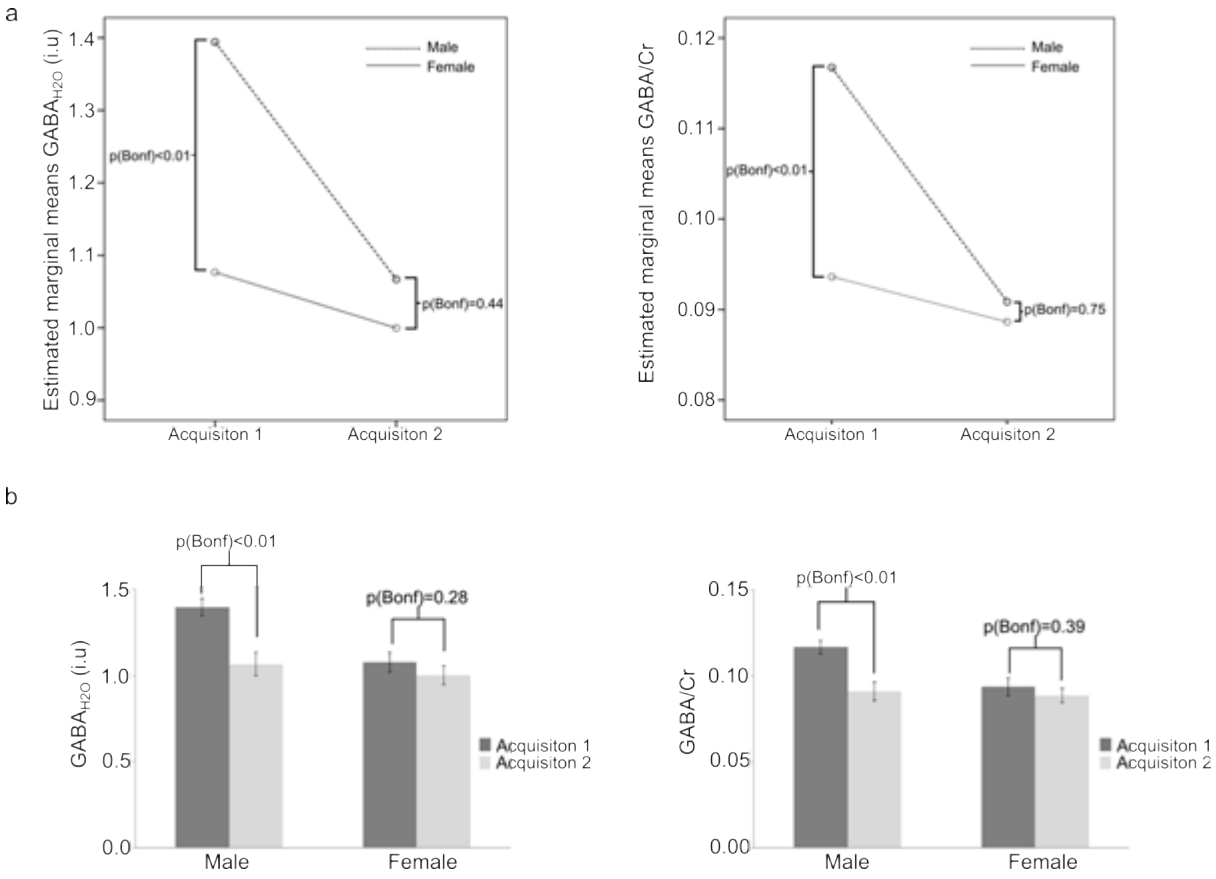

Figure 5.5: a) Estimated marginal means of $GABA_{H2O}$(left) and GABA/Cr (right) for males and females in medial parietal cortex (PAR) for the first and second acquisitions, showing significant gender differences only for the first acquisition. b) Effects of time on $GABA_{H2O}$ (left) and GABA/Cr (right) in PAR. Only male participants reveal significant differences between the two acquisitions. p_{Bonf}: Bonferroni corrected *p* values.

In this study, we implemented 3D EPI double (motion and shim) volumetric navigators in the SV MEGA-SPECIAL sequence (Saleh et al., 2016) to acquire GABA without MM contamination. The motion navigator permits data acquisition at the correct brain region, while the shim navigator enhances spectral quality and ensures that the frequency selective RF pulses are applied symmetrically about 1.7 ppm, as previously demonstrated (Saleh et al., 2016). It is evident upon visual inspection (Figure 5.2) that the spectra from both regions are of excellent quality and in agreement with previous GABA studies (ACC spectra from Figure 2 in (Mikkelsen et al., 2015) and PAR spectra from Figure 4 in (R. Edden, Puts, et al., 2012)).

The CRLB values from LCModel fitting indicate good reliability. Most studies use 20% as a rough criterion for acceptable reliability (Long et al., 2013; Provencher, 2005; Wijtenburg et al., 2013). In

our study, the maximum and overall average CRLB's are 15% and 10%, respectively. Both are well below the criterion and in agreement with values that have been reported in previous studies (Long et al., 2013; Wijtenburg et al., 2013).

In this study, linear regression analysis was employed to determine GABA concentrations in GM and WM. This method for extrapolating metabolite concentrations of pure GM (GM_{ratio}= 1) and WM (GM_{ratio} = 0) has been demonstrated in previous studies using CSI (I.-Y. Choi et al., 2006; Gasparovic et al., 2006; Jensen et al., 2005). The major benefit of CSI over SV spectroscopy (SVS) is that the former acquires a large number of data points (one per voxel) from a single acquisition compared to SVS and is therefore less susceptible to error. In our study, we performed repeated measures (4 per subject) to obtain sufficient data to effectively perform the analysis. For example, Jensen et al. performed the analysis using 68 data points (voxels) compared to the 64 data points in our study (Jensen et al., 2005).

I-Y Choi et al., through structural image based segmentation and non-linear least square fitting, reported about eight-fold higher $GABA_{H2O}$ (GM: 1.30 ± 0.36 mM vs WM: 0.16 ± 0.16 mM) and about five-fold higher GABA/Cr (GM: 0.16 ± 0.04 vs WM: 0.03 ± 0.03) in GM relative to WM across prefrontal and parietal regions using MQF CSI (I.-Y. Choi et al., 2006). Jensen et al., reported 2-fold higher $GABA_{H2O}$ (GM: 0.96 ± 0.24 mM vs WM: 0.44 ± 0.16 mM) in GM than WM across dorsolateral prefrontal and parieto-occipital regions using 2D J-resolved CSI (Jensen et al., 2005). The GM and WM concentrations of $GABA_{H2O}$ in Jensen et al., (Jensen et al., 2005) were derived from multiplying GM GABA/Cr with literature values of GM Cr_{H2O} (8.3 mM) and WM GABA/Cr with literature values of WM Cr_{H2O} (6.5 mM). Using this method with values for GABA/Cr in GM and WM from our study, yields a GM to WM ratio for $GABA_{H2O}$ of 1.7, which is comparable with the value of 2 reported by Jensen et al. C Choi et al. reported that $GABA_{H2O}$ levels in GM were about 3 times higher than in WM (GM: 1.1 ± 0.1 mM vs WM: 0.4 ± 0.1 mM) in prefrontal and left frontal cortices using SV localized double quantum filtering (DQF) (C. Choi et al., 2007).

Our study yielded three-fold higher $GABA_{H2O}$ in GM relative to WM, which is in close agreement with C Choi et al. (C. Choi et al., 2007), while GABA/Cr was about 1.5 times higher in GM compared to WM, similar to values reported by Jensen et al. (Jensen et al., 2005). Notably the latter agreement gets even better when using the method performed by Jensen et al. (Jensen et al., 2005) to derive $GABA_{H2O}$ in GM and WM, respectively. Caution should be taken when comparing results with those from literature as differences in approach could affect these. For example, the relatively larger GM $GABA_{H2O}$ and GABA/Cr found by I-Y Choi et al. (I.-Y. Choi et al., 2006) could be due to the non-linear least square estimation of the non-linear model implemented, in contrast with the

non-linear least square estimation of the linear model implemented here. Another possible reason could be the larger field of view chosen in their study (I.-Y. Choi et al., 2006) that encompassed brain regions, such as sensorimotor cortex (Bhattacharyya et al., 2011), with higher levels of GABA in GM relative to WM. Overall, the higher $GABA_{H2O}$ and GABA/Cr in GM found in the two regions examined in our study along with the disparate results from literature (C. Choi et al., 2007; I.-Y. Choi et al., 2006; Jensen et al., 2005) reflect the highly heterogeneous distribution of GABA in the human brain (Rothman et al., 1993).

Due to the low SNR of GABA, the SV sequences usually acquire data from large voxels of interest (VOI) inevitably comprising all tissue types (GM, WM, CSF). Acquiring data from any group of participants will most likely result in some degree of variation in tissue fractions. Given the aforementioned differences in GM and WM concentrations of GABA, the variations in tissue fractions would result in variances in GABA concentrations and could impact GABA-based evaluation of disease (A. Harris et al., 2015). Recently, Harris et al. demonstrated effects of differences in tissue fractions on $GABA+_{H2O}$ and developed a new technique involving a correction factor (α) – defined as the ratio of $GABA+_{H2O}$ in WM to GM – to minimize the dependence of $GABA+_{H2O}$ on tissue fractions (A. Harris et al., 2015). Harris et al. suggested an α value of 0.43 deduced using *in vivo* measurements of $GABA+_{H2O}$ in the OCC, DLPFC, sensorimotor cortex (SMC), frontal eye fields and auditory cortex (A. Harris et al., 2015). In this study, we suggest an α value of 0.34 - the ratio of $GABA_{H2O}$ in WM to GM – to adjust $GABA_{H2O}$ to correct for different tissue fractions.

While $GABA_{H2O}$ was associated with GM_{ratio}, GABA/Cr was not. However, Cr_{H2O} was found to be strongly associated with GM_{ratio} ($r = 0.53$, $p < 0.01$) and was about 1.6-fold higher in GM (GM: 13.20 ± 0.37 i.u vs WM: 8.38 ± 0.61 i.u) than in WM, similar to results of a previous study (Gasparovic et al., 2006). Since both $GABA_{H2O}$ and Cr_{H2O} were independently related to GM_{ratio}, the ratio of $GABA_{H2O}$ to Cr_{H2O} would reduce the dependence on GM_{ratio}. This is also reflected by the reduction in GM/WM concentrations of GABA/Cr to 1.5 from 3 for $GABA_{H2O}$. Since GABA/Cr is independent of GM_{ratio},Cr may be a suitable internal reference in MRS studies (Puts & Edden, 2012). This may, however, not be ideal for some neurological studies (Gruber et al., 2003), and thus $GABA_{H2O}$ can be used in such cases along with the aforementioned tissue correction technique (A. Harris et al., 2015).

Several studies have performed GABA-based evaluation of neurological conditions through GABA+ measurements (Levy & Degnan, 2013). The weak to no correlation between GABA+ and GABA could be due to the problems related with the MM suppression technique. This also suggests that GABA+ cannot be used as a substitute for underlying GABA (Harris et al., 2014; Mikkelsen et

al., 2015). Furthermore, observed gender-related differences in GABA+ (O'Gorman et al., 2011; Sanacora et al., 1999) may be attributable to varying levels of MM (≈40-60%) in individuals (Harris et al., 2014; Near et al., 2011). To our knowledge, only one study has examined gender differences in MM-suppressed GABA in only one region, namely ACC. This study found no gender-related differences (Aufhaus et al., 2013).

In our study we also found no gender differences in GABA in the ACC. In contrast, males had higher GABA and GABA/Cr in PAR. These results, together with those from previous studies showing gender-related differences in GABA+ in the DLPFC and OCC (O'Gorman et al., 2011; Sanacora et al., 1999), provide evidence that effects of gender on GABA levels may vary regionally. Furthermore, the fact that gender-related differences have been observed in both GABA+ and GABA may indicate that contributions from MM are similar in males and females so that gender differences are not impacted. Future research assessing the levels of MM in different regions of the brain in both male and female participants is necessary.

Since each acquisition was repeated twice in each subject in our study (with the start of repeated acquisitions separated by about 15 minutes), we performed ANOVA with repeated measures to examine gender effects. Notably, there was an effect of time only in males and only in PAR. The absence of an effect of time in ACC suggests concentrations of GABA in ACC are stable over time in both male and female participants. In contrast, GABA levels in PAR were stable over time in females, while concentrations in males decreased significantly from the first to the second acquisition, with GABA levels for the second acquisition being similar to those of females. This lack of stability in GABA levels in PAR in males does not appear to be due to dissimilar tissue fractions between genders or regions, since tissue fractions between males and females differed significantly in both ACC and PAR, and GM_{ratio}'s were higher in PAR for both sexes (Table 5.1).

The neurophysiological reasons for the decreasing GABA levels with time in males in PAR are not yet fully understood. Neuroactive steroids, including ovary-produced progesterone and testis-produced testosterone, are known to have modulatory effects on the release of neurotransmitters, including GABA (Zheng, 2009). The mechanisms by which the modulatory effects occur are complex and may depend on many factors, including type of neuroactive steroids, and may vary by region (Zheng, 2009). The observed effect of time on gender differences could be due to the neuroactive steroidal-related modulation of GABA, however further studies are needed to determine correlation between concentrations of GABA and plasma hormone levels.

Another possible reason could be the involvement of GABA in regulating circadian rhythm (Liu & Reppert, 2000) due to the presence of clock genes in the parietal cortex (Masubuchi et al., 2000). Duffy et al. demonstrated using measurements of core body temperature and plasma melatonin that the intrinsic circadian period is significantly shorter in women than in men (Duffy et al., 2011). This difference may explain the absence in females of the changes in GABA levels observed in males with time. In the present study, these time-related changes in GABA levels were observed over a period of about 40 minutes. It is possible that GABA levels may be stable at certain times of day, as demonstrated previously for GABA+ in OCC and SMC (Evans et al., 2010).

Given the neuroactive steroidal-related modulation of GABA, GABA-based regulation of circadian rhythm and gender-related differences in circadian rhythm, it would be beneficial to investigate diurnal stability of GABA along with plasma hormone levels in both male and female participants in future research. The diurnal measurements of GABA could provide information as to the time of day when GABA levels are stable, thus facilitating investigations of alterations in GABA associated with neurological conditions.

The scanning protocol for almost all subjects was such that GABA measurements in PAR were performed ≈15 min apart. Subjects were requested not to move during the scanning session as this could cause data to be acquired from an incorrect region. It is, however, possible that males are less able to keep their head still over time, since substantial variation in GABA levels are observed in male participants only.

It has been shown previously that heating of the iron shim coils throughout gradient-intensive scanning (such as diffusion tensor imaging or BOLD fMRI) will cause frequency drifts of up to 15 Hz over roughly 6 minutes of scanning, which will increase further over time with repeated acquisitions (Alhamud et al., 2016; Harris et al., 2013). Since the data acquired in the present scans were typically not the first scans of the day, it is therefore possible that such heating may have occurred, resulting in gradient-induced frequency shifts, and that this may be the reason for the time-changing GABA measurements observed in PAR in males. However, since all participants (males and females) were scanned in an interleaved manner and the PAR region was scanned second and last in all subjects (except for two males in whom PAR acquisitions were done before ACC acquisitions), we do not believe that this is the reason for the observed time-related changes in GABA levels in males in PAR, since prior heating would have affected the first ACC acquisitions most severely (Harris et al., 2013). This change in GABA in PAR was also not evident in females in whom the same scanning order was used. Prospective shim correction employed here would further ensure correct frequency settings for these acquisitions despite potential drift from heating of the shim coils (Saleh et al., 2016).

Although the outcomes of our study might be limited by small sample size, previous studies demonstrating tissue-specific concentrations of GABA and effects of gender on GABA used similar sample sizes (Gasparovic et al., 2006; Jensen et al., 2005; O'Gorman et al., 2011; Sanacora et al., 1999). In this study, the ACC and PAR regions were selected due to the role of GABA in several neurological conditions where these regions are implicated (Bai et al., 2014; Puts & Edden, 2012). Future research should involve other regions of the brain, such as OCC, SMC and DLPFC, due to their important role in both healthy behaviour and pathology (Puts & Edden, 2012), especially in view of the fact that alterations in GABA appear to be region specific.

5.6 CONCLUSION

The motion and shim navigated MEGA-SPECIAL sequence acquired data with superior quality from both ACC and PAR regions, allowing us to determine tissue-specific $GABA_{H2O}$ and GABA/Cr, and to investigate gender-related differences in $GABA_{H2O}$ and GABA/Cr. The higher $GABA_{H2O}$ and GABA/Cr in GM reflect the heterogeneous distribution of GABA in the brain. The gender difference in GABA observed in PAR, and how it changes over time, emphasizes the importance of not only gender- but also time-matching when evaluating changes in GABA in neurological conditions.

5.7 ACKNOWLEDGEMENTS

Support was provided by the NRF/DST South African Research Chairs Initiative, NIH grant R01HD071664 and the South African Medical Research Council (MRC).

Chapter 6 Discussion

In this work, we presented a motion and shim corrected MEGA-SPECIAL sequence for accurate quantification of MM-suppressed GABA. Reproducibility (over a period of about 40 minutes) of GABA measurements was highest for LCModel processing. GABA levels in ACC did not change over time, while GABA levels in PAR decreased over time. Although GABA levels did not differ between males and females in ACC, they were higher in males in PAR. This difference was only present in the first acquisition, as GABA levels in PAR decreased significantly for the second acquisition in males *only*.

GABA is the primary inhibitory neurotransmitter in the brain and accounts for almost half of the synaptic activity (Levy & Degnan, 2013). Measurement of GABA is becoming increasingly important due to its link with neurological conditions (Levy & Degnan, 2013; Mullins et al., 2012; Puts & Edden, 2012). At the University of Cape Town (UCT) there has been a long-standing interest in studying learning deficits in children with prenatal alcohol exposure and the ability to measure changes in GABA during learning tasks – such as motor learning (Floyer-Lea et al., 2006) or eyeblink conditioning (Jacobson et al., 2011) – could provide new insights into the physiological basis of these learning deficits.

In vivo measurement of GABA is challenging because of the low signal to noise ratio (SNR), and overlap with macromolecules (MM) and more concentrated metabolites, such as NAA and Cr, rendering direct observation challenging (Mullins et al., 2012; Puts & Edden, 2012). Consequently, spectral editing methods, such as MEGA-SPECIAL and MEGA-PRESS (Mescher et al., 1998; Near et al., 2011), are typically implemented that separate GABA at 3 ppm (C4-GABA) from overlapping metabolites. Removal of MM is challenging and most studies acquire GABA with MM, commonly referred to as GABA+ (Mullins et al., 2012; Puts & Edden, 2012). Other approaches to acquire GABA, such as acquisition at higher field strengths, are not feasible due to the fact that high-field scanners (> 3 T) are not widely available and have not been optimised for routine clinical use (Ke et al., 2000).In this study, we implemented an optimised motion and shim corrected single voxel (SV) MEGA-SPECIAL (Near et al., 2011) sequence and used it to acquire GABA without MM contamination.

Compared to the more widely used MEGA-PRESS sequence, MEGA-SPECIAL demonstrates reduced spatial variations within the volume of interest (VOI) and yields a 10% improvement in editing efficiency of GABA (Near et al., 2011). However, At the same TR, the MEGA-SPECIAL

sequence requires twice the time to localize a VOI compared to MEGA-PRESS ((Near et al., 2011)), rendering it more sensitive to subject motion. Since the GABA signal suffers from low SNR, a large number of measurements are required, further increasing the scan time and sensitivity to motion and B_0 inhomogeneity. These limitations have been addressed in this study by implementing a technique involving pairs of three-dimensional (3D) echo planar imaging (EPI) volumetric navigators to correct in real time for subject motion and B_0 inhomogeneity throughout the acquisition.

In vitro phantom scans demonstrated that the individual shim terms affect the final edited spectra differently. Manually added frequency offsets of 15 Hz led to substantial subtraction artefacts, while manually added first-order shim distortions of 10 μT led to severe line broadening and loss of the pseudo-doublet pattern of the GABA peak. These results suggest that subtraction artefacts are caused by frequency drifts, while broadening of peaks and loss of multiplet structure may be due to first-order shim terms.

Spectra acquired *in vivo* demonstrated that subject motion can lead to artefacts beyond the commonly reported choline artefact (Evans et al., 2013; Harris et al., 2013), and that larger head motion can cause severe spectral distortions. Furthermore, motion-related effects could be present in edit-on or edit-off spectra without prominent artefacts in the edited spectra, so that referencing GABA relative to metabolites from the edited spectra should be done with extreme caution (Durst et al., 2015).

Most MRS studies rely on spectral linewidth (FWHM) and SNR as indices for spectral quality (Hess et al., 2011; Keating & Ernst, 2012; Kreis, 2004). In GABA MRS, FWHM values of GABA ranging between 0.11 ppm and 0.19 ppm are considered indicative of good spectral quality (Bhattacharyya et al., 2007; Harris et al., 2014; Mescher et al., 1998). However, in the present study GABA spectra acquired in the presence of limited motion (< 3.1°) without any correction yielded a similar range of FWHM values (0.12-0.14 ppm), indicating that FWHM of GABA as a measure of spectral quality should be used with caution. Similarly, SNR from the GABA scans could be misleading (Dharmadhikari et al., 2015) due to signal elevations arising from inadequate suppression of MM due to motion-related frequency drift.

In view of the above, we recommend that GABA-edited spectra should be assessed quantitatively – through indices such as Cramer-Rao Lower Bounds in LCModel , fitting error in GANNET or Cramer-Rao standard deviation in jMRUI – and visually to ensure reliable concentration

quantification, as explained in (Dharmadhikari et al., 2015; R. A. Edden et al., 2013; Gao et al., 2013; Kreis, 2004; Provencher, 2001, 2005).

Several methods are used to gauge the quality of data, including CRLBs that provide a measure of how well the fitting algorithm could fit the data (Kreis, 2004). It is standard practice to reject GABA+ measurements with relative CRLB values – expressed as a percentage of the estimated area or concentration of the metabolite – exceeding 20% (Long et al., 2013; Wijtenburg et al., 2013). However, GABA will typically have higher relative CRLBs than GABA+, which should be interpreted with caution as this could be the result of a decrease in concentration rather than being indicative of a less reliable fit (Kreis, 2016).

Motion-related frequency drifts can severely compromise spectral editing during GABA acquisition especially when scanning paediatric and patient populations (Alhamud et al., 2015; A. T. Hess et al., 2014) resulting in MM contamination in the edited GABA signal. The present study provides an efficient technique that mitigates motion-related frequency drifts and permits symmetric editing of C4-GABA without MM contamination. Since previous studies have demonstrated weak to no relationship between GABA+ and GABA, there is no support for using GABA+ as a substitute for underlying GABA (Harris et al., 2014; Mikkelsen et al., 2015), and MM suppression is recommended. Further, differences in levels of MM have been observed in patients with tumours, multiple sclerosis and stroke (Graham et al., 2001; Howe et al., 2003; Mader et al., 2001), and age-related decreases of GABA+ (Gao et al., 2013) did not persist when MM were suppressed (Aufhaus et al., 2013).

A previous study involving a cohort of 8 participants (1 female) reported diurnal stability of GABA+ in occipital cortex (OCC) and sensorimotor cortex (SMC) (Evans et al., 2010). In view of the differences in stability of GABA levels over time found between males and females in PAR *only* in our study, it may not be appropriate to extrapolate these results to females in general, or to other brain regions. For instance, GABA levels in regions such as suprachiasmatic nucleus and PAR have been shown to exhibit changes that may be associated with the control of circadian rhythms (Liu & Reppert, 2000; Masubuchi et al., 2000). Some studies also choose to exclude female participants due to reported variations in GABA+ levels with the menstrual cycle (Harada et al., 2011; Near et al., 2014; Puts & Edden, 2012). In contrast, in our study GABA levels in females were stable over time in both regions, even though we did not control for menstrual cycle. In view of variations in MM levels between individuals and in neurological conditions, it is possible that the

observations described above for GABA+ may not reflect accurately the levels of pure GABA. As such, results obtained for GABA+ require validation for pure GABA.

Previous studies have demonstrated that behavioural interventions cause changes in GABA levels. Floyer-Lea et al. demonstrated that GABA decreases significantly in the SMC after 50 minutes of performing a repetitive motor learning task in a cohort of 23 subjects. These learning-related changes in GABA were not observed in 10 and 7 different subjects after performing random and rest tasks, respectively (Floyer-Lea et al., 2006). Levy et al. demonstrated significant reductions of GABA in SMC during an ischemic nerve block in 12 subjects (2 females) (Levy et al., 2002). Kupers et al. performed painful heat stimuli on 13 subjects (7 females) that led to a significant increase in GABA in ACC (Kupers et al., 2009). Sanacora et al. reported that cognitive behavioural therapy as a treatment for major depression has a moderate effect on GABA in OCC relative to both electroconvulsive therapy (ECT) and selective serotonin reuptake inhibitor (SSRI) treatments in 8 medication-free subjects with major depression (Sanacora et al., 2006).

Given the differences in reproducibility found between males and females in different brain regions in the present study, gender-related effects may have introduced bias in the above studies. For example, Floyer Lea et al. used different groups of subjects for the different tasks, which may have affected the results if the groups were not matched for gender (and possibly age). In the study by Levy et al. 83% of the subjects were male (Levy et al., 2002). Although gender could be used as a covariate (Sanacora et al., 1999), this might not be feasible due to lack of statistical power to detect group differences for the small sample sizes typically used in these studies (Kupers et al., 2009; Levy et al., 2002; Sanacora et al., 2006; Sanacora et al., 1999).The author recommends that future studies should emphasize gender-matching prior to conducting GABA-based investigations.

Limitations and future work

A technical limitation of the navigator system implemented is that the EPI specific frequency updates are disabled after the start of the motion correction to avoid interaction between frequency adjustment and motion correction. By not updating the EPI frequency in real time, the image is displaced in the phase encode direction and the slice profile will be shifted. A solution to this interaction would be to subtract the frequency-based phase encode translation estimate from that applied. This would permit simultaneous frequency and translation estimates to be applied to the EPI acquisition.

Subject motion can result in second-order shim changes that cause B_0 distortion (Figures 5 and 6 in (Hess et al., 2011)). One possible solution is to update the second order-shim estimates in a similar manner to that of first-order shim updates. Although the EPI navigator estimates the second-order shim in the present work, the current Siemens hardware does not allow real-time control of the higher-order shims due to the lack of eddy current compensation.

This work has not addressed the reacquisition technique to further enhance the spectral quality (Bogner et al., 2014). This technique could lead to subject fatigue due to prolonged scan time. Here we removed individual corrupted spectra during post-processing, as previously done (Near et al., 2013), rather than performing reacquisition.

Evans et al. demonstrated – on GABA spectra acquired by MEGA-PRESS – that pairwise (edit-on/off) frequency updates are superior and reduces subtraction artefacts (Evans et al., 2013). Bogner et al. demonstrated – on GABA spectra acquired by MEGA-LASER – that updating motion and shim terms once every pair of edit-on/off reduces choline artefacts and enhances spectral quality (Bogner et al., 2014). The MEGA-SPECIAL sequence requires four acquisitions (4 x TR = 16s for this study) to acquire a single GABA edited spectrum, rendering it very sensitive to motion compared to MEGA-PRESS and MEGA-LASER, which both require two TR's per edited spectrum. Therefore, in this work, the motion and shim estimates were updated every TR, rather than once for every set of measurements, to reduce the impact of motion and B_0 inhomogeneity on the final GABA spectrum. Nevertheless, comparison between the individual and pairwise updates of motion and shim terms during MEGA-SEPCIAL acquisition would be favourable.

The long TR of 4 s was necessary for this study to reduce specific absorption rate (SAR) due to strong outer volume suppression (OVS) pulses – a necessity for MEGA-SPECIAL (Near et al., 2011) – to eliminate any signal outside the VOI. Previous studies have demonstrated that long TRs ranging from 4s to 5s increase SNR by 20-30%. Furthermore, GABA editing has been well established for a TR of 4 s (Andreychenko et al., 2012).

In this study, the reproducibility, tissue-specific concentrations of GABA, and effects of gender and time on GABA concentrations were evaluated in the ACC and PAR due to the role of GABA in several neurological conditions (Bai et al., 2014; Puts & Edden, 2012) in which these regions are implicated. Future research should involve other regions of the brain, such as OCC, SMC and DLPFC, due to the correlation of GABA levels in these regions with pathology and healthy behaviour (Levy & Degnan, 2013; Mullins et al., 2012; Puts & Edden, 2012). Given the neuroactive

steroidal-related modulation of GABA and GABA-based regulation of circadian rhythm, it is important to investigate diurnal stability of GABA along with plasma hormone levels in both male and female participants.

In this study, the reproducibility of GABA levels was performed within a session. Repetition of session would have been more informative. However, the scope of the study was to determine reproducibility using different analysis packages, and therefore within session examination is adequate to achieve this objective. Furthermore, the scope and the outcome of the study support the findings of a previous GABA+ study (O'Gorman et al., 2011).

Finally, as previously mentioned, at University of Cape Town, there has been long-standing interest in studying learning deficits in children with prenatal alcohol exposure. Therefore, future work will include GABA-based investigation into the physiological basis of these learning deficits by implementing GABA acquisition before and after performing learning tasks, such as motor learning (Floyer-Lea et al., 2006) or eyeblink conditioning (Jacobson et al., 2011).

Chapter 7 CONCLUSION

γ-aminobutyric acid (GABA) is the primary inhibitory neurotransmitter and is of great interest to the MRS community due to its relevance with several neurological diseases and disorders. GABA acquisition is challenging and susceptible to motion and B_0 inhomogeneity. A novel technique has been presented that performs prospective motion, zero- and first-order shim correction using 3D EPI volumetric navigators. The registration of the navigator images using the PACE technique provides robust estimates of head position and orientation for motion correction. The field map generated by the navigator provides reliable B_0 estimates for zero- and first-order shim correction.

The navigators were incorporated in the MEGA-SPECIAL sequence with no impact on the acquisition time, producing GABA edited spectra with superior spectral quality. The navigators maintain spectral quality in the presence and absence of motion. Scans with B_0 disruptions, and with and without correction in the presence of motion, unequivocally demonstrate the necessity of real-time motion and shim correction.

The motion and shim navigated MEGA-SPECIAL sequence was used to acquire GABA spectra from the anterior cingulate (ACC) and medial parietal (PAR) cortices with superior quality and permitted investigations of reproducibility, variations of GABA levels in different tissues, and effects of gender. It was found that GABA measurements are most reproducible in both regions using LCModel followed by jMRUI and then GANNET. However, GABA levels were significantly lower for the second measurement in PAR.

Although GABA concentrations did not differ between males and females in ACC, the concentration in PAR was significantly higher in males, emphasizing the importance of gender-matching during GABA-based investigations of neurological conditions in mixed-gender groups. In addition, the concentration of GABA in male participants decreased over roughly 40 minutes in PAR *only*, stressing the need to determine the time of day during which GABA is stable in brain regions of interest prior to conducting GABA-based evaluations of neurological conditions.

References

Alhamud, A, Taylor, Paul A, Laughton, Barbara, van der Kouwe, André JW, & Meintjes, Ernesta M. (2015). Motion artifact reduction in pediatric diffusion tensor imaging using fast prospective correction. *Journal of Magnetic Resonance Imaging,* 41(5), 1353-1364.

Alhamud, A, Taylor, Paul A, van der Kouwe, Andre JW, & Meintjes, Ernesta M. (2016). Real-time measurement and correction of both B0 changes and subject motion in diffusion tensor imaging using a double volumetric navigated (DvNav) sequence. *Neuroimage,* 126, 60-71.

Andreychenko, Anna, Boer, Vincent O, Arteaga de Castro, Catalina S, Luijten, Peter R, & Klomp, Dennis WJ. (2012). Efficient spectral editing at 7 T: GABA detection with MEGA-sLASER. *Magnetic resonance in medicine,* 68(4), 1018-1025.

Ashburner, John, & Friston, Karl J. (2005). Unified segmentation. *Neuroimage,* 26(3), 839-851.

Aufhaus, E, Weber−Fahr, W, Sack, M, Tunc−Skarka, N, Oberthuer, G, Hoerst, M, Meyer−Lindenberg, A, Boettcher, U, & Ende, G. (2013). Absence of changes in GABA concentration with age and gender in the human anterior cingulate cortex: A MEGA-PRESS study with symmetric editing pulse frequencies for macromolucule suppression. *Magnetic resonance in medicine,* 69(2), 317-320.

Bai, Xue, Edden, Richard AE, Gao, Fei, Wang, Guangbin, Wu, Lebin, Zhao, Bin, Wang, Minzhong, Chan, Queenie, Chen, Weibo, & Barker, Peter B. (2014). Decreased γ-aminobutyric acid levels in the parietal region of patients with Alzheimer's disease. *Journal of Magnetic Resonance Imaging,* 41, 1326-1331.

Behar, Kevin L, Rothman, Douglas L, Petersen, Kitt F, Hooten, Michael, Delaney, Richard, Petroff, Ognen AC, Shulman, Gerald I, Navarro, Victor, Petrakis, Ismene L, Charney, Dennis S, & Krystal, JH. (1999). Preliminary evidence of low cortical GABA levels in localized 1H-MR spectra of alcohol-dependent and hepatic encephalopathy patients. *American Journal of Psychiatry,* 156, 952-954.

Bhattacharyya, PK, Lowe, MJ, & Phillips, MD. (2007). Spectral quality control in motion-corrupted single-voxel J-difference editing scans: An interleaved navigator approach. *Magnetic resonance in medicine,* 58(4), 808-812.

Bhattacharyya, PK, Phillips, MD, Stone, LA, & Lowe, MJ. (2011). In-vivo MRS measurement of gray-matter and white-matter GABA concentration in sensorimotor cortex using a motion-controlled MEGA-PRESS Sequence. *Magnetic resonance imaging,* 29(3), 374.

Bigal, ME, Hetherington, H, Pan, J, Tsang, A, Grosberg, B, Avdievich, N, Friedman, B, & Lipton, RB. (2008). Occipital levels of GABA are related to severe headaches in migraine. *Neurology,* 70(22), 2078-2080.

Block, Wolfgang, Träber, Frank, von Widdern, Olrik, Metten, Martin, Schild, Hans, Maier, Wolfgang, Zobel, Astrid, & Jessen, Frank. (2009). Proton MR spectroscopy of the hippocampus at 3 T in patients with unipolar major depressive disorder: correlates and predictors of treatment response. *International Journal of Neuropsychopharmacology,* 12(3), 415-422.

Bogner, W, Gagoski, Borjan, Hess, Aaron T, Bhat, Himanshu, Tisdall, M Dylan, van der Kouwe, Andre JW, Strasser, Bernhard, Marjańska, Małgorzata, Trattnig, Siegfried, Grant, Ellen, Rosen, B, & Andronesi, OC. (2014). 3D GABA imaging with real-time motion correction, shim update and reacquisition of adiabatic spiral MRSI. *Neuroimage,* 103, 290-302.

Bogner, W, Gruber, S, Doelken, M, Stadlbauer, A, Ganslandt, O, Boettcher, U, Trattnig, S, Doerfler, A, Stefan, H, & Hammen, T. (2010). In vivo quantification of intracerebral GABA by single-voxel (1)H-MRS-How reproducible are the results? *European journal of radiology,* 73(3), 526-531.

Bottomley, Paul A. (1987). Spatial localization in NMR spectroscopy in vivo. *Annals of the New York Academy of Sciences,* 508(1), 333-348.

Buckens, Constantinus F, de Jong, Pim A, Mol, Christian, Bakker, Eric, Stallman, Hein P, Mali, Willem P, van der Graaf, Yolanda, & Verkooijen, Helena M. (2013). Intra and interobserver

reliability and agreement of semiquantitative vertebral fracture assessment on chest computed tomography. *PloS one,* 8(8), e71204.

Choi, Changho, Bhardwaj, Paramjit P, Kalra, Sanjay, Casault, Colin A, Yasmin, Umme S, Allen, Peter S, & Coupland, Nicholas J. (2007). Measurement of GABA and contaminants in gray and white matter in human brain in vivo. *Magnetic resonance in medicine,* 58(1), 27-33.

Choi, In-Young, Lee, Sang-Pil, Merkle, Hellmut, & Shen, Jun. (2006). In vivo detection of gray and white matter differences in GABA concentration in the human brain. *Neuroimage,* 33(1), 85-93.

De Graaf, Robin A. (2008). *In vivo NMR spectroscopy: principles and techniques*: John Wiley & Sons.

Deicken, Raymond F, Eliaz, Yael, Feiwell, Robert, & Schuff, Norbert. (2001). Increased thalamic N-acetylaspartate in male patients with familial bipolar I disorder. *Psychiatry Research: Neuroimaging,* 106(1), 35-45.

Dharmadhikari, Shalmali, Ma, Ruoyun, Yeh, Chien-Lin, Stock, Ann-Kathrin, Snyder, Sandy, Zauber, S Elizabeth, Dydak, Ulrike, & Beste, Christian. (2015). Striatal and thalamic GABA level concentrations play differential roles for the modulation of response selection processes by proprioceptive information. *Neuroimage,* 120, 36-42.

Donahue, Manus J, Near, Jamie, Blicher, Jakob U, & Jezzard, Peter. (2010). Baseline GABA concentration and fMRI response. *Neuroimage,* 53(2), 392-398.

Drost, Dick J, Riddle, William R, & Clarke, Geoffrey D. (2002). Proton magnetic resonance spectroscopy in the brain: report of AAPM MR Task Group# 9. *Medical physics,* 29(9), 2177-2197.

Duffy, Jeanne F, Cain, Sean W, Chang, Anne-Marie, Phillips, Andrew JK, Münch, Mirjam Y, Gronfier, Claude, Wyatt, James K, Dijk, Derk-Jan, Wright, Kenneth P, & Czeisler, Charles A. (2011). Sex difference in the near-24-hour intrinsic period of the human circadian timing system. *Proceedings of the National Academy of Sciences,* 108(Supplement 3), 15602-15608.

Durst, Christopher R, Michael, Navin, Tustison, Nicholas J, Patrie, James T, Raghavan, Prashant, Wintermark, Max, & Velan, S Sendhil. (2015). Noninvasive evaluation of the regional variations of GABA using magnetic resonance spectroscopy at 3 Tesla. *Magnetic resonance imaging,* 33(5), 611-617.

Edden, R, Intrapiromkul, Jarunee, Zhu, He, Cheng, Ying, & Barker, Peter B. (2012). Measuring T2 in vivo with J-difference editing: Application to GABA at 3 tesla. *Journal of Magnetic Resonance Imaging,* 35(1), 229-234.

Edden, R, Puts, Nicolaas AJ, & Barker, Peter B. (2012). Macromolecule-suppressed GABA-edited magnetic resonance spectroscopy at 3T. *Magnetic resonance in medicine,* 68(3), 657-661.

Edden, Richard AE, & Barker, Peter B. (2007). Spatial effects in the detection of γ-aminobutyric acid: Improved sensitivity at high fields using inner volume saturation. *Magnetic resonance in medicine,* 58(6), 1276-1282.

Edden, Richard AE, Puts, Nicolaas AJ, Harris, Ashley D, Barker, Peter B, & Evans, C John. (2013). Gannet: A batch-processing tool for the quantitative analysis of gamma-aminobutyric acid–edited MR spectroscopy spectra. *Journal of Magnetic Resonance Imaging,* 40, 1445-1452.

Edden, Richard AE, Schär, Michael, Hillis, Argye E, & Barker, Peter B. (2006). Optimized detection of lactate at high fields using inner volume saturation. *Magnetic resonance in medicine,* 56(4), 912-917.

Epperson, C Neill, Haga, Kristin, Mason, Graeme F, Sellers, Edward, Gueorguieva, Ralitza, Zhang, Wenjiang, Weiss, Erica, Rothman, Douglas L, & Krystal, John H. (2002). Cortical gamma-aminobutyric acid levels across the menstrual cycle in healthy women and those with Premenstrual Dysphoric Disorder: a proton magnetic resonance spectroscopy study. *Archives of General Psychiatry,* 59(9), 851-858.

Evans, Christopher John, McGonigle, David John, & Edden, Richard Anthony Edward. (2010). Diurnal stability of γ-aminobutyric acid concentration in visual and sensorimotor cortex. *Journal of Magnetic Resonance Imaging,* 31(1), 204-209.

Evans, Christopher John, Puts, Nicolaas AJ, Robson, Siân E, Boy, Frederic, McGonigle, David J, Sumner, Petroc, Singh, Krish D, & Edden, Richard AE. (2013). Subtraction artifacts and frequency (Mis-) alignment in J-difference GABA editing. *Journal of Magnetic Resonance Imaging,* 38(4), 970-975.

Floyer-Lea, Anna, Wylezinska, Marzena, Kincses, Tamas, & Matthews, Paul M. (2006). Rapid modulation of GABA concentration in human sensorimotor cortex during motor learning. *Journal of neurophysiology,* 95(3), 1639-1644.

Fu, Zhuo Wu, Wang, Yi, Grimm, Roger C, Rossman, Phillip J, Felmlee, Joel P, Riederer, Stephen J, & Ehman, Richard L. (1995). Orbital navigator echoes for motion measurements in magnetic resonance imaging. *Magnetic resonance in medicine,* 34(5), 746-753.

Fuchs, Alexander, Luttje, Mariska, Boesiger, Peter, & Henning, Anke. (2013). SPECIAL semi-LASER with lipid artifact compensation for 1H MRS at 7 T. *Magnetic resonance in medicine,* 69(3), 603-612.

Gao, Fei, Edden, Richard AE, Li, Muwei, Puts, Nicolaas AJ, Wang, Guangbin, Liu, Cheng, Zhao, Bin, Wang, Huiquan, Bai, Xue, Zhao, Chen, Wang, X, & Barker, PB. (2013). Edited magnetic resonance spectroscopy detects an age-related decline in brain GABA levels. *Neuroimage,* 78, 75-82.

Gasparovic, Charles, Song, Tao, Devier, Deidre, Bockholt, H Jeremy, Caprihan, Arvind, Mullins, Paul G, Posse, Stefan, Jung, Rex E, & Morrison, Leslie A. (2006). Use of tissue water as a concentration reference for proton spectroscopic imaging. *Magnetic resonance in medicine,* 55(6), 1219-1226.

Goddard, Andrew W, Mason, Graeme F, Almai, Ahmad, Rothman, Douglas L, Behar, Kevin L, Petroff, Ognen AC, Charney, Dennis S, & Krystal, John H. (2001). Reductions in occipital cortex GABA levels in panic disorder detected with 1h-magnetic resonance spectroscopy. *Archives of General Psychiatry,* 58(6), 556-561.

Govindaraju, Varanavasi, Young, Karl, & Maudsley, Andrew A. (2000). Proton NMR chemical shifts and coupling constants for brain metabolites. *NMR in Biomedicine,* 13(3), 129-153.

Graham, Glenn D, Hwang, Jong-Hee, Rothman, Douglas L, & Prichard, James W. (2001). Spectroscopic assessment of alterations in macromolecule and small-molecule metabolites in human brain after stroke. *Stroke,* 32(12), 2797-2802.

Gruber, Stephan, Frey, Richard, Mlynárik, Vladimir, Stadlbauer, Andreas, Heiden, Angela, Kasper, Siegfried, Kemp, Graham J, & Moser, Ewald. (2003). Quantification of metabolic differences in the frontal brain of depressive patients and controls obtained by 1H-MRS at 3 Tesla. *Investigative radiology,* 38(7), 403-408.

Harada, Masafumi, Kubo, Hitoshi, Nose, Ayumi, Nishitani, Hiromu, & Matsuda, Tsuyoshi. (2011). Measurement of variation in the human cerebral GABA level by in vivo MEGA-editing proton MR spectroscopy using a clinical 3 T instrument and its dependence on brain region and the female menstrual cycle. *Human brain mapping,* 32(5), 828-833.

Harris, A, Puts, N, & Edden, R. (2015). Tissue correction for GABA-edited MRS: Considerations of voxel composition, tissue segmentation, and tissue relaxations. *Journal of Magnetic Resonance Imaging,* 42(5), 1431-1440.

Harris, Ashley D, Glaubitz, Benjamin, Near, Jamie, John Evans, C, Puts, Nicolaas AJ, Schmidt-Wilcke, Tobias, Tegenthoff, Martin, Barker, Peter B, & Edden, Richard AE. (2013). Impact of frequency drift on gamma-aminobutyric acid-edited MR spectroscopy. *Magnetic resonance in medicine,* 72(4), 941-948.

Harris, Ashley D, Puts, Nicolaas AJ, Anderson, Brian A, Yantis, Steven, Pekar, James J, Barker, Peter B, & Edden, Richard AE. (2015). Multi-Regional Investigation of the Relationship between Functional MRI Blood Oxygenation Level Dependent (BOLD) Activation and GABA Concentration. *PloS one,* 10(2), e0117531.

Harris, Ashley D, Puts, Nicolaas AJ, Barker, Peter B, & Edden, Richard AE. (2014). Spectral-editing measurements of GABA in the human brain with and without macromolecule suppression. *Magnetic resonance in medicine,* 74(6), 1523-1529.

Hasler, Gregor, van der Veen, Jan Willem, Tumonis, Toni, Meyers, Noah, Shen, Jun, & Drevets, Wayne C. (2007). Reduced prefrontal glutamate/glutamine and {gamma}-aminobutyric acid levels in major depression determined using proton magnetic resonance spectroscopy. *Archives of General Psychiatry,* 64(2), 193-200.

Henry, Pierre-Gilles, Dautry, Caroline, Hantraye, Philippe, & Bloch, Gilles. (2001). Brain GABA editing without macromolecule contamination. *Magn. Reson. Med.,* 45(3), 517-520.

Hess, A, Jacobson, SW, Jacobson, JL, Molteno, CD, van der Kouwe, André JW, & Meintjes, Ernesta M. (2014). A comparison of spectral quality in magnetic resonance spectroscopy data acquired with and without a novel EPI-navigated PRESS sequence in school-aged children with fetal alcohol spectrum disorders. *Metabolic brain disease,* 29(2), 323-332.

Hess, Aaron T, Andronesi, Ovidiu C, Dylan Tisdall, M, Gregory Sorensen, A, Kouwe, André JW, & Meintjes, Ernesta M. (2012). Real-time motion and B0 correction for localized adiabatic selective refocusing (LASER) MRSI using echo planar imaging volumetric navigators. *NMR in Biomedicine,* 25(2), 347-358.

Hess, Aaron T, Dylan Tisdall, M, Andronesi, Ovidiu C, Meintjes, Ernesta M, & van der Kouwe, André JW. (2011). Real-time motion and B0 corrected single voxel spectroscopy using volumetric navigators. *Magnetic resonance in medicine,* 66(2), 314-323.

Hess, Aaron T, Kouwe, André JW, Mbugua, Kenneth K, Laughton, Barbara, & Meintjes, Ernesta M. (2014). Quality of 186 child brain spectra using motion and B0 shim navigated single voxel spectroscopy. *Journal of Magnetic Resonance Imaging,* 40(4), 958-965.

Hodkinson, Duncan J, Krause, Kristina, Khawaja, Nadine, Renton, Tara F, Huggins, John P, Vennart, William, Thacker, Michael A, Mehta, Mitul A, Zelaya, Fernando O, Williams, Steven CR, & Howard, MA. (2013). Quantifying the test–retest reliability of cerebral blood flow measurements in a clinical model of on-going post-surgical pain: A study using pseudo-continuous arterial spin labelling. *NeuroImage: Clinical,* 3, 301-310.

Howe, FA, Barton, SJ, Cudlip, SA, Stubbs, M, Saunders, DE, Murphy, M, Wilkins, P, Opstad, KS, Doyle, VL, McLean, MA, Bell, BA, & Griffiths, JR. (2003). Metabolic profiles of human brain tumors using quantitative in vivo 1H magnetic resonance spectroscopy. *Magnetic resonance in medicine,* 49(2), 223-232.

Jacobson, Sandra W, Stanton, Mark E, Dodge, Neil C, Pienaar, Mariska, Fuller, Douglas S, Molteno, Christopher D, Meintjes, Ernesta M, Hoyme, H Eugene, Robinson, Luther K, Khaole, Nathaniel, & Jacobson, JL. (2011). Impaired Delay and Trace Eyeblink Conditioning in School-Age Children With Fetal Alcohol Syndrome. *Alcoholism: Clinical and Experimental Research,* 35, 250-264.

Jenkinson, Mark. (2003). Fast, automated, N-dimensional phase-unwrapping algorithm. *Magnetic resonance in medicine,* 49(1), 193-197.

Jensen, JE, Frederick, Bde B, & Renshaw, PF. (2005). Grey and white matter GABA level differences in the human brain using two-dimensional, J-resolved spectroscopic imaging. *NMR in Biomedicine,* 18(8), 570-576.

Ke, Yong, Cohen, Bruce M, Bang, Jeannette Y, Yang, Manqiu, & Renshaw, Perry F. (2000). Assessment of GABA concentration in human brain using two-dimensional proton magnetic resonance spectroscopy. *Psychiatry Research: Neuroimaging,* 100(3), 169-178.

Keating, Brian, Deng, Weiran, Roddey, J Cooper, White, Nathan, Dale, Anders, Stenger, V Andrew, & Ernst, Thomas. (2010). Prospective motion correction for single-voxel 1H MR spectroscopy. *Magnetic resonance in medicine,* 64(3), 672-679.

Keating, Brian, & Ernst, Thomas. (2012). Real-time dynamic frequency and shim correction for single-voxel magnetic resonance spectroscopy. *Magnetic resonance in medicine,* 68(5), 1339-1345.

Klose, Uwe. (1990). In vivo proton spectroscopy in presence of eddy currents. *Magnetic resonance in medicine*, 14(1), 26-30.

Kreis, Roland. (2004). Issues of spectral quality in clinical 1H-magnetic resonance spectroscopy and a gallery of artifacts. *NMR in Biomedicine*, 17(6), 361-381.

Kreis, Roland. (2016). The trouble with quality filtering based on relative Cramér−Rao lower bounds. *Magnetic resonance in medicine*, 75(1), 15-18.

Kupers, Ron, Danielsen, Else R, Kehlet, Henrik, Christensen, Rune, & Thomsen, Carsten. (2009). Painful tonic heat stimulation induces GABA accumulation in the prefrontal cortex in man. *Pain*, 142(1), 89-93.

Levy, L, & Degnan, AJ. (2013). GABA-based evaluation of neurologic conditions: MR spectroscopy. *American Journal of Neuroradiology*, 34, 259-265.

Levy, L, Levy-Reis, Igor, Fujii, Mavis, & Dalakas, Marinos C. (2005). Brain Gamma-Aminobutyric Acid Changes in Stiff-Person Syndrome. *Archives of neurology*, 62(6), 970-974.

Levy, L, Ziemann, Ulf, Chen, Robert, & Cohen, Leonardo G. (2002). Rapid modulation of GABA in sensorimotor cortex induced by acute deafferentation. *Annals of neurology*, 52(6), 755-761.

Liu, Chen, & Reppert, Steven M. (2000). GABA synchronizes clock cells within the suprachiasmatic circadian clock. *Neuron*, 25(1), 123-128.

Long, Zaiyang, Medlock, Carla, Dzemidzic, Mario, Shin, Yong-Wook, Goddard, Andrew W, & Dydak, Ulrike. (2013). Decreased GABA levels in anterior cingulate cortex/medial prefrontal cortex in panic disorder. *Progress in Neuro-Psychopharmacology and Biological Psychiatry*, 44, 131-135.

Mader, I, Seeger, U, Weissert, R, Klose, U, Naegele, T, Melms, A, & Grodd, W. (2001). Proton MR spectroscopy with metabolite-nulling reveals elevated macromolecules in acute multiple sclerosis. *Brain*, 124(5), 953-961.

Mason, Graeme F, Petrakis, Ismene L, de Graaf, Robin A, Gueorguieva, Ralitza, Guidone, Elizabeth, Coric, Vladimir, Epperson, C Neill, Rothman, Douglas L, & Krystal, John H. (2006). Cortical gamma-aminobutyric acid levels and the recovery from ethanol dependence: preliminary evidence of modification by cigarette smoking. *Biological psychiatry*, 59(1), 85-93.

Masubuchi, Satoru, Honma, Sato, Abe, Hiroshi, Ishizaki, Kouji, Namihira, Masakazu, Ikeda, Masaaki, & Honma, Ken−ichi. (2000). Clock genes outside the suprachiasmatic nucleus involved in manifestation of locomotor activity rhythm in rats. *European Journal of Neuroscience*, 12(12), 4206-4214.

Mescher, M, Merkle, H, Kirsch, J, Garwood, M, & Gruetter, R. (1998). Simultaneous in vivo spectral editing and water suppression. *NMR in Biomedicine*, 11(6), 266-272.

Mescher, M, Tannus, A, Johnson, M, & Garwood, M. (1996). Solvent suppression using selective echo dephasing. *Journal of Magnetic Resonance, Series A*, 123(2), 226-229.

Michaelis, T, Merboldt, KD, Bruhn, H, Hänicke, W, & Frahm, J. (1993). Absolute concentrations of metabolites in the adult human brain in vivo: quantification of localized proton MR spectra. *Radiology*, 187(1), 219-227.

Michels, Lars, Martin, Ernst, Klaver, Peter, Edden, Richard, Zelaya, Fernando, Lythgoe, David J, Lüchinger, Rafael, Brandeis, Daniel, & O'Gorman, Ruth L. (2012). Frontal GABA levels change during working memory. *PloS one*, 7(4), e31933.

Mikkelsen, Mark, Singh, Krish D, Sumner, Petroc, & Evans, C John. (2015). Comparison of the repeatability of GABA-edited magnetic resonance spectroscopy with and without macromolecule suppression. *Magnetic resonance in medicine*, 75(3), 946-953.

Mlynárik, Vladimír, Gambarota, Giulio, Frenkel, Hanne, & Gruetter, Rolf. (2006). Localized short-echo-time proton MR spectroscopy with full signal-intensity acquisition. *Magnetic resonance in medicine*, 56(5), 965-970.

Mlynárik, Vladimír, Gruber, Stephan, & Moser, Ewald. (2001). Proton T1 and T2 relaxation times of human brain metabolites at 3 Tesla. *NMR in Biomedicine,* 14(5), 325-331.

Mullins, Paul G, McGonigle, David J, O'Gorman, Ruth, Puts, Nicolaas AJ, Vidyasagar, Rishma, Evans, C John, & Edden, Richard AE. (2012). Current Practice in the use of MEGA-PRESS spectroscopy for the detection of GABA. *Neuroimage,* 86, 43-52.

Muthukumaraswamy, Suresh D, Edden, Richard AE, Jones, Derek K, Swettenham, Jennifer B, & Singh, Krish D. (2009). Resting GABA concentration predicts peak gamma frequency and fMRI amplitude in response to visual stimulation in humans. *Proceedings of the National Academy of Sciences,* 106(20), 8356-8361.

Naressi, A, Couturier, C, Devos, JM, Janssen, M, Mangeat, C, De Beer, R, & Graveron-Demilly, D. (2001). Java-based graphical user interface for the MRUI quantitation package. *Magnetic Resonance Materials in Physics, Biology and Medicine,* 12(2-3), 141-152.

Near, Jamie, Andersson, Jesper, Maron, Eduard, Mekle, Ralf, Gruetter, Rolf, Cowen, Philip, & Jezzard, Peter. (2013). Unedited in vivo detection and quantification of γ-aminobutyric acid in the occipital cortex using short-TE MRS at 3 T. *NMR in Biomedicine,* 26, 1353-1362.

Near, Jamie, Edden, Richard, Evans, C John, Paquin, Raphaël, Harris, Ashley, & Jezzard, Peter. (2015). Frequency and phase drift correction of magnetic resonance spectroscopy data by spectral registration in the time domain. *Magnetic resonance in medicine,* 73(1), 44-50.

Near, Jamie, Evans, C John, Puts, Nicolaas AJ, Barker, Peter B, & Edden, Richard AE. (2012). J-difference editing of gamma-aminobutyric acid (GABA): Simulated and experimental multiplet patterns. *Magnetic resonance in medicine,* 70(5), 1183-1191.

Near, Jamie, Ho, Yi-Ching Lynn, Sandberg, Kristian, Kumaragamage, Chathura, & Blicher, Jakob Udby. (2014). Long-term reproducibility of GABA magnetic resonance spectroscopy. *Neuroimage,* 99, 191-196.

Near, Jamie, Simpson, Robin, Cowen, Philip, & Jezzard, Peter. (2011). Efficient γ-aminobutyric acid editing at 3T without macromolecule contamination: MEGA-SPECIAL. *NMR in Biomedicine,* 24(10), 1277-1285.

O'Gorman, R , Edden, R, Michels, L, Murdoch, JB, & Martin, E. (2007). *Precision and repeatability of in vivo GABA and glutamate quantification*. Paper presented at the Proceedings of the 19th scientific meeting, International Society for Magnetic Resonance in medicine, Montreal, Canada.

O'Gorman, R , Michels, Lars, Edden, Richard A, Murdoch, James B, & Martin, Ernst. (2011). In vivo detection of GABA and glutamate with MEGA-PRESS: Reproducibility and gender effects. *Journal of Magnetic Resonance Imaging,* 33(5), 1262-1267.

Pallant, J. (2001). *SPSS survival manual: a step by step to data analysis using SPSS*.

Provencher, Stephen W. (2001). Automatic quantitation of localized in vivo 1H spectra with LCModel. *NMR in Biomedicine,* 14(4), 260-264.

Provencher, Stephen W. (2005). LCModel & LCMgui user's manual. *Stephen W. Provencher*.

Puts, Nicolaas AJ, Barker, Peter B, & Edden, Richard AE. (2013). Measuring the longitudinal relaxation time of GABA in vivo at 3 Tesla. *Journal of Magnetic Resonance Imaging,* 37(4), 999-1003.

Puts, Nicolaas AJ, & Edden, Richard AE. (2012). In vivo magnetic resonance spectroscopy of GABA: A methodological review. *Progress in nuclear magnetic resonance spectroscopy,* 60, 29-41.

Rothman, Douglas L, Petroff, OA, Behar, Kevin L, & Mattson, Richard H. (1993). Localized 1H NMR measurements of gamma-aminobutyric acid in human brain in vivo. *Proceedings of the National Academy of Sciences,* 90(12), 5662-5666.

Saleh, Muhammad G., Alhamud, A., Near, Jamie, van der Kouwe, André JW, & Meintjes, Ernesta M. (2016). Volumetric navigated MEGA-SPECIAL for real-time motion and shim corrected GABA editing. *NMR in Biomedicine,* 29, 248-255.

Sanacora, Gerard, Fenton, Lisa R, Fasula, Madonna K, Rothman, Douglas L, Levin, Yael, Krystal, John H, & Mason, Graeme F. (2006). Cortical γ-aminobutyric acid concentrations in

depressed patients receiving cognitive behavioral therapy. *Biological psychiatry,* 59(3), 284-286.

Sanacora, Gerard, Mason, Graeme F, Rothman, Douglas L, Behar, Kevin L, Hyder, Fahmeed, Petroff, Ognen AC, Berman, Robert M, Charney, Dennis S, & Krystal, John H. (1999). Reduced cortical γ-aminobutyric acid levels in depressed patients determined by proton magnetic resonance spectroscopy. *Archives of General Psychiatry,* 56(11), 1043-1047.

Sanacora, Gerard, Mason, Graeme F, Rothman, Douglas L, & Krystal, John H. (2002). Increased occipital cortex GABA concentrations in depressed patients after therapy with selective serotonin reuptake inhibitors. *American Journal of Psychiatry,* 159, 663-665.

Stagg, Charlotte J, Wylezinska, Marzena, Matthews, Paul M, Johansen-Berg, Heidi, Jezzard, Peter, Rothwell, John C, & Bestmann, Sven. (2009). Neurochemical effects of theta burst stimulation as assessed by magnetic resonance spectroscopy. *Journal of neurophysiology,* 101(6), 2872-2877.

Terpstra, Melissa, Ugurbil, Kamil, & Gruetter, Rolf. (2002). Direct in vivo measurement of human cerebral GABA concentration using MEGA-editing at 7 Tesla. *Magnetic resonance in medicine,* 47(5), 1009-1012.

Thesen, Stefan, Heid, Oliver, Mueller, Edgar, & Schad, Lothar R. (2000). Prospective acquisition correction for head motion with image-based tracking for real-time fMRI. *Magnetic resonance in medicine,* 44(3), 457-465.

Ticku, Maharaj K. (1990). Alcohol and GABA-benzodiazepine receptor function. *Annals of medicine,* 22(4), 241-246.

Tkáć, I, & Gruetter, R. (2005). Methodology of ^{1}H NMR spectroscopy of the human brain at very high magnetic fields. *Applied Magnetic Resonance,* 29(1), 139-157.

Tkáć, I, Starcuk, Z, Choi, IY, & Gruetter, R. (1999). In Vivo ^{1}H NMR Spectroscopy of Rat Brain at 1 ms Echo Time. *Magnetic resonance in medicine,* 41, 649-656.

van der Kouwe, André JW, Benner, Thomas, & Dale, Anders M. (2006). Real-time rigid body motion correction and shimming using cloverleaf navigators. *Magnetic resonance in medicine,* 56(5), 1019-1032.

van der Kouwe, André JW, Benner, Thomas, Salat, David H, & Fischl, Bruce. (2008). Brain morphometry with multiecho MPRAGE. *Neuroimage,* 40(2), 559-569.

Vanhamme, Leentje, van den Boogaart, Aad, & Van Huffel, Sabine. (1997). Improved method for accurate and efficient quantification of MRS data with use of prior knowledge. *Journal of Magnetic Resonance,* 129(1), 35-43.

Waddell, Kevin W, Avison, Malcolm J, Joers, James M, & Gore, John C. (2007). A practical guide to robust detection of GABA in human brain by J-difference spectroscopy at 3 T using a standard volume coil. *Magnetic resonance imaging,* 25(7), 1032-1038.

Weir, Joseph P. (2005). Quantifying test-retest reliability using the intraclass correlation coefficient and the SEM. *The Journal of Strength & Conditioning Research,* 19(1), 231-240.

Welch, Edward Brian, Manduca, Armando, Grimm, Roger C, Ward, Heidi A, & Jack Jr, Clifford R. (2002). Spherical navigator echoes for full 3D rigid body motion measurement in MRI. *Magn. Reson. Med.,* 47(1), 32-41.

White, Nathan, Roddey, Cooper, Shankaranarayanan, Ajit, Han, Eric, Rettmann, Dan, Santos, Juan, Kuperman, Josh, & Dale, Anders. (2010). PROMO: Real-time prospective motion correction in MRI using image-based tracking. *Magnetic resonance in medicine,* 63(1), 91-105.

Wijtenburg, S Andrea, Rowland, Laura M, Edden, Richard AE, & Barker, Peter B. (2013). Reproducibility of brain spectroscopy at 7T using conventional localization and spectral editing techniques. *Journal of Magnetic Resonance Imaging,* 38(2), 460-467.

Winkelman, John W, Buxton, Orfeu M, Jensen, J Eric, Benson, Kathleen L, O'Connor, Shawn P, Wang, Wei, & Renshaw, Perry F. (2008). Reduced brain GABA in primary insomnia: preliminary data from 4T proton magnetic resonance spectroscopy (1H-MRS). *Sleep,* 31(11), 1499-1506.

Wong, C, Bottiglieri, Teodoro, & Snead, O Carter. (2003). Gaba, γ-hydroxybutyric acid, and neurological disease. *Annals of neurology*, 54(S6), S3-S12.

Yamamoto, Mitsutoshi, Takahashi, Shigeru, Otsuki, Saburo, Kugoh, Toshiaki, Hosokawa, Kiyoshi, & Ogawa, Norio. (1985). GABA levels in cerebrospinal fluid of patients with epilepsy. *Psychiatry and Clinical Neurosciences*, 39(4), 515-519.

Zaitsev, M, Speck, O, Hennig, J, & Büchert, M. (2010). Single-voxel MRS with prospective motion correction and retrospective frequency correction. *NMR in Biomedicine*, 23(3), 325-332.

Zheng, Ping. (2009). Neuroactive steroid regulation of neurotransmitter release in the CNS: action, mechanism and possible significance. *Progress in neurobiology*, 89(2), 134-152.

Zhu, He, Edden, Richard AE, Ouwerkerk, Ronald, & Barker, Peter B. (2011). High resolution spectroscopic imaging of GABA at 3 Tesla. *Magn. Reson. Med.*, 65(3), 603-609.